Copyright Warning & Restrictions

The copyright law of the United States (Title 17, United States Code) governs the making of photocopies or other reproductions of copyrighted material.

Under certain conditions specified in the law, libraries and archives are authorized to furnish a photocopy or other reproduction. One of these specified conditions is that the photocopy or reproduction is not to be "used for any purpose other than private study, scholarship, or research." If a, user makes a request for, or later uses, a photocopy or reproduction for purposes in excess of "fair use" that user may be liable for copyright infringement,

This institution reserves the right to refuse to accept a copying order if, in its judgment, fulfillment of the order would involve violation of copyright law.

Please Note: The author retains the copyright while the New Jersey Institute of Technology reserves the right to distribute this thesis or dissertation

Printing note: If you do not wish to print this page, then select "Pages from: first page # to: last page #" on the print dialog screen

Softening Response of Concrete in Direct Tension

by

Teresa Cintora

November 12, 1987

Thesis submitted to the faculty of the Graduate School of
the New Jersey Institute of Technology in partial fulfillment of
the requirements for the degree of
Master of Science in Civil Engineering
1987

APPROVAL SHEET

Title of Thesis: Softening Response of Concrete in Direct Tension

Name of Candidate: Teresa Cintora
Master of Science in Civil Engineering, 1988

Thesis and Abstract Approved:

Dr. Methi Wecharatana
Associate Professor
Department of Civil Engineering

Date

Signatures of other members of the thesis committee

Dr. Farhad Ansari
Associate Professor of Civil Engineering

Date

Dr. Dorairaja Raghu
Associate Professor of Civil Engineering

Date

VITA

Name: Teresa Cintora

Degree and Date to be Conferred: M.S. in Civil Engineering, 1988

Secondary Education: Carl Schurz High School, Chicago Ill., 1980

Collegiate Institutions Attended	Dates	Degree	Date of Degree
New Jersey Institute of Technology	1986-1987	M.S.C.E.	1987
New Jersey Institute of Technology	1983-1986	B.S.C.E.	1987

Major: Civil Engineering

Positions held: 1984-1987 Graduate Assistant
New Jersey Institute of Technology
Newark, New Jersey 07102

Abstract

Title of Thesis: Softening Response of Concrete in Direct Tension
Teresa Cintora, Master of Science in Civil Engineering, 1987

Thesis directed by: Dr. Methi Wecharatana, Associate Professor of Civil Engineering

Due to the increased attention in nonlinear fracture mechanics and numerical methods of cementitious material, it has become necessary to have a reliable investigation of the post-peak softening response of concrete under direct uniaxial loading. But due to the brittleness of the material previous researchers have encountered great difficulty in obtaining complete data regarding the load-deformation behavior. This study uses a strain-controlled testing method and therefore the post-peak curve can be more easily obtained. Based on these results a unique formula for the normalized load vs. deformation curve has been proposed to be applied in fracture analysis applications.

ACKNOWLEDGMENT

I like to express my deepest gratitude to my family and friends for their support through this very important endeavor. I must make special mention of my advisor Dr. Methi Wecharatana for his vital counseling. And most of all I would like to thank Vasil Hlinka, it must have taken a lot of patience to put up with me during the writing of this thesis.

Contents

List of Figures

Chapter I

INTRODUCTION

1. General

The tensile capacity of concrete, due to its low magnitude, has up to now been disregarded when designing regular reinforced and especially prestressed concrete structures. In recent years nonlinear finite element analysis and other numerical methods have proved to be efficient and highly accurate. These methods require the use of crack models, which can only be generated if complete stress-deformation curves are available. This information is necessary so as to obtain accurate predictions of crack widths, deflections, and fracture energy. Data regarding this is sparse due to the difficulties of the uniaxial tension test. But with the development of electro-hydraulic feedback controlled testing machines, new techniques are posssible.

Available studies on tensile softening are conflicting. Some show the stress-deformation curve to become asymptotic. Others have incomplete post-peak response. But since the fracture energy is considered to be the area under the curve, either of these type of results would be misleading. Obtaining a complete curve was one of the main objectives of this study. Closed-loop strain control testing was used, ensuring a stable post-peak response (without abrupt brittle failure) until the specimen no longer had the capacity to carry any tensile load. Five controlled grain sizes of sand were used (passing sieve # 70, between sieve # 40 and # 70, between sieve # 40 and # 50, between sieve # 30 and # 40, and between # 10 and # 40), with a similar mix proportion of 1 part cement, 2 parts sand, and varying water cement ratios. Some concrete specimens, with a coarse aggregate size of 3/8 inch gravel, were also included.

2. Literature Review

In the recent past many models have been proposed to be used in non-linear fracture mechanics. Among the many are: the fictitious crack model by Hillerborg [5]; the crack band model by Bazant [1] and the modified strain energy model by Wecharatana and Shah [11]. The above mentioned models used assumed post-peak portions of the uniaxial tension process, since no data was available on this type of test. Therefore, the accuracy of the assumptions made in order to arrive at such models cannot really be ascertained without actual uniaxial tension test results. The reasons for this lack of information on this subject are the brittleness of the material and unavailability of equipment sensitive enough to control the cracking process.

Various attempts have been made to carry out a uniaxial tension test. Evans and Marathe [3] try to resolve the problem by increasing the stiffness of the equipment by conducting the test on the concrete specimen plus four parallel steel rods. But after the load dropped to about 1/5 of the peak load, abrupt failure occurred. Petersson [6], also used the approach of externally increasing the stiffness of the testing machine. This was done by placing aluminum columns on either side of the specimen. These columns were then electrically heated causing them to expand. It was this expansion that forced the actuator head upward and therefore applying a tensile force on the specimen. However these tests were not carried out to complete unloading (or failure) of the specimen, and they were only used to obtain the peak tensile force. In fact the results showed an asymptotic behavior once the stress reached about 60 psi (pounds per square inch). It seemed doubtfull that the concrete could hold a constant load while its strain increased indefinitely. Both of these approaches seemed to be limited by the setup used.

With the development of better testing equipment new setups have been used. Closed-loop testing now permits much greater control throughout the tests. The output from high precision extensometers is used as the feedback signal to the MTS controller. The controller in turn adjusts the actuator movement accordingly, thus, avoiding the abrupt failure caused by the otherwise erratic rate of crack opening. Reinhardt [8] used a direct tension specimen which was held in place through the use of steel plates glued to the ends of the specimen with epoxy. The alignment of the plates on the specimen is critical to a successful test. Gopalaratnam and Shah [4] used plates which were clamped on to the specimen. These plates secured the specimen through the friction force created by them. This method proved to

be restrictive. If the size of the specimen was increased beyond that which they used, the friction force would not be sufficient to hold the specimen, therefore resulting in slippage.

Even though some of these researchers had the capability to run the uniaxial tension test to its entirety, they did not. Others were using highly sensistive gages which had a limited amount of travel. The test were terminated in the range of 1600 $\mu inch$ to 2400 $\mu inch$ of displacement. One assumption made was that the response became asymptotic after this point, another assumption was that the contribution made by the remaining unseen portion would be irrelevant. So the fracture energy G_f, which is the area under the stress-strain curve, obtained from this data could be inaccurate.

3. Objectives

It is the objective of this research to obtain a more realistic and complte load-displacement response which includes both the loading and unloading portion. The effects of mix proportion and grain size will also be analyzed. A load-displacement law similar to those reported by Wecharatana and Shah [11] and Visalvanich and Naaman [10], was to be considered. However an attempt will be made to include the ascending portion of the curve.

If successful the obtained formula will enable researchers and engineers to predict the entire (both ascending and descending) load-deformation curve of concrete, provided that tensile strength, grain size and mix proportion are given.

Chapter II

TESTING PROCEDURE

1. Specimen

A rectangular shaped section with tapered ends was chosen for the specimens to be tested. This was done to facilitate a method of securing the specimen. At first, the use of a rectangular specimen with uniform section was considered, but upon further investigation, it was found that it would have been inadequate. The reason for this was that the force required to create enough friction force to prevent slippage would be very close to the capacity of the material. The final design had a rectangular cross-section of about 1 in. by 3 in.. The rectangular portion was 3 inches in length, after which the width tapered out at a ratio slope of 1 in 5 (see Figure 2.1).

Having the above explained specimen, it was possible for the crack to occur anywhere along the narrow portion of the specimen. This posed a problem: how to monitor the crack without knowing its location. In order to solve this problem notches were introduced; one on each side of the specimen at the middle. Then the 1 inch extensometers could be positioned at the potential crack zone [4]. The effects of stress concentration at the notch due to the cutting process were assumed to be negligible. This assumption was confirmed when the cross-sectional strain distribution was analyzed (see Figure 3.5).

2. Grips

The grips were fabricated from an alloy steel and polyvinylchloride (PVC). The main considerations during the design and building process were:

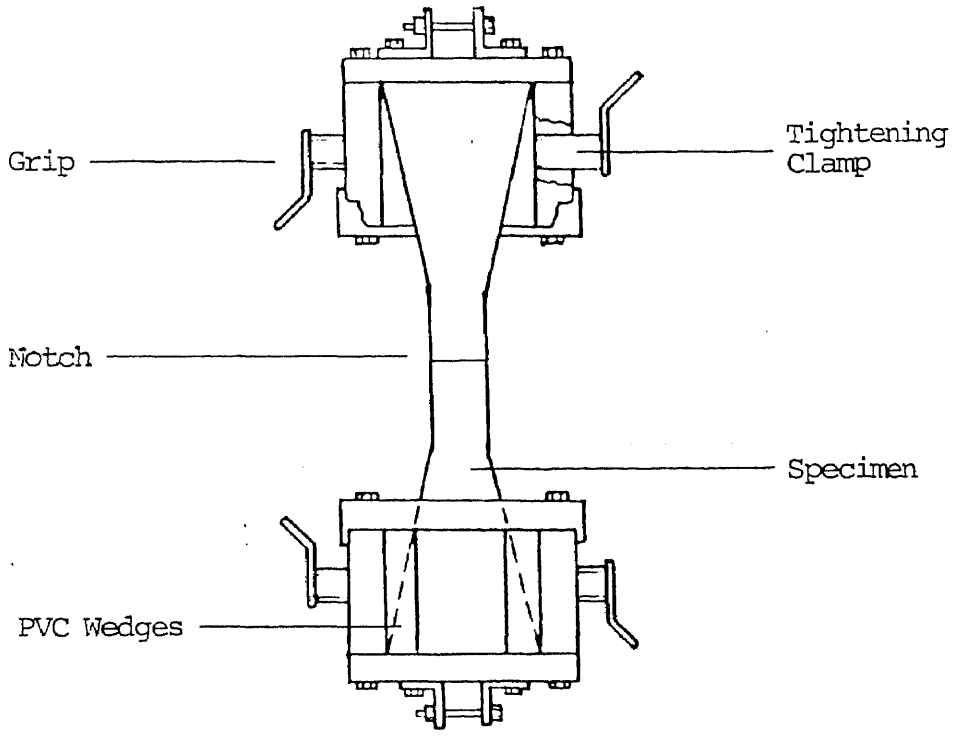

Figure 2.1: Friction grips.

1. To ensure that the load applied to the specimen would be easily transfered through the grips without any yielding or failure.

2. To ensure that enough pulling force would be provided without creating undesired compression at the transition zone.

The grips were box-shaped, measuring 6" by 4" by 5". It consisted of 3 steel plates (one 6" × 5", and two 3" × 6"), and two 3/2" × 3/2" × 1/8" angles. The two 3" × 6" plates were connected to the edges of the 6" × 5" plate, using 6 1/2" bolts, which in turn were linked to each other using the two steel angles (see Figure 2.1). Within this box were two PVC wedges, with angles complementing those of the specimen, which would secure the specimen in place. The grips were connected to the testing machine using two universal joints, one at the top and the other at the bottom. The above described setup was then connected to a custom-made adjustable steel rod, which in turn was secured into the base of the load frame.

3. Specimen Casting

A total of twelve different mixes were used in this study (see Table III.1 page 9). The type of cement used was Type III. The fine aggregate was silicious sand, which was sieved to obtain a total of five groups of different grain size. The mix was prepared by hand. Enough mix was made to cast three tension specimens and three compression specimens each time. On the average the total amount of mortar being prepared ranged between 20 to 30 pounds. After the mix was poured into the molds, it was vibrated on a vibrating table to drive out the excess air and obtain a well compacted specimen. When 24 hours had elapsed, (so that the specimens were strong enough to be removed from their molds) they were placed in a lime-water solution and left to cure for a period of at least one week. The testing age of the specimens varied from 28 days to a year. More details about each individual test can be observed in Appendix C. Just prior to testing, the notches were made using a diamond saw.

4. Closed Loop Testing

The testing was conducted with a MTS closed-loop machine (model 810-442 controllers). The specimens were loaded so as to maintain a steady rate of increase in elongation, which was being measured by extensometers. Two extensometers (1 in. gage length each) were positioned opposite each other on the specimen where the crack was expected to occur. The averaged reading of the two gages was then used as feedback to control the test. Two gages were found to be necessary since the non-homogeneity of the material makes it most probable that the crack will start from one side. Therefore, two gages will permit better control. For example, if a crack starts to generate very quickly on one side, the machine will hold or lower load in order to compensate, while also allowing the strain on the opposite side to approach the same degree as that of the first.

The specimens were initially loaded at a rate of 0.1 $\mu strains$ per second, therefore allowing the specimen to reach the critical peak without sudden failure. Once the load had dropped about 20% of the peak load, the rate was increased at regular intervals until it reached 4 $\mu strains$ per second. On average, the rate applied was approximately 0.5 $\mu strains$ per second. Readings were recorded every 15 seconds, using a computer interfaced with the MTS-442 data display. The data was also simultaneously recorded on a

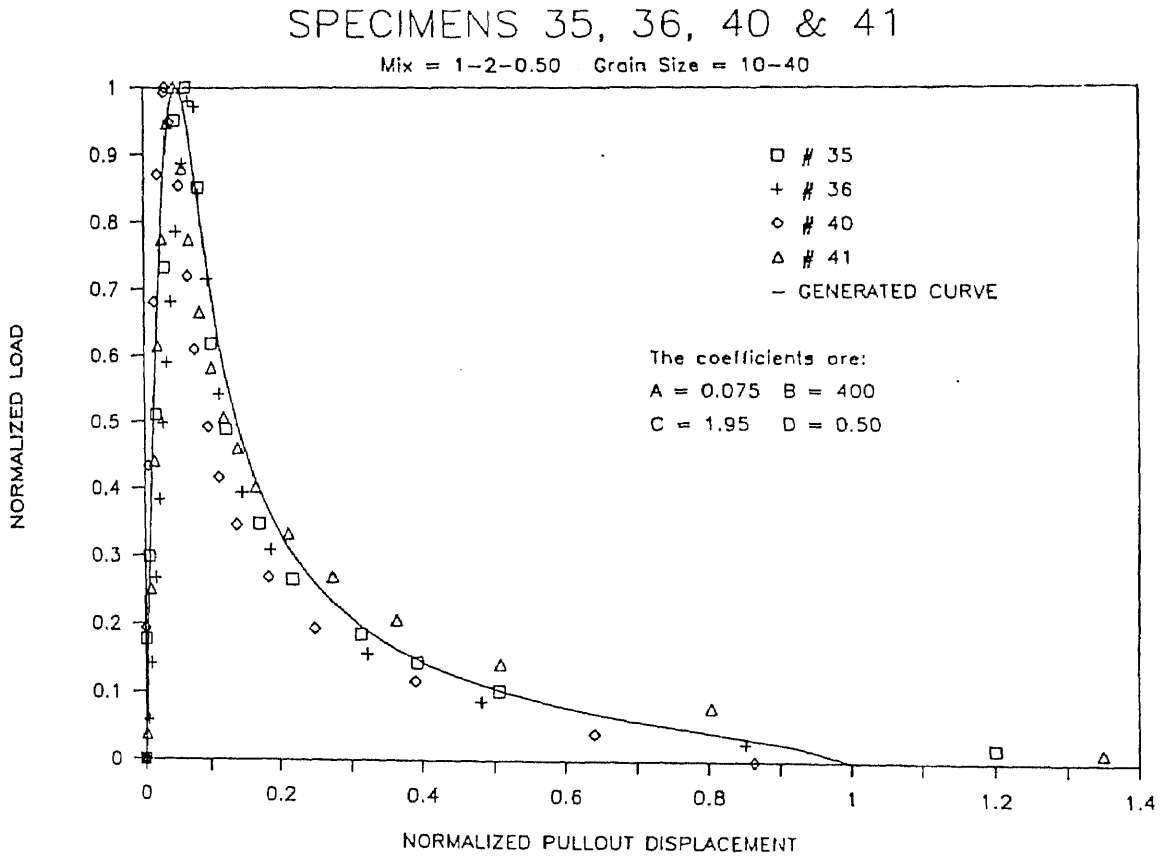

Figure 3.3: Comparison of recommended formula with results from present study.

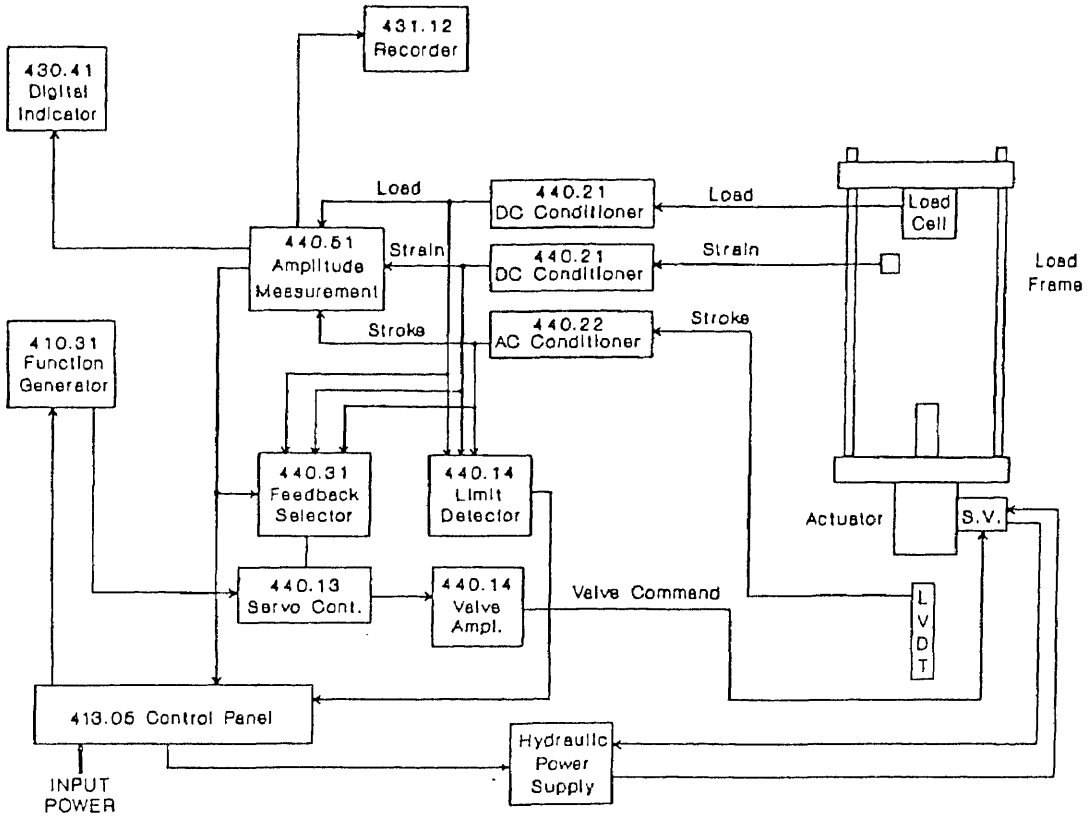

Figure 2.2: Block diagram of closed-loop system.

XY Recorder (see Figure 2.2).

As explained above, the extensometers yielded the average strain (displacement) of the cross sectional area in the fracture zone. In order to obtain some insight into the strain distribution, four foil strain gages were mounted on specimens between the two notches. These gages were connected to a bridge circuit which in turn was connected to a CYBORG ISAAC 2000 Data Acquisition system (see Figure 2.3). The ISAAC unit provided all the necessary signal conditioning (voltage amplification) to allow the bridge voltage to be measured and recorded. Readings were taken every 15 seconds, each one consisting of an average of five readings taken at 1 millisecond intervals. The ISAAC was also recording data being measured by the MTS; such as the load, stroke, and strain (from extensometers); in order to synchronize these with the strain readings from the foil gages.

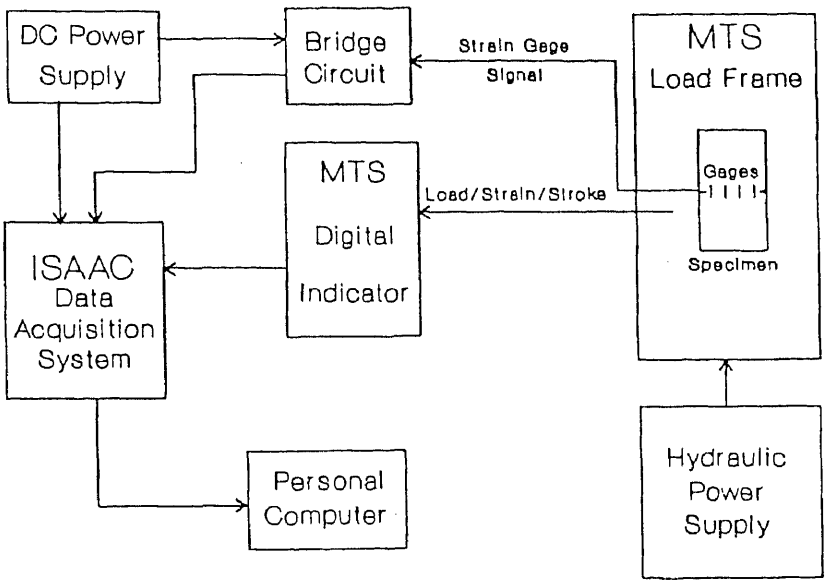

Figure 2.3: Block diagram of ISAAC-MTS interface.

Chapter III

RESULTS AND DISCUSSION

Table III.1 presents the results obtained. The numbers indicate the averages of all the specimens tested for that particular mix. Included in the table are: the grain size of the sand used in terms of the sieves passing; the peak load in tension; the strain at which the peak tensile load was observed; the strain value corresponding to the point where the specimen has reached zero load, or is incapable of carrying any tensile forces; the compressive strenght; the tensile strength; and finally the fracture energy, G_f, calculated as the entire area under the stress versus strain curve. The Modulus of Elasticity (Young's Modulus), though not listed in the table was in the range of 1.8 EE6 psi to 2.5 EE6 psi. This value was obtained from the compression test results, by taking the tangent at the most linear portion of the curve.

1. Load Displacement Relationship

Figure 3.1, represents a typical load versus displacement relationship. Responses for each of the specimens tested can be found in Appendix A. The same behavior was observed in every test. The ascending part is non-linear. After the peak the load (stress) drops gradually until it reaches zero. This contradicts the asymptotic behavior indicated by other researchers, [4] [6] [8]. The maximum post-peak displacement represents the pullout distance where no traction remains across the crack plane. Figure 3.1, shows that in the post-peak region there is a loading and unloading type of response. This is caused by the brittleness of the material and the somewhat limiting capacity of the pump being used. Because the speed with which the machine responds to the input is dependent on the power that the pump can provide.

Table III.1: Overall Observed Parameters

Mix	Mix Proportion (C:S:W)	Sand Size (sieve)	Peak Load (lbs)	Strain at Peak Load	Maximum Strain	Compr. Strength (psi)	Tensile Strength (psi)	G_f (energy) (lb/in)
I	1:2:0.40	10-30	999	2.33E-04	8.10E-03	9116	425	0.344
II	1:2:0.40	10-40	506	2.70E-04	8.07E-03	10356	220	0.277
III	1:2:0.40	30-40	1023	2.35E-04	5.28E-03	9655	469	0.371
IV	1:2:0.45	10-40	717	3.60E-04	7.78E-03	8616	276	0.272
V	1:2:0.45	30-40	614	3.10E-04	1.10E-02	8140	208	0.368
VI	1:2:0.45	40-50	692	3.05E-04	7.49E-03	6763	333	0.354
VII	1:2:0.45	40-70	648	2.95E-04	5.36E-03	8230	316	0.252
VIII	1:2:0.50	10-40	454	3.98E-04	7.45E-03	7174	211	0.262
IX	1:2:0.50	40-50	678	2.23E-04	7.70E-03	6275	283	0.328
X	1:2:0.50	40-70	502	4.20E-04	6.48E-03	6663	246	0.229
XI	1:2:0.55	10-40	796	2.63E-04	7.46E-03	6941	363	0.392
XII	1:2:0.55	40-70	859	3.20E-04	4.10E-03	7233	392	0.322

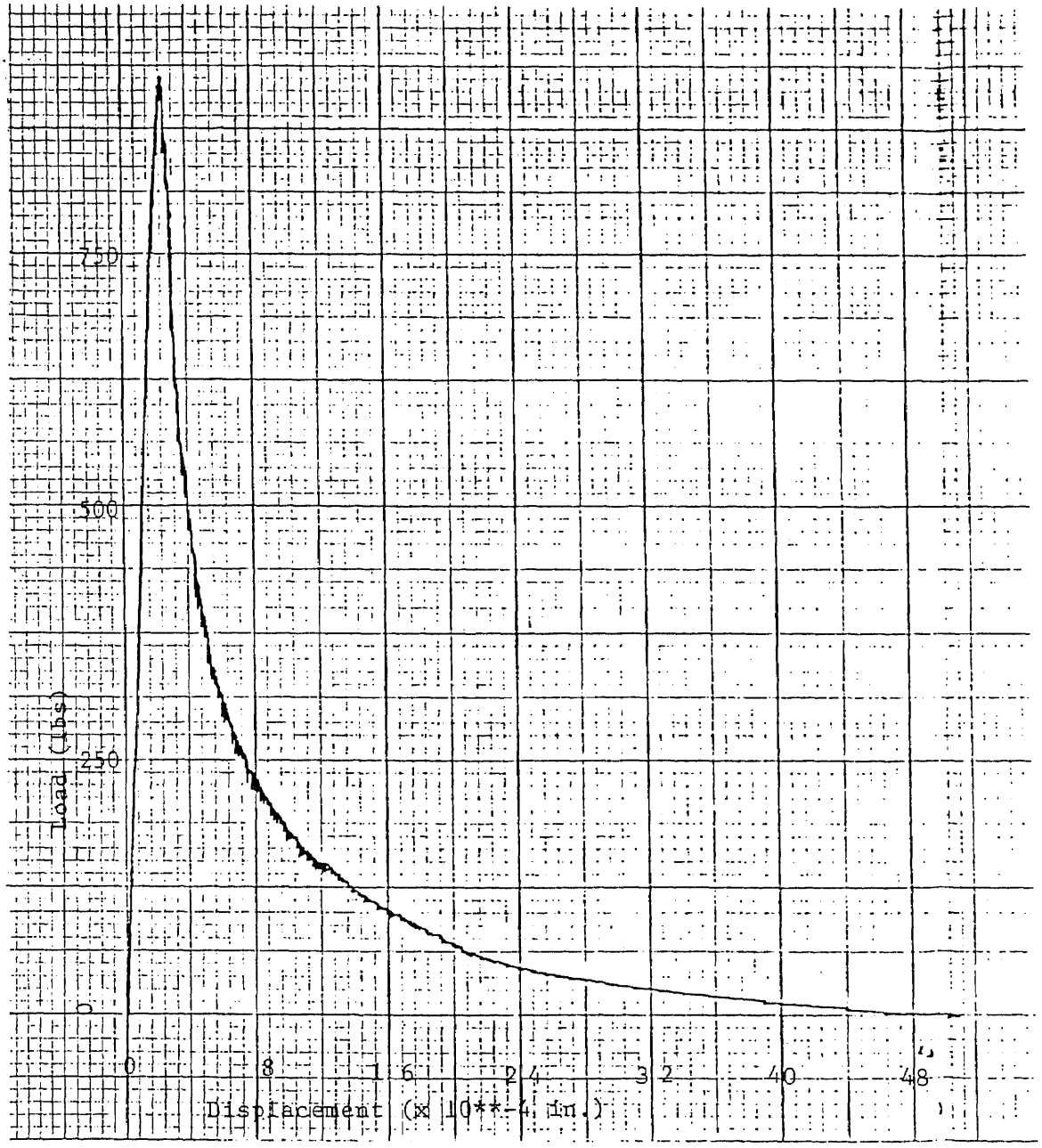

Figure 3.1: Load vs. Displacement

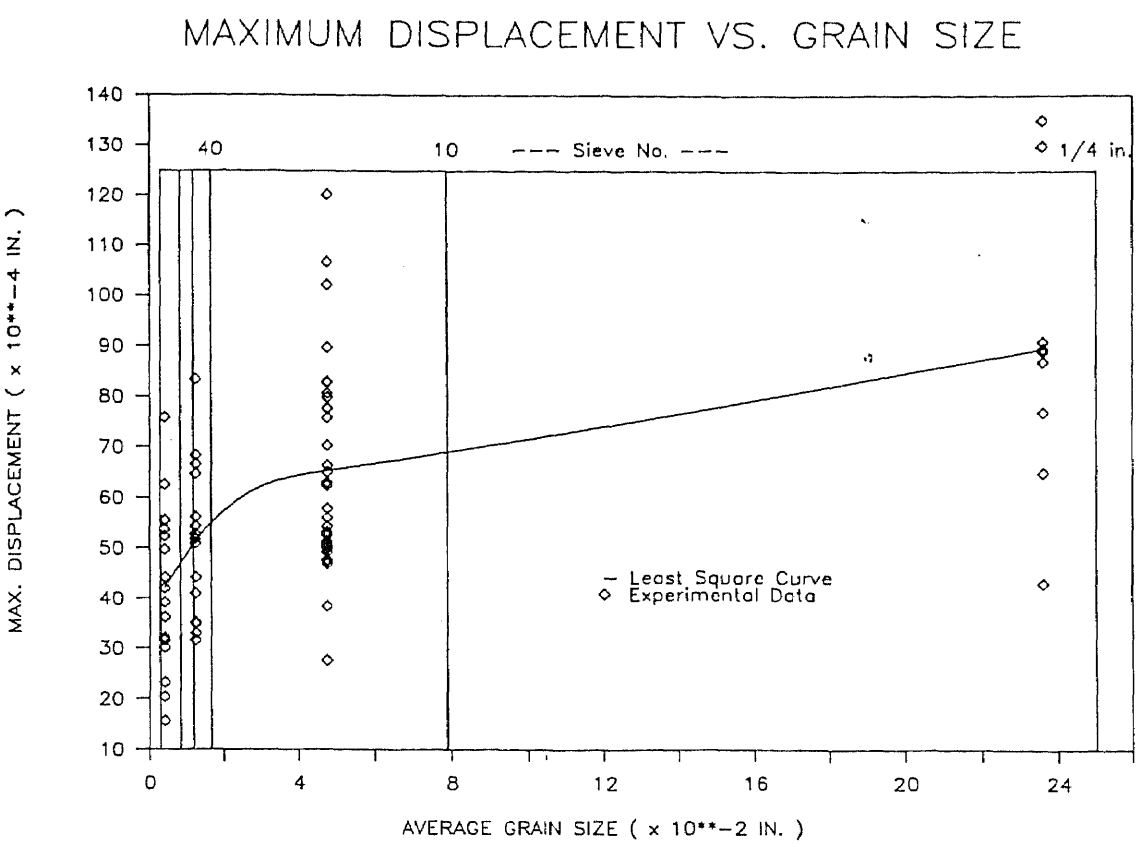

Figure 3.2: Relation of maximum displacement to grain size.

provide. This unsteadiness is reduced as the strain rate is increased. The tests were started with a rate of 0.1 $\mu strains$ per second, this slow rate was necessary to obtain the peak portion smoothly and without sudden rupture. The rate was then slowly increased up to 4 $\mu strains$ per second, otherwise the total time required to complete a test would have been over ten hours. These steps reduced the possible creep effects to a negligible amount.

One of the parameters observed was the relation of the maximum displacement to the grain size of the aggregate used. Figure 3.2 shows the results obtained and a least square fit of the general curve.

2. Normalized Load Displacement Relationship

It was anticipated that there would be a unique relation of the load versus the displacement for the material. However, due to the different mix proportions used and the varying strengths of the specimens, it became apparent that something had to be done to view the data from a better perspective. In order to facilitate the analysis, it was necessary to normalize the results

obtained. The load was normalized with respect to the peak load, and the displacement with respect to the maximum post-peak displacement (see Appendix B).

Many types of equations were tested in an attempt to fit the data obtained from the tests. But most of the formulas which had been proposed by other researchers consisted of only the post-peak portion [11], or two different equations, one for the ascending portion and another for the descending portion [4]. It was preferable to arrive at a single continuous equation for the entire response curve. One of the reasons being that having a discontinuity in the approximation of the softening behavior would create instabilities when applied to numerical analysis methods.

The first attempts at solving this problem consisted of making modifications to formulas presented in other papers. Various, and sometimes unlikely combinations were used to generate curves which were compared to the data being obtained from the tests. These efforts met with little success. A new formula would have to be developed, if a single homogeneous formula were to be used to represent the tensile behavour of concrete.

The following formula was developed.

$$\frac{\sigma}{\sigma_{max}} = \frac{A}{\left(\frac{\delta}{\delta_{max}}\right)}\left(1 - e^{-B\left(\frac{\delta}{\delta_{max}}\right)^C}\right)\left(1 - \frac{\delta}{\delta_{max}}\right)^D$$

where;

σ	=	tensile stress	A	=	0.075
σ_{max}	=	maximum tensile stress	B	=	400
δ	=	displacement	C	=	1.95
δ_{max}	=	maximum displacement	D	=	0.50

It has been found to provide a good fit for all of the data obtained in this investigation. In fact, the curve generated by this formula fits all of the data with the coefficients held constant. The curve was also applied to data from Gopalaratnam [4], Petersson [6], and Reinhardt [8] (as shown in Figure 3.4). Again the data matched the curve rather well, even though different sized specimens and different mixes were used.

Figures 3.3 and 3.4 clearly shows that the curve obtained from the formula recommended in this study closely matches the data from this study along with the results reported by other researchers. It should be pointed out that the specimens used in this study were all the same shape, and they were all tested in direct tension. However the specimens used by the other

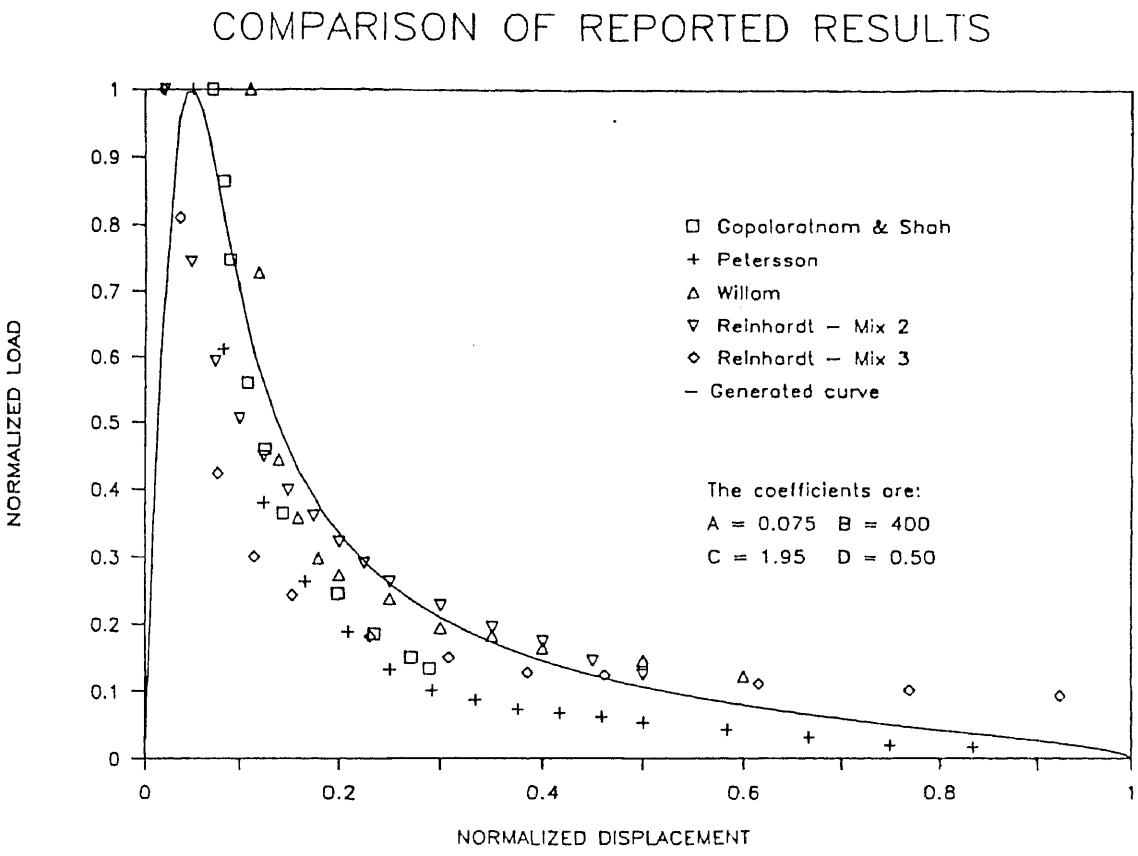

Figure 3.4: Comparison of formula with other reported results.

investigators vary in overall size and geometry. Furthermore, the testing methods which were used, differed from those applied to the present research. Even with these discrepancies, the generated curve correlates well to the results from the other studies.

The coefficients which were used do not necessarily have to be maintained at the reported value. They can be changed to make the curve steeper and narrower or vice versa.

3. Strain Distribution

As mentioned earlier, the strain being measured by the MTS represented the average strain across the specimen. Since some insight into the distribution of the strain across the notched portion was needed, it became necessary to attach strain gages across the cross section of the specimens. The data from these tests were compared to data from similar tests done by [1] and [2]. These tests were also needed to observe the nature of the crack opening. That is, whether a crack is initiated from both ends or from just one end of the specimen.

From Figure 3.5, it becomes apparent that the crack starts from one side of the specimen. The theory of a crack starting from both ends simultaneously has not been observed in any of the tests conducted. In fact, it would seem that the nature of the material would prohibit this phenomenon from occuring.

Figure 3.5 illustrates what was observed in virtually every test in which the cross sectional strain distribution was measured. For initial loading, the strain is basically distributed uniformly throughout the cross section of the specimen. However, as the loading increased, the strain reading on one end of the specimen would start to increase at a far greater rate than the rest of the specimen. This trend continued until failure occured.

When the analysis of the data began, there was speculation as to whether the test apparatus was inducing moment on the specimen, thus causing the crack to start from one end. Indeed, this was the motivation for monitoring the strain distribution, which was an expensive and laborious process. The results showed what was intuitively deduced earlier, that the crack always starts from one end of the notched specimen. They also seemed to dispel any notions of induced moment.

If moment was indeed introduced by some portion of the testing equipment, one would expect that one end of the specimen would always show

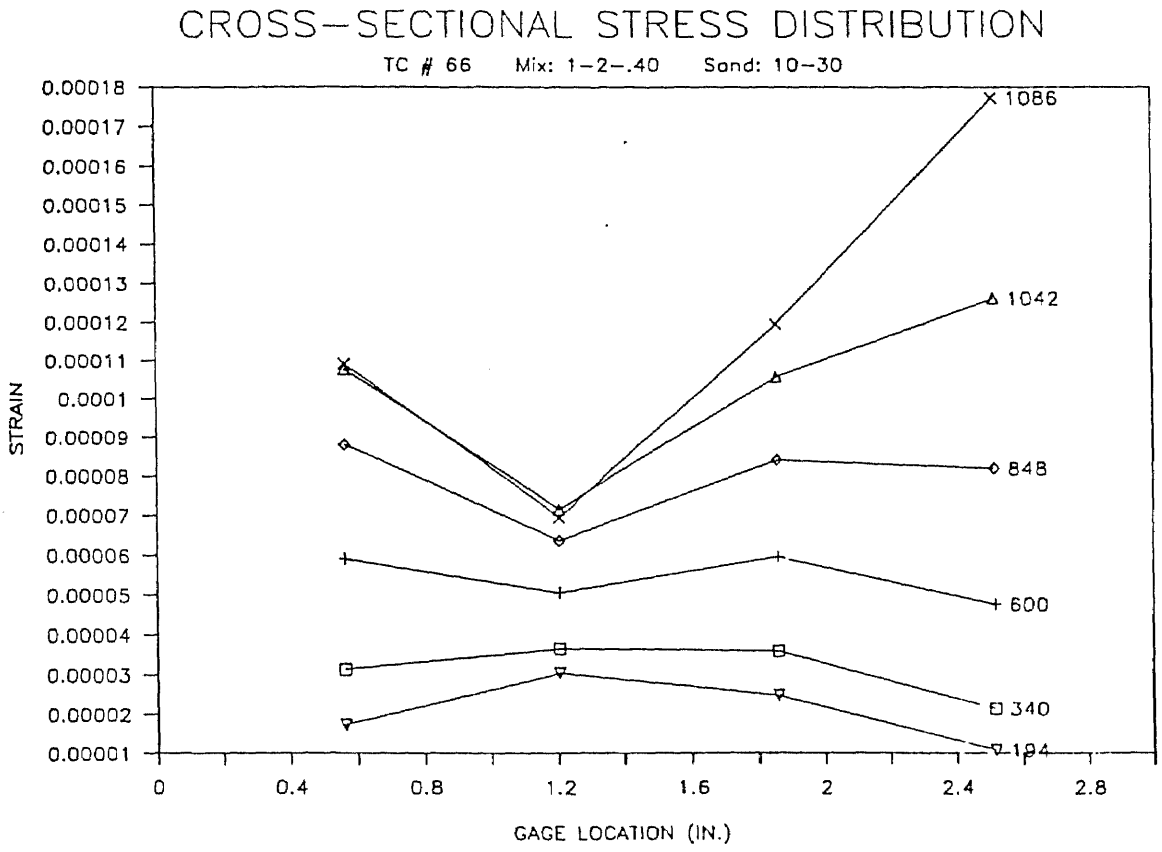

Figure 3.5: A typical strain distribution.

a marked increase in local strain. A pattern would become prevalent and obvious in the graphing of the results. One would expect that the graphs would show a distribution sloped to one side, a slope which would increase with increasing loads. There should be a consistency to the graphs, that is, once the graph begins to slope in a certain direction, it should continue in that direction. And finally, the crack would form at the end where the graph pointed to from almost the start of the test.

In fact, this did not happen. What was found was that the curves (see Figure 3.5) representing the strain distributions were fairly flat up to a third of the peak load. From then on, there would be a see-sawing effect until finally a crack formed on one side of the specimen. This see-sawing effect is used to describe the graphs of the strain distributions. First one end would show higher strain reading than the rest of the specimen, and then, as the load increased, the other end of the specimen would begin to give larger strain values. There was no apparent pattern as to which side would develop the crack, unlike what would be true if there was moment present in the system.

With the results showing that there was little chance of moment, questions may arise pertaining to the accuracy of the measurements. As a response to these possible questions, it may be beneficial to describe some of the methods used to measure the cross sectional strain.

The gages were the standard foil type (Micro-Measurements CEA-06-500UW-120) strain gages used extensively in applications involving concrete. The gages were connected to a multi-channel bridge completion circuit using high quality shielded cable. This was in turn, connected to CYBORG's ISAAC 2000 data acquisition system. This system provided the necessary signal amplification and internal noise suppression required to obtain readings from the strain gages. Shielding was used extensively throughout the setup, including inside the ISAAC itself. An average of five samples was taken for every reading. This was done to compensate for noise from various sources such as power supplies and generators. All switching was done automatically by the ISAAC system, thus eliminating another possible source for error (switch impedance, switching speed, etc). The entire system was calibrated according to a Vishay Strain Calibration Bar and a Vishay Strain Indicator which had a nominal accuracy of +/- one $\mu strains$. The ISAAC system was found to be comparable in accuracy.

The conclusions reached here are in stark contrast to those reached by some others who are doing research in this area. One paper [4] suggested that the crack is initiated from both sides of the specimen. There was

evidence provided in the form of strain distribution graphs which were used to support these conclusions. The distributions given were remarkably flat during the initial loading of the specimen. And as the loading continued to increase, the strain on both ends of the specimen increased equally. The data provided in these graphs were puzzling. In the paper it was mentioned that two LVDT's were positioned on either end of the specimen to provide a feedback signal to the loading apparatus. The reason given for using two LVDT's was as follows : *" If the feedback signal is monitored only using a single extensometer mounted across one of the two notches, then an unstable failure may result if the crack initiates at the opposite notch."* But if the strain was truly distributed throughout the specimen as was given in the graphs, there was no need for two LVDT's. According to the graphs, one LVDT placed at either end would have provided for a stable post peak response. The fact that this could not be done, suggests that perhaps the strain distributions would not be symmetrical.

In fact, the statement that the crack initiates from both ends of a notched specimen seemed to be disproved by the same logic used above. Since the tests could only be conducted with an averaged strain reading across the specimen, a symmetrical strain distribution seemed highly unlikely. And without a symmetrical strain distribution, it would be very difficult for a crack to form on both ends of a specimen.

4. Fracture Energy

The averaged fracture energies, G_f, (see Table III.1 page 10) for the different mixes tested are in close agreement with each other. The values ranged from 0.229 lb/in to 0.392 lb/in. However when these values are compared to those reported by other investigators (see Table III.2) it becomes clear that the fracture energy is size and mix dependent. This observation has been made earlier by other investigators [2].

5. Application of the Post-Peak Response

One of the applications of the observed tension softening is to provide a more accurate constitutive relationship for crack tip modelling. Many of the proposed models have used different assumptions for this crucial relationship, and therefore, lead to inaccurate predictions.

Table III.2: Fracture Energy.

Author	*Mix C:S:A:W*	*Type of Specimen*	*Fracture Energy (lb/in)*
Gopalaratnam and Shah [4]	1:2:2:0.45 1:2:2:0.60 1:2:0:0.50	Plate Tension	0.297 0.322 0.415
Reinhardt [8] [9]	1:3.38:0.50	Plate Tension	0.771
Chiou [2]	1:2:0:0.40 1:2:0:0.50 1:2:0:0.55 1:2:2:0.50	Dog Bone	0.287 0.223 0.216 0.385
Present Study	1:2:0:0.40 1:2:0:0.45 1:2:0:0.50 1:2:0:0.55	Tapered Specimen	0.331 0.312 0.295 0.357

ment method based on the fictitious crack model proposed by Hillerborg [5] was employed. Figure 3.6 shows the finite element mesh and boundary conditions used in this study. Three different constitutive laws, (i.e. stress-displacement relationship), proposed by Petersson [6], Reinhardt [8], and the present study were used to theoretically predict the responses of a notched beam. The general concept and details of the fictitious crack model is available in [6] and [8]. The results were then compared with the observed experimental data. It can be seen that the proposed formula provides good agreement of the predicted response when compared with the test results (see Figure 3.7. Reinhardt's formula gives a slightly higher value while Petersson's linear model shows a much larger error. These results indicate that the proposed tension softening is accurate and critical to fracture modelling of concrete.

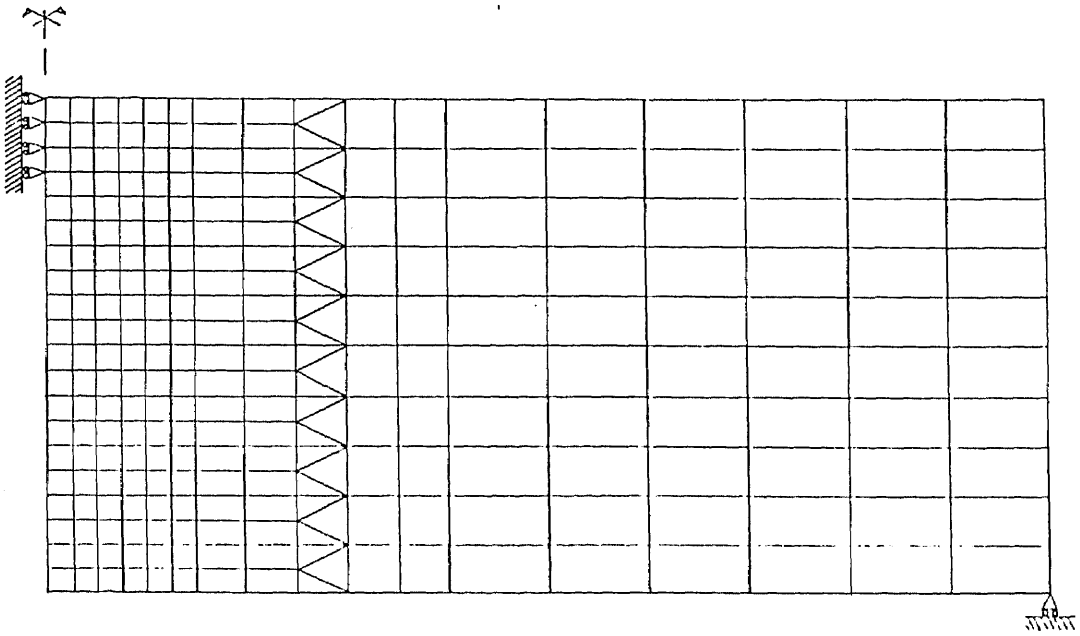

Figure 3.6: Finite element mesh for notched beam.

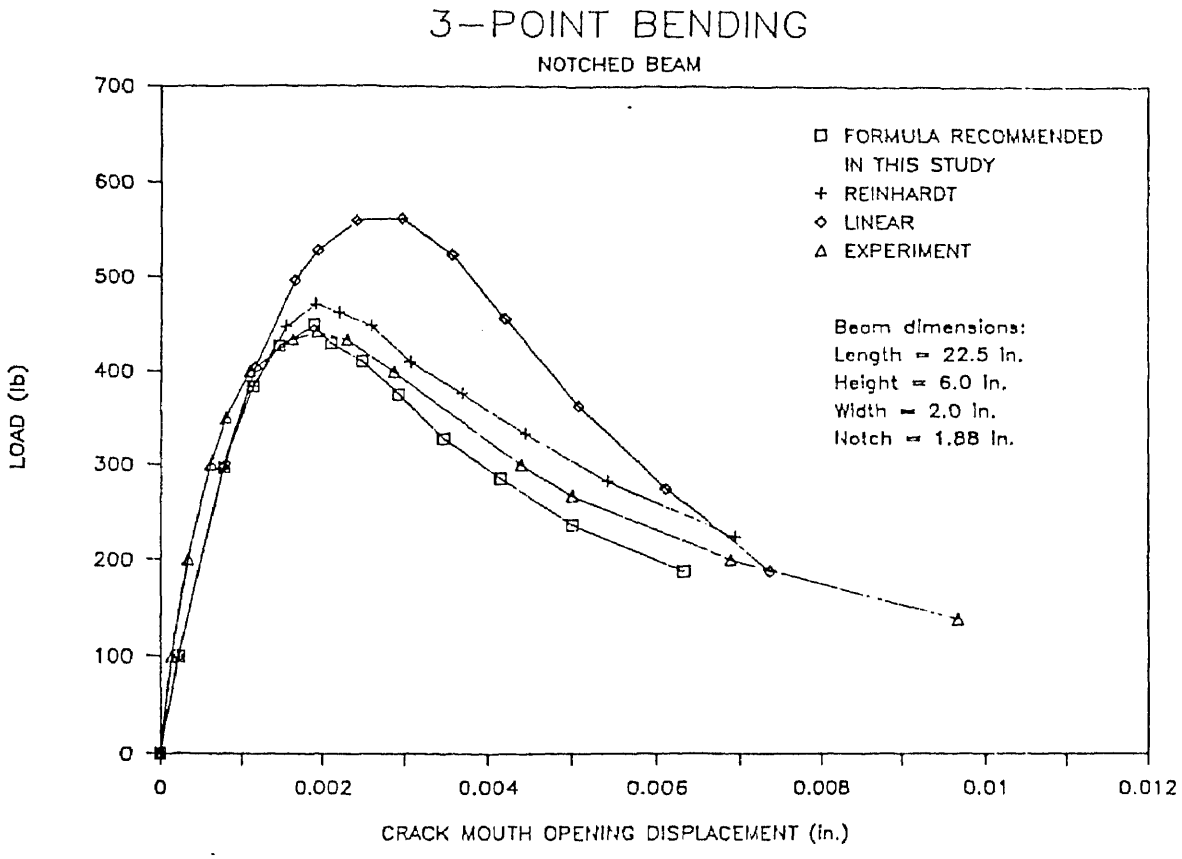

Figure 3.7: Finite Element Method application.

Chapter IV

CONCLUSION

This investigation yielded a large amount of data pertaining to the softening response of concrete in uniaxial tension. The data clearly shows that there is a exponentially decaying post-peak behavior, with a defined limit on displacement. This limit is reached when the tensile capacity of the material becomes zero. The point at which this occurs (i.e. the maximum strain) is related to the grain size of the aggregate. It was concluded from this study that the fracture energy is not a unique material property. It is dependent on the specimen shape and geometry. This agrees with the conclusion arrived at by Wen-Jinn Chiou [2].

The formula which was derived in this study is currently being used in a Fictitious Crack Model [7]. The above mentioned on-going research has proved this formula to be efficient and accurate when applied in Finite Element Methods. The results obtained with its use are concurrent with those obtained from other similar Crack Models (see Figure 3.7, and agree closely to the experimental results.

Finally, the author would like to suggest that further investigations of this behavior of the material be made taking into account the possible effects of geometry and size. The study should include specimens which are larger than those presented here. Also, various shapes should be used, such as rectangular, dog-bone, notched and unnotched, and so on. The results for these test should determine the relation of the coefficients in the recommended formula to the shape and size, if any exists.

Bibliography

[1] Bazant, Z. P. and Oh, B. H. 1983. *Crack Band Theory for Fracture of Concrete*, Materiaux et Constructions, Vol. 16, No.93, pp. 155–177.

[2] Chiou W. J. 1986. *Fracture Energy and Tensile Behavior of Concrete*, M.S. Thesis, New Jersey Institute of Technology.

[3] Evans, R. H., and Marathe, M. S. 1968. *Microcracking and Stress-Strain Curves for Concrete in Tension*, Materiaux et Constructions, No. 1, January-February, pp. 61–64.

[4] Gopalaratnam, V.S., and Shah, S.P. 1985. *Softening of Plain Concrete in Direct Tension*, ACI Journal, Vol. 82, No. 3, May–June.

[5] Hillerborg, A., Modeer, H., and Petersson, P. E. 1976. *Analysis of Crack Formation and Crack Growth in Concrete by Means of Fracture Mechanics and Finite Elements*, Cement and Concrete Research, Vol. 6, pp. 773–781.

[6] Petersson, P. E. 1981. *Crack Growth and Development of Fracture Zones in Plain Concrete and Similar Materials*, Report No. TVBM-1006, Lund Institute of Technology, Sweden.

[7] Ratanalert, S. (expected) 1988. , Doctoral Dissertation , New Jersey Institute of Technology.

[8] Reinhardt, H. W. 1985. *Crack Softening Zone in Plain Concrete under Static Loading*, Cement and Concrete Research, Vol. 15, pp. 42–52.

[9] Reinhardt, H. W., and Cornelissen, H. A. W. 1984. *Post-Peak Cyclic Behavior of Concrete in Uniaxial Tensile and Alternating Tensile and Compressive Loading*, Cement and Concrete Research, Vol. 14, pp. 263–270.

[10] Visalvanich, K., and Naaman, A. E. 1983. *Fracture Model for Fiber Reinforced Concrete*, ACI Journal, Vol. 80, No. 2, pp.128–138.

[11] Wecharatana, M. and Shah, S. P. 1983. *Predictions of Nonlinear Fracture Process Zone in Concrete*, Journal of Engineering Mechanics Division, ASCE, Vol. 109, No. EMD5, October, pp. 1231–1246.

[12] Willam, K. J., Bicanic, N., and Sture, S. 1984. *Constitutive and Computational Aspects of Strain Softening and Localization in Solids*, Presented at the ASME-WAM 1984 Symposium on Constitutive Equations, New Orleans, December 10–14.

APPENDIX A

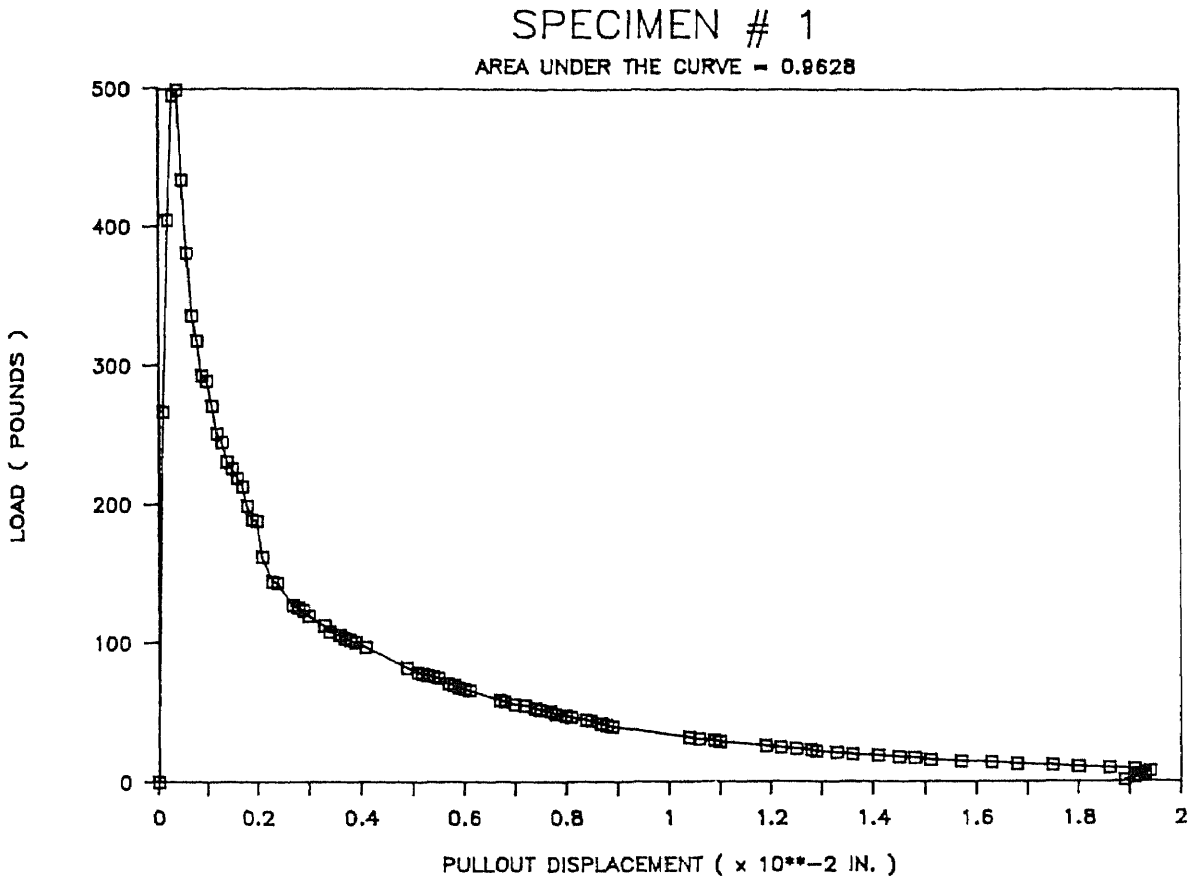
SPECIMEN # 1
AREA UNDER THE CURVE = 0.9628
LOAD (POUNDS)
500
400
300
200
100
0
0
0.2
0.4
0.6
0.8
1
1.2
1.4
1.6
1.8
2
PULLOUT DISPLACEMENT (x 10**-2 IN.)

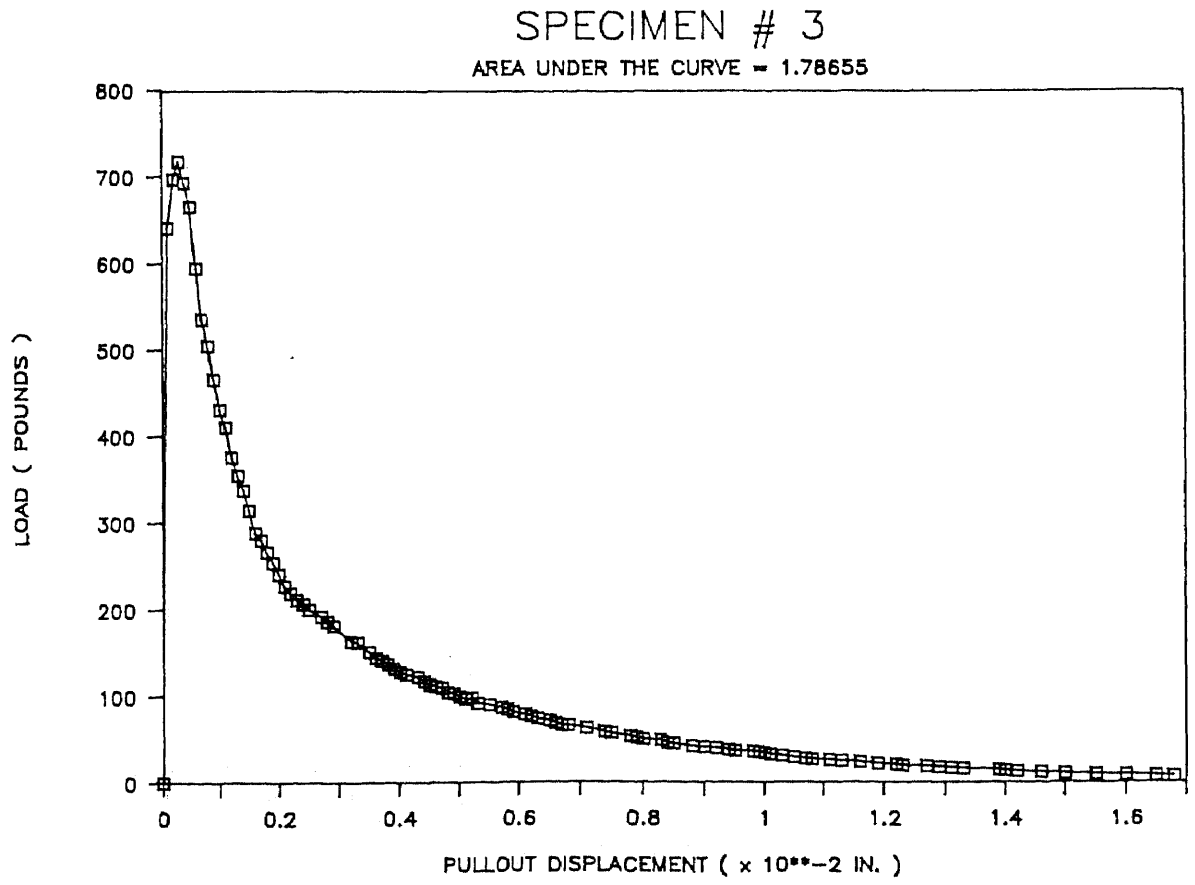
SPECIMEN # 3
AREA UNDER THE CURVE = 1.78655
LOAD (POUNDS)
800
700
600
500
400
300
200
100
0
0
0.2
0.4
0.6
0.8
1
1.2
1.4
1.6
PULLOUT DISPLACEMENT (x 10**-2 IN.)

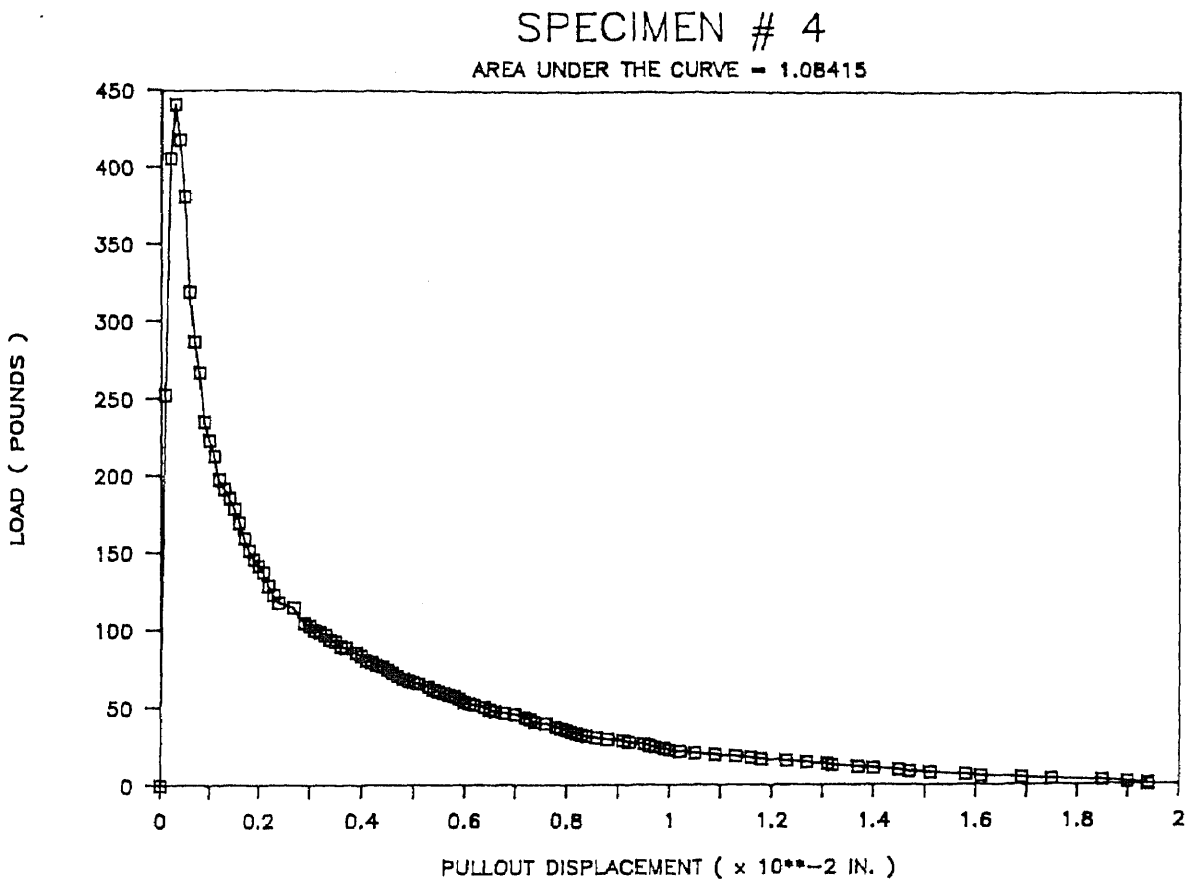
SPECIMEN # 4
AREA UNDER THE CURVE = 1.08415
LOAD (POUNDS)
450
400
350
300
250
200
150
100
50
0
0
0.2
0.4
0.6
0.8
1
1.2
1.4
1.6
1.8
2
PULLOUT DISPLACEMENT (x 10**-2 IN.)

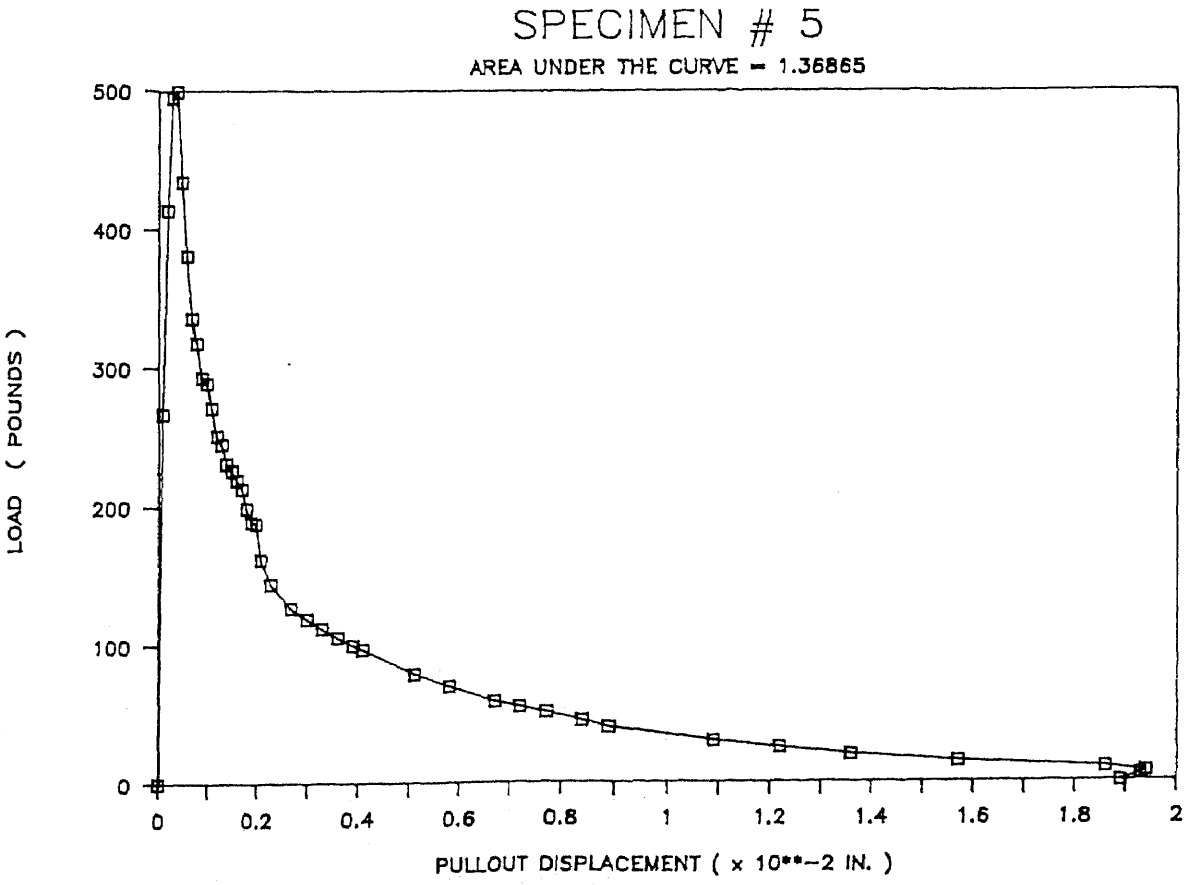
SPECIMEN # 5
AREA UNDER THE CURVE = 1.36865
LOAD (POUNDS)
500
400
300
200
100
0
0
0.2
0.4
0.6
0.8
1
1.2
1.4
1.6
1.8
2
PULLOUT DISPLACEMENT (x 10**-2 IN.)

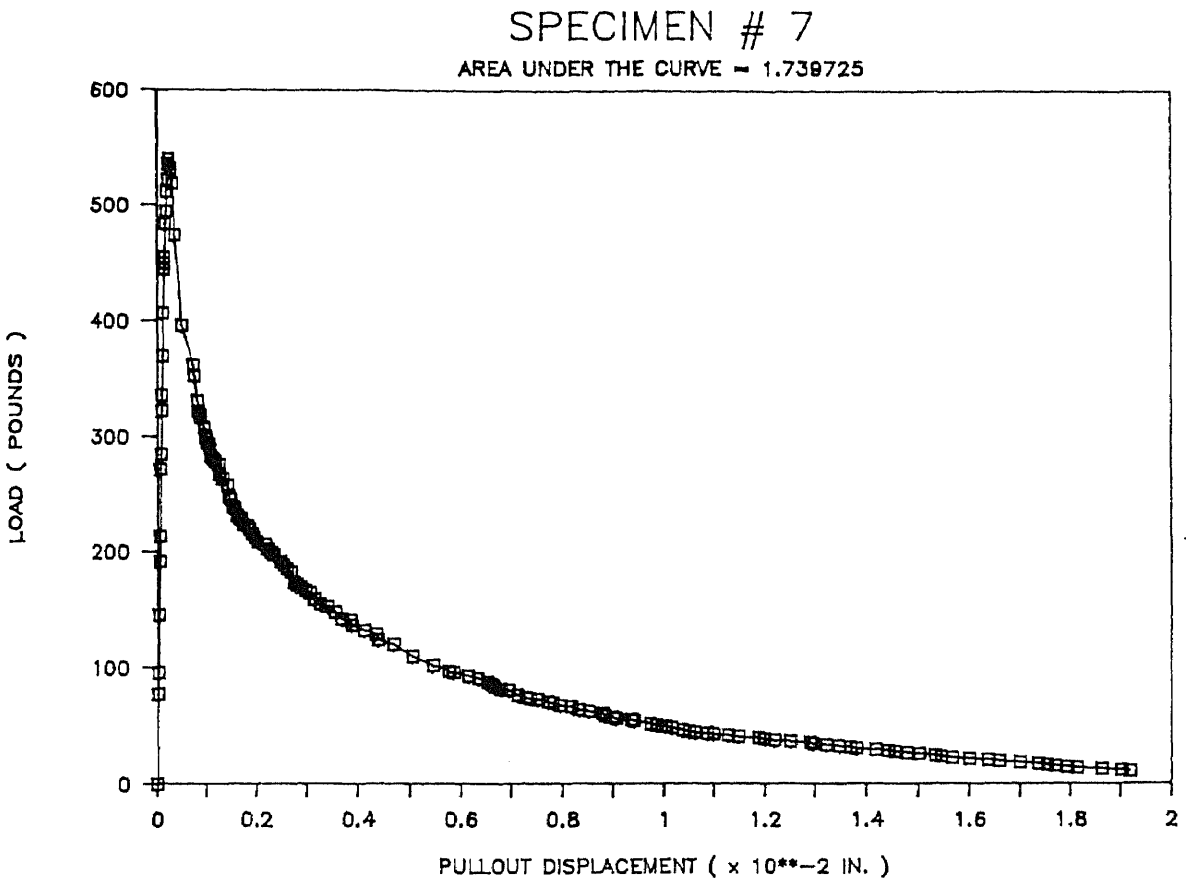
SPECIMEN # 7
AREA UNDER THE CURVE = 1.739725
LOAD (POUNDS)
600
500
400
300
200
100
0
0
0.2
0.4
0.6
0.8
1
1.2
1.4
1.6
1.8
2
PULLOUT DISPLACEMENT (x 10**-2 IN.)

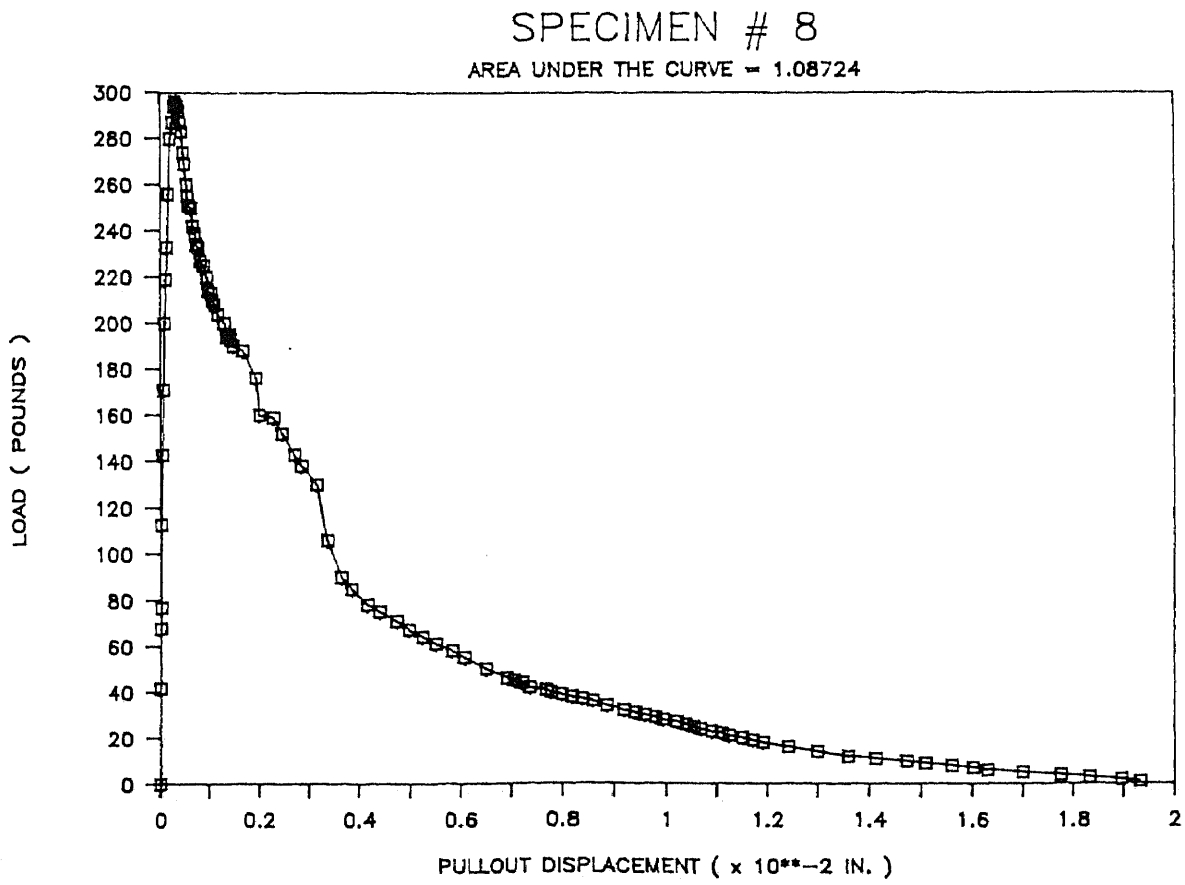
SPECIMEN # 8
AREA UNDER THE CURVE = 1.08724
LOAD (POUNDS)
300
280
260
240
220
200
180
160
140
120
100
80
60
40
20
0
0
0.2
0.4
0.6
0.8
1
1.2
1.4
1.6
1.8
2
PULLOUT DISPLACEMENT (x 10**-2 IN.)

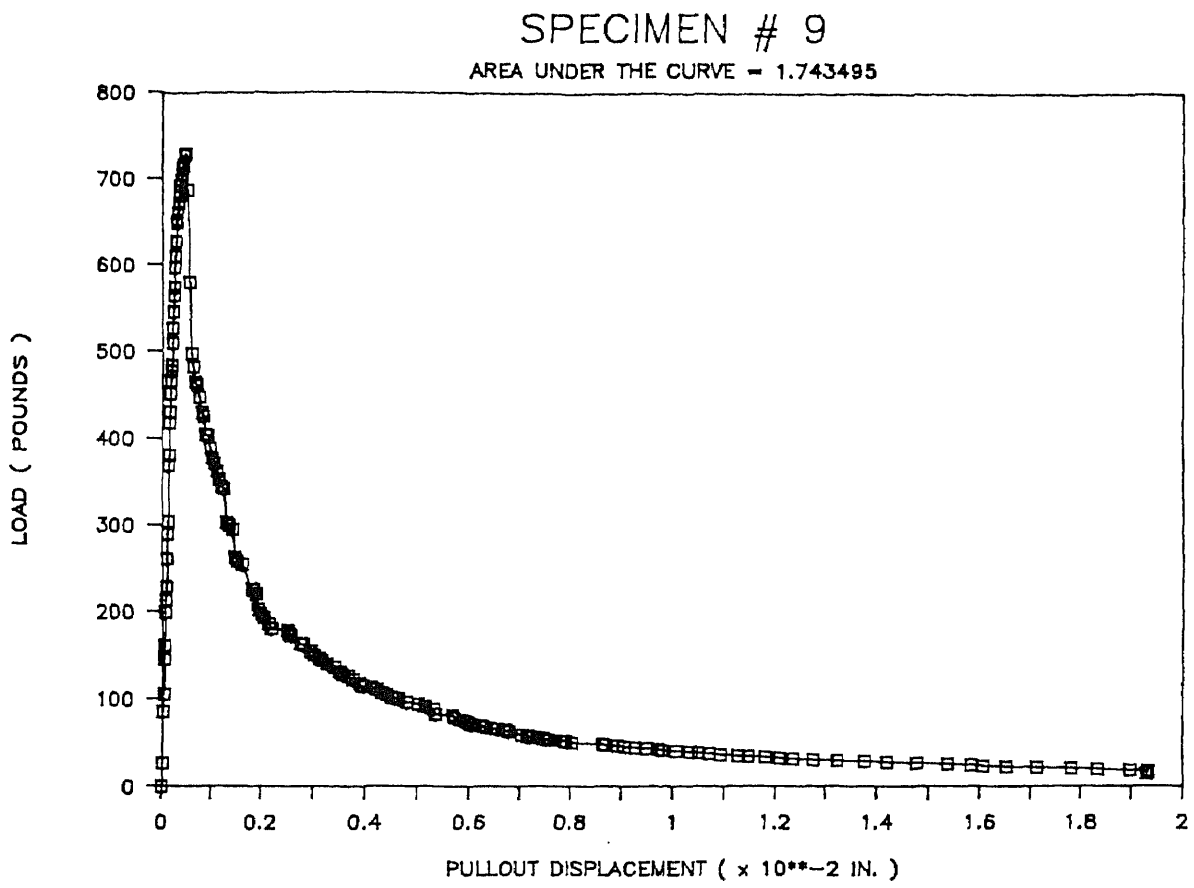
SPECIMEN # 9
AREA UNDER THE CURVE = 1.743495
LOAD (POUNDS)
800
700
600
500
400
300
200
100
0
0
0.2
0.4
0.6
0.8
1
1.2
1.4
1.6
1.8
2
PULLOUT DISPLACEMENT (x 10**-2 IN.)

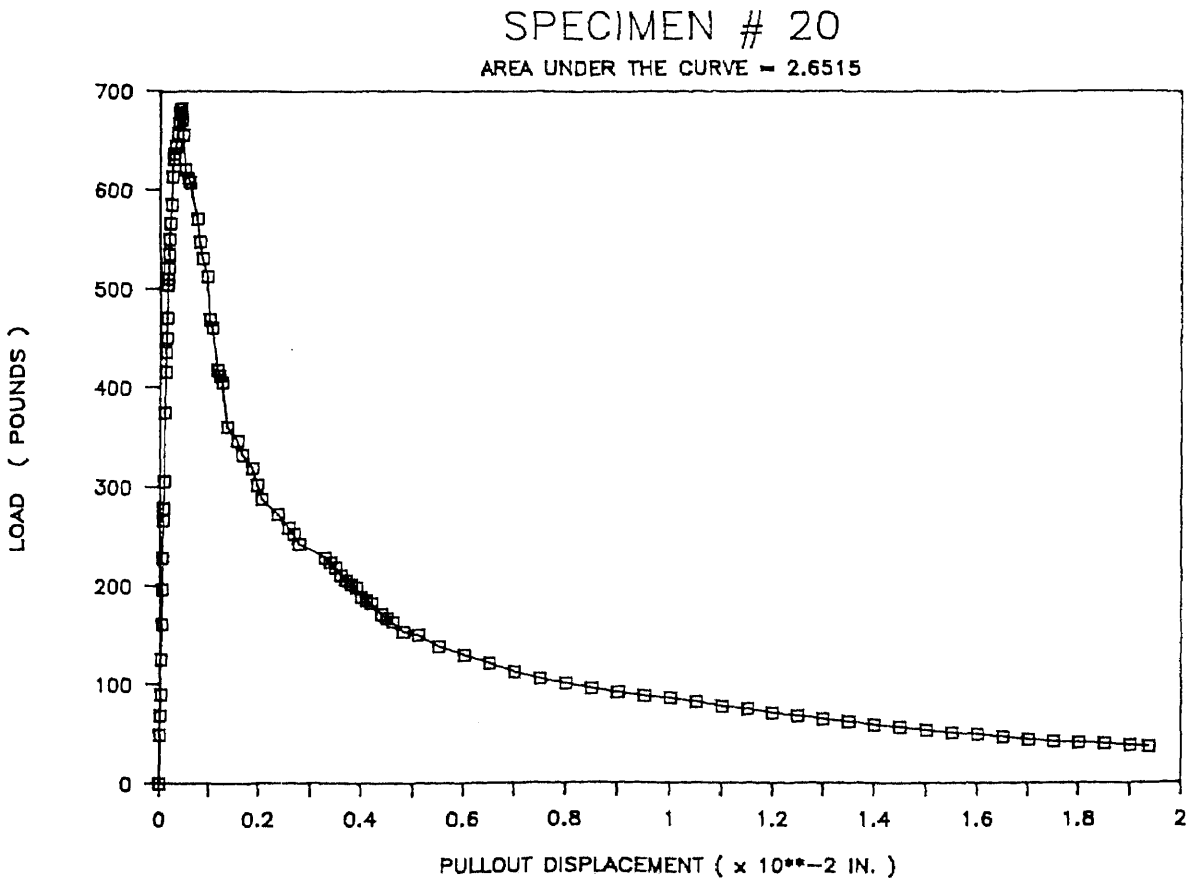
SPECIMEN # 20
AREA UNDER THE CURVE = 2.6515
LOAD (POUNDS)
700
600
500
400
300
200
100
0
0
0.2
0.4
0.6
0.8
1
1.2
1.4
1.6
1.8
2
PULLOUT DISPLACEMENT (x 10**-2 IN.)

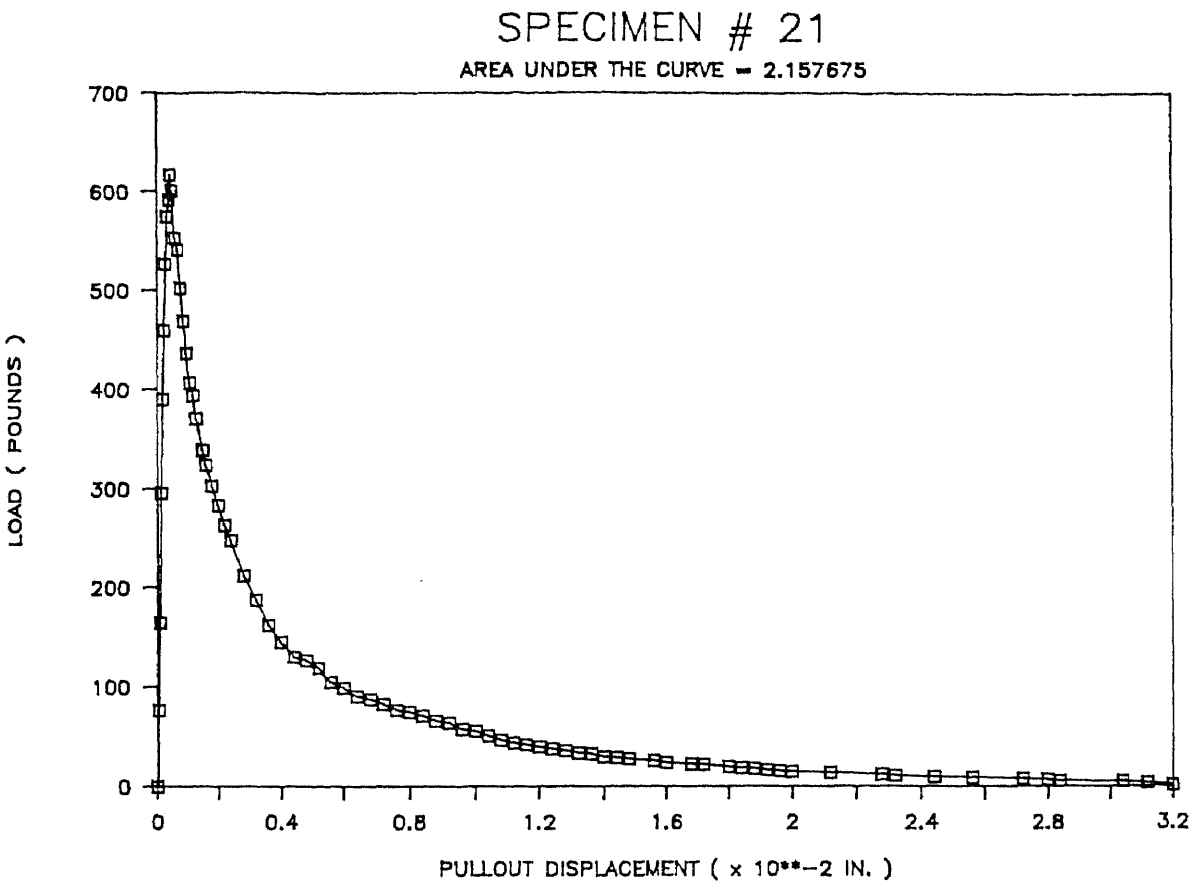
SPECIMEN # 21
AREA UNDER THE CURVE = 2.157675
LOAD (POUNDS)
700
600
500
400
300
200
100
0
0
0.4
0.8
1.2
1.6
2
2.4
2.8
3.2
PULLOUT DISPLACEMENT (x 10**-2 IN.)

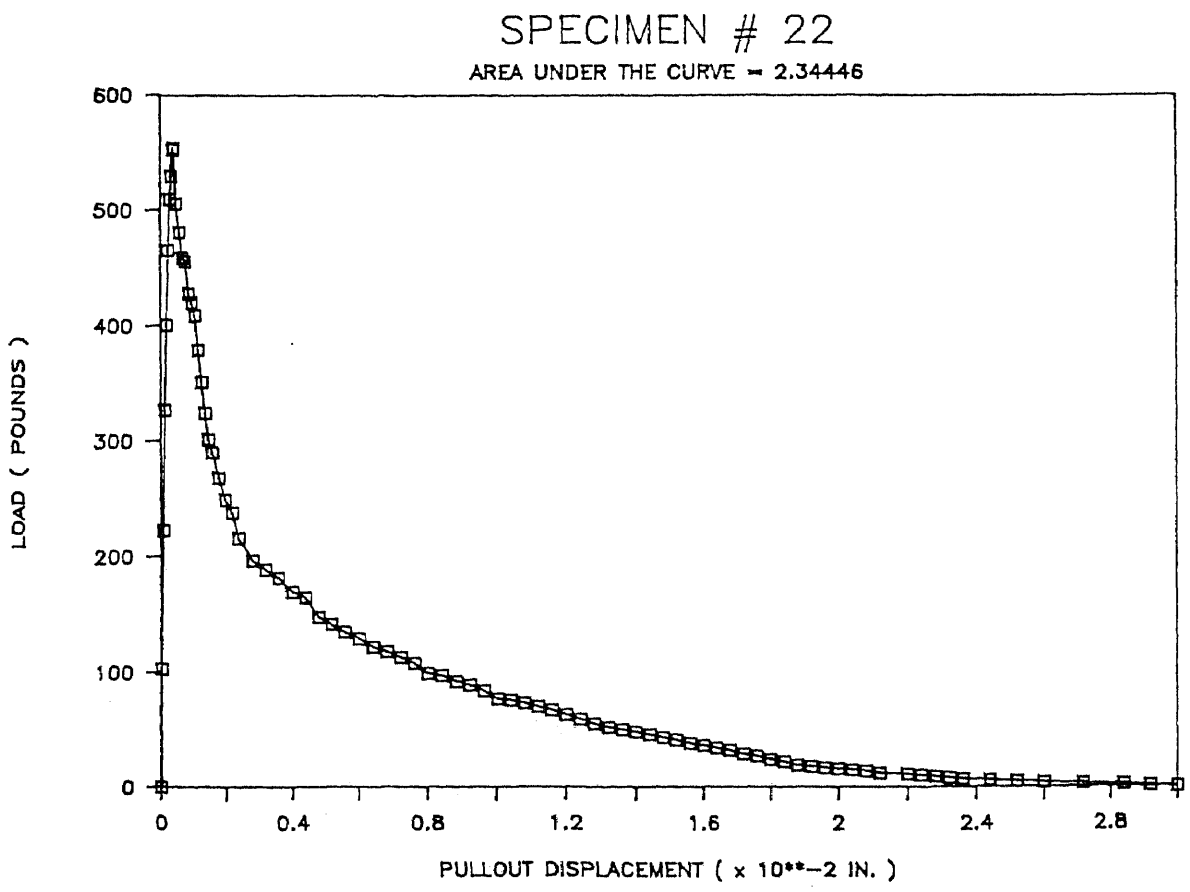
SPECIMEN # 22
AREA UNDER THE CURVE = 2.34446
LOAD (POUNDS)
600
500
400
300
200
100
0
0
0.4
0.8
1.2
1.6
2
2.4
2.8
PULLOUT DISPLACEMENT (x 10**-2 IN.)

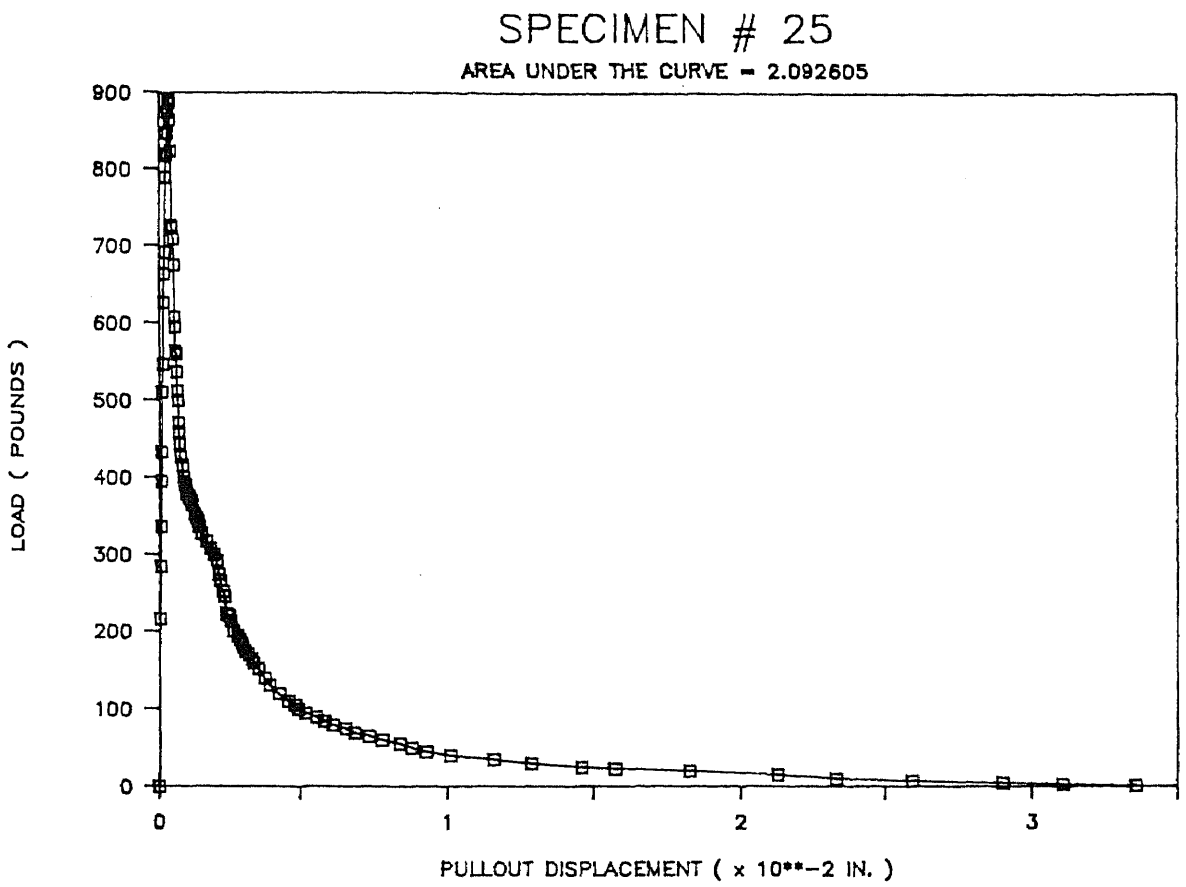
SPECIMEN # 25
AREA UNDER THE CURVE = 2.092605
LOAD (POUNDS)
900
800
700
600
500
400
300
200
100
0
0
1
2
3
PULLOUT DISPLACEMENT (x 10**-2 IN.)

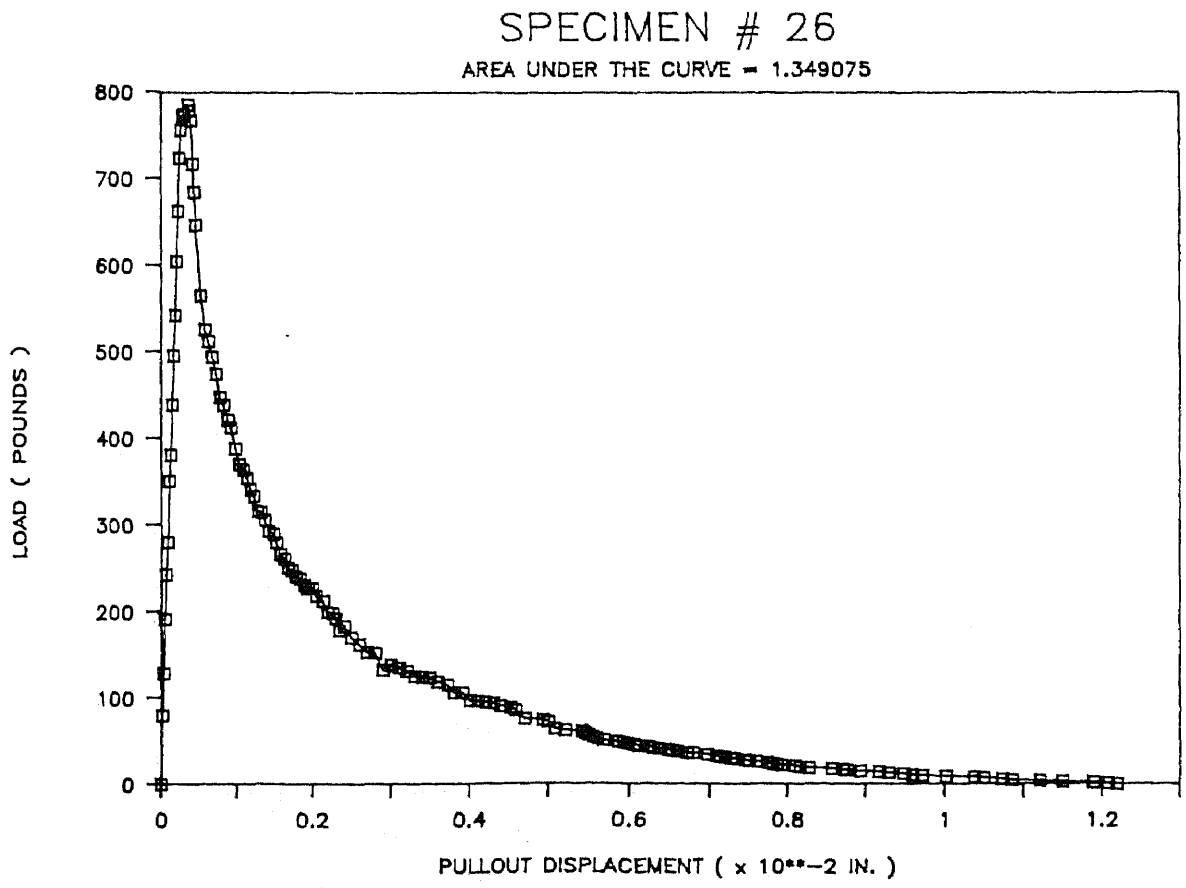
SPECIMEN # 26
AREA UNDER THE CURVE = 1.349075
LOAD (POUNDS)
800
700
600
500
400
300
200
100
0
0
0.2
0.4
0.6
0.8
1
1.2
PULLOUT DISPLACEMENT (x 10**-2 IN.)

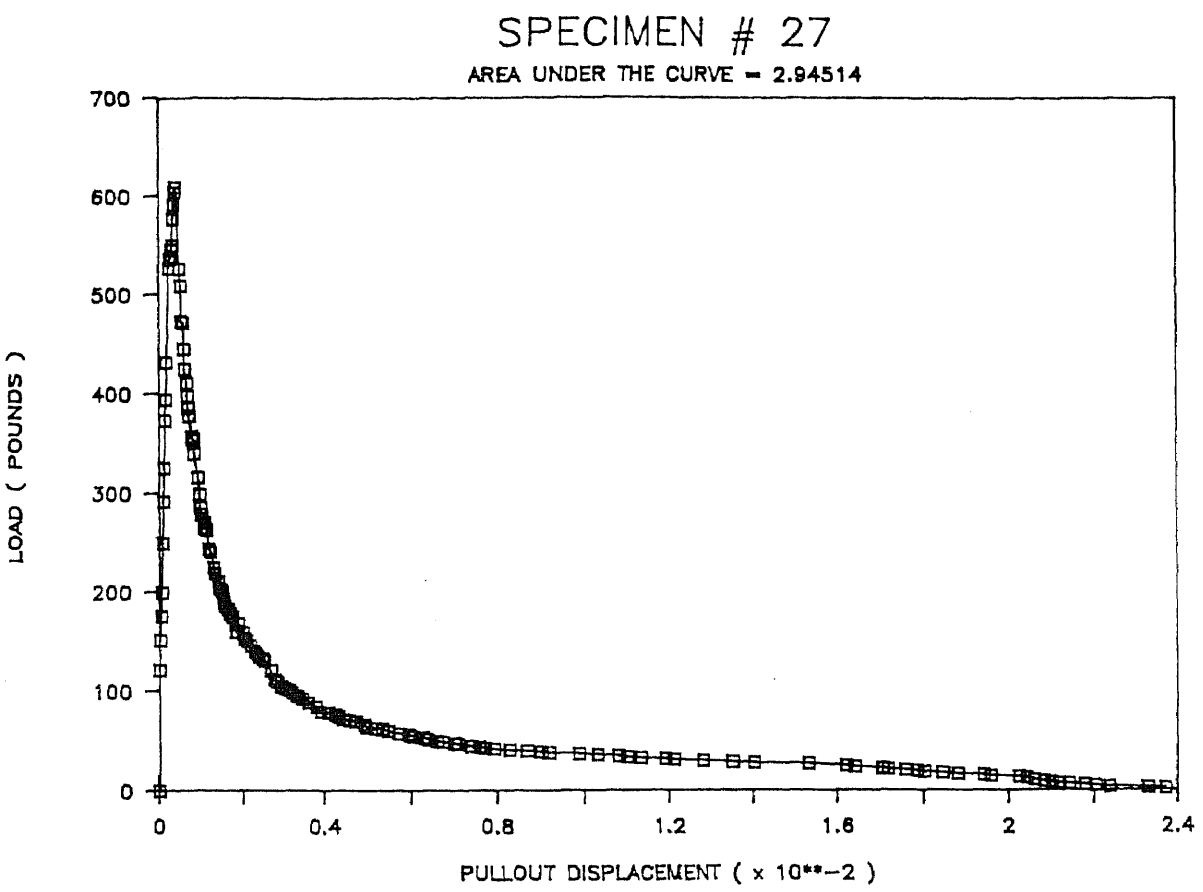
SPECIMEN # 27
AREA UNDER THE CURVE = 2.94514
LOAD (POUNDS)
700
600
500
400
300
200
100
0
0
0.4
0.8
1.2
1.6
2
2.4
PULLOUT DISPLACEMENT (x 10**-2)

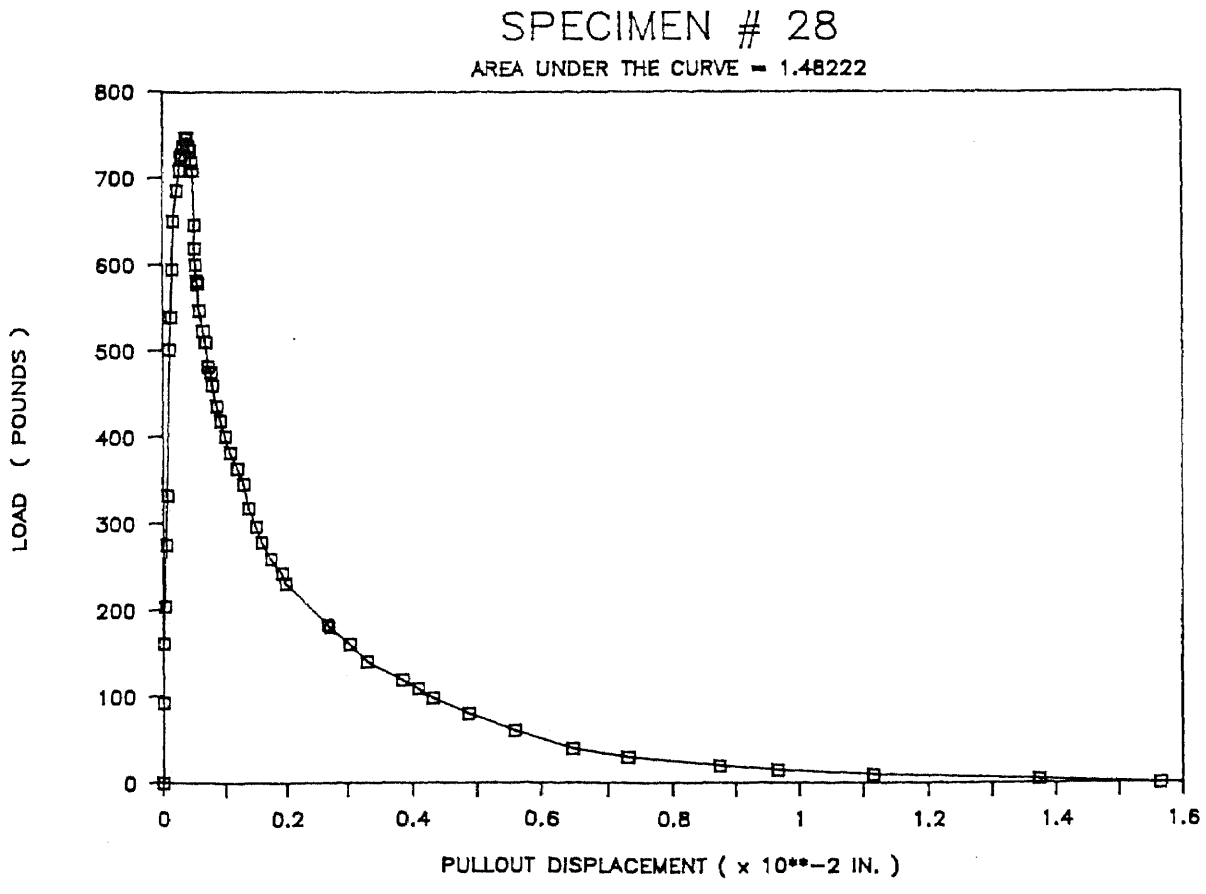
SPECIMEN # 28
AREA UNDER THE CURVE = 1.48222
LOAD (POUNDS)
800
700
600
500
400
300
200
100
0
0
0.2
0.4
0.6
0.8
1
1.2
1.4
1.6
PULLOUT DISPLACEMENT (x 10**-2 IN.)

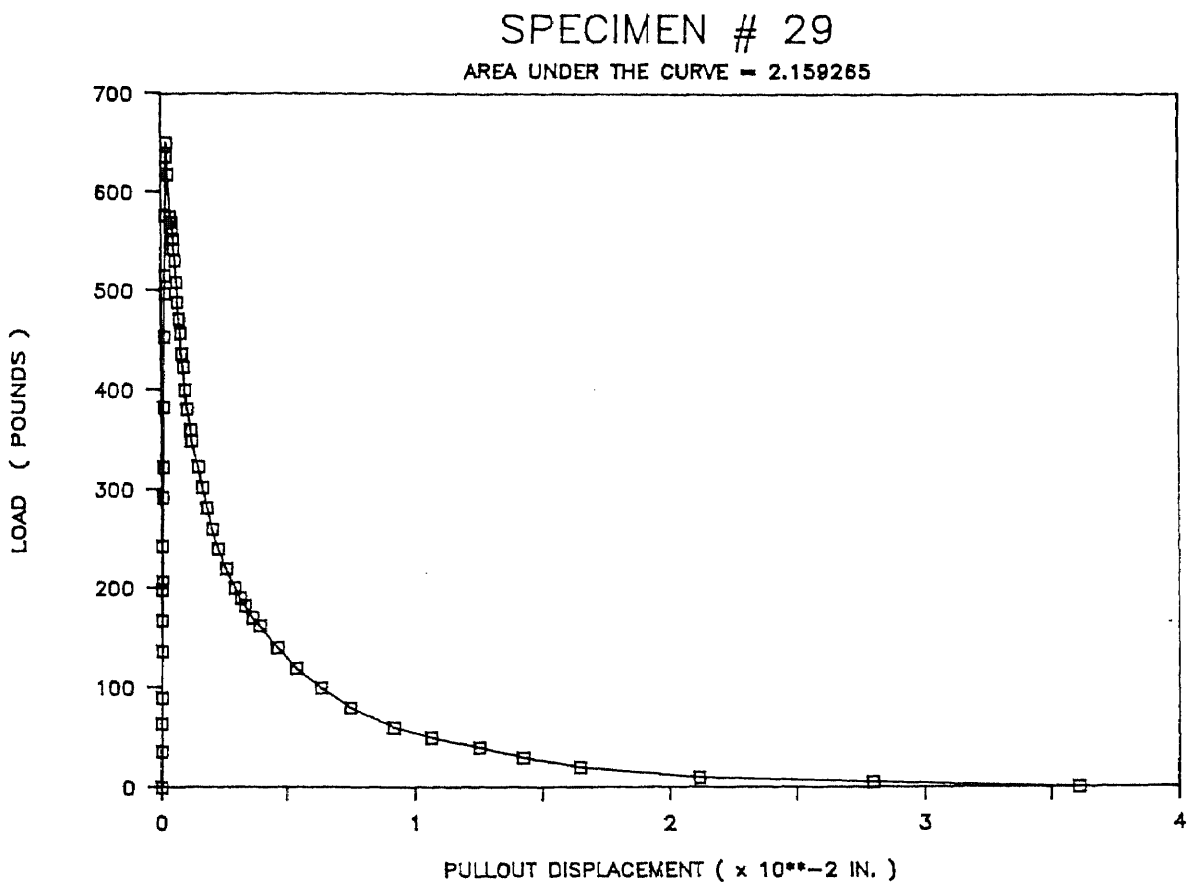
SPECIMEN # 29
AREA UNDER THE CURVE = 2.159265
LOAD (POUNDS)
700
600
500
400
300
200
100
0
0
1
2
3
4
PULLOUT DISPLACEMENT (x 10**-2 IN.)

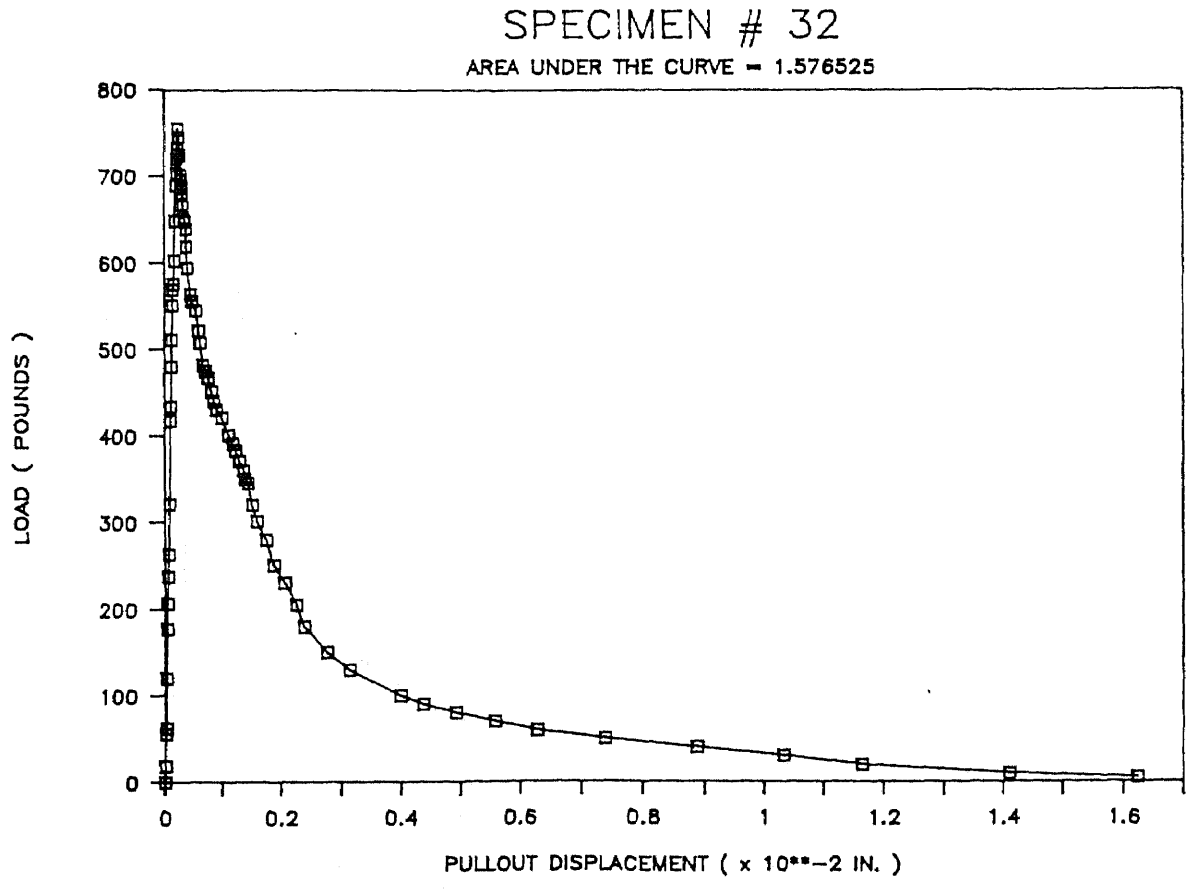
SPECIMEN # 32
AREA UNDER THE CURVE = 1.576525
LOAD (POUNDS)
800
700
600
500
400
300
200
100
0
0
0.2
0.4
0.6
0.8
1
1.2
1.4
1.6
PULLOUT DISPLACEMENT (x 10**-2 IN.)

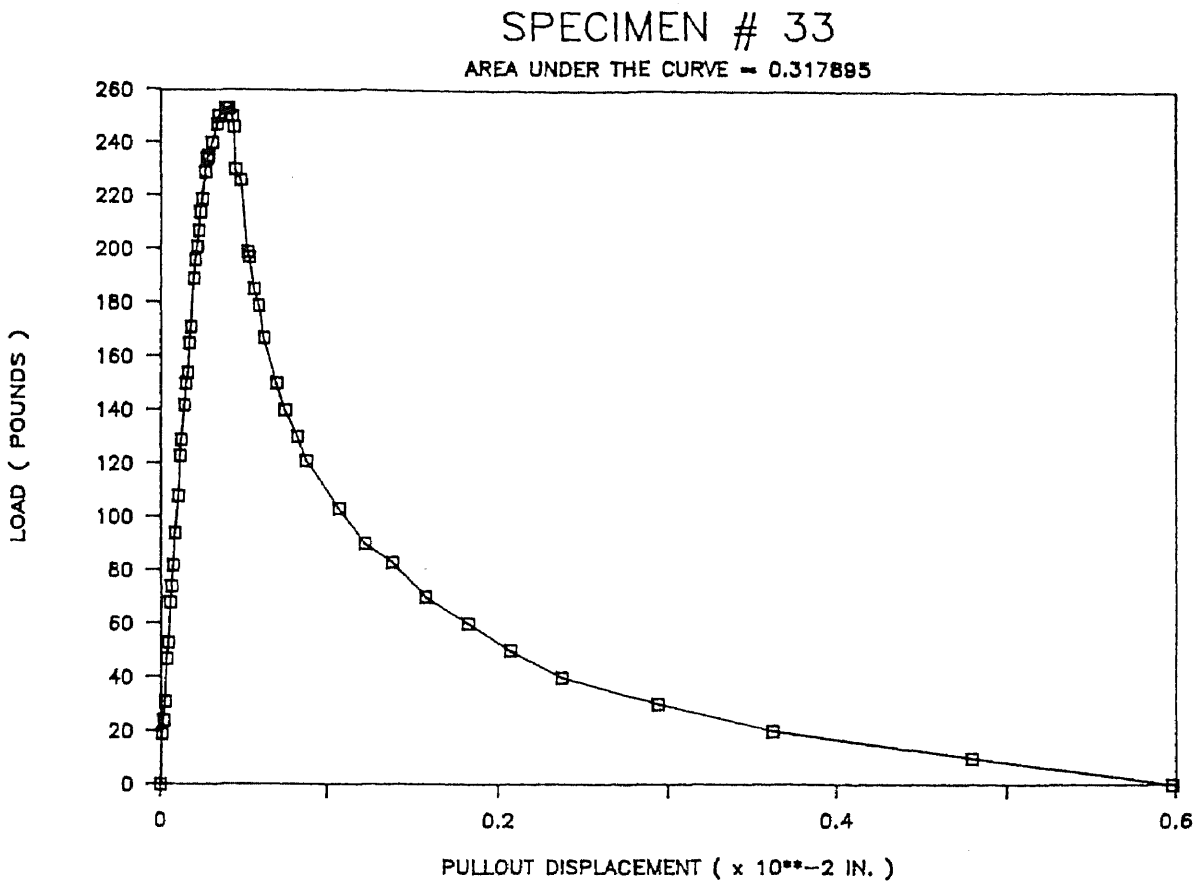
SPECIMEN # 33
AREA UNDER THE CURVE = 0.317895
LOAD (POUNDS)
260
240
220
200
180
160
140
120
100
80
60
40
20
0
0
0.2
0.4
0.6
PULLOUT DISPLACEMENT (x 10**-2 IN.)

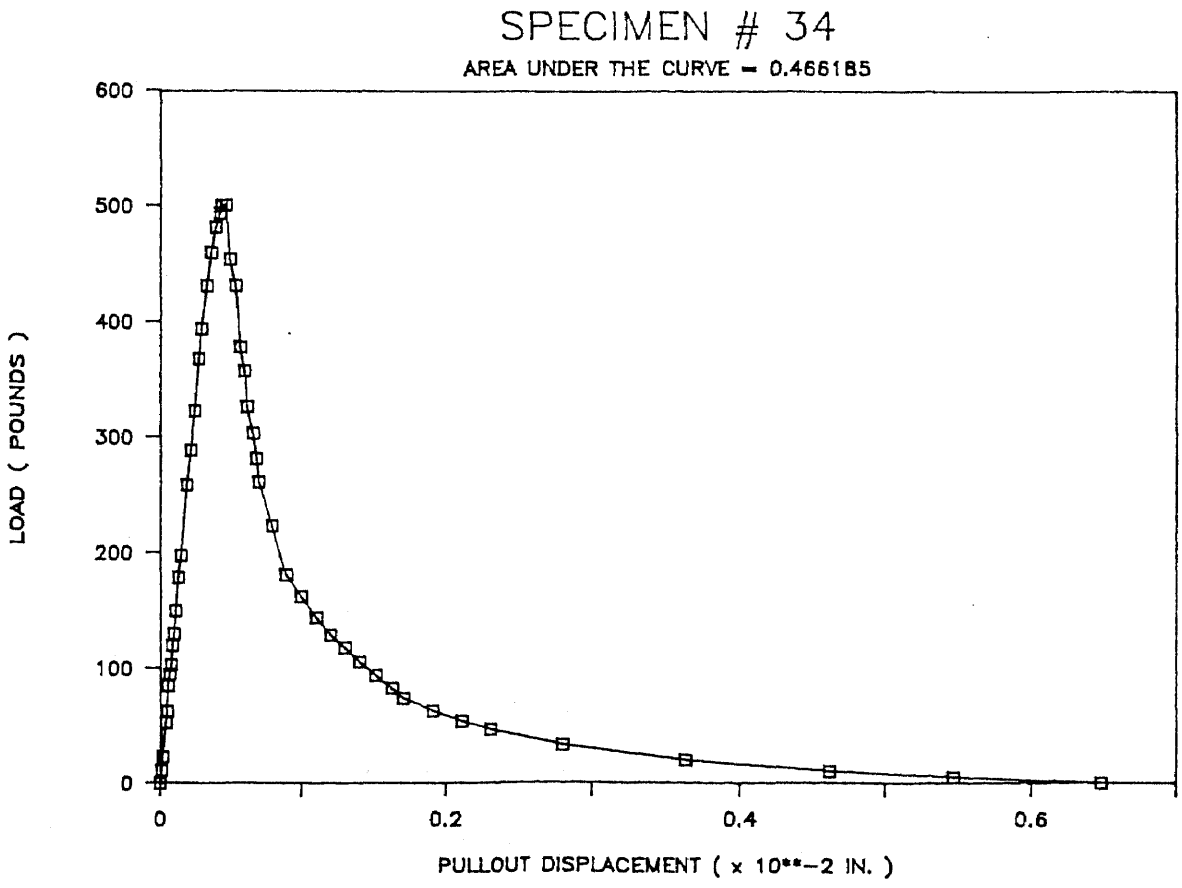
SPECIMEN # 34
AREA UNDER THE CURVE = 0.466185
LOAD (POUNDS)
600
500
400
300
200
100
0
0
0.2
0.4
0.6
PULLOUT DISPLACEMENT (x 10**-2 IN.)

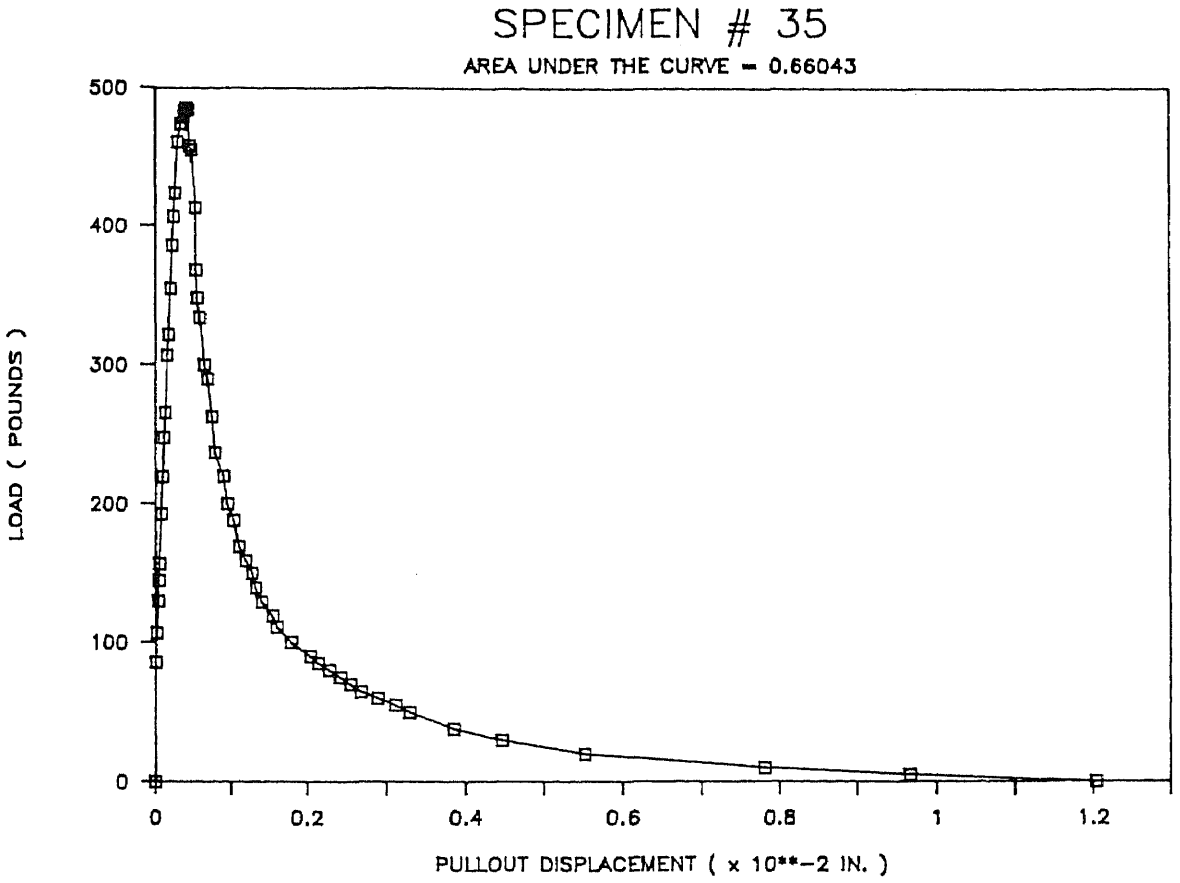
SPECIMEN # 35
AREA UNDER THE CURVE = 0.66043
LOAD (POUNDS)
500
400
300
200
100
0
0
0.2
0.4
0.6
0.8
1
1.2
PULLOUT DISPLACEMENT (x 10**-2 IN.)

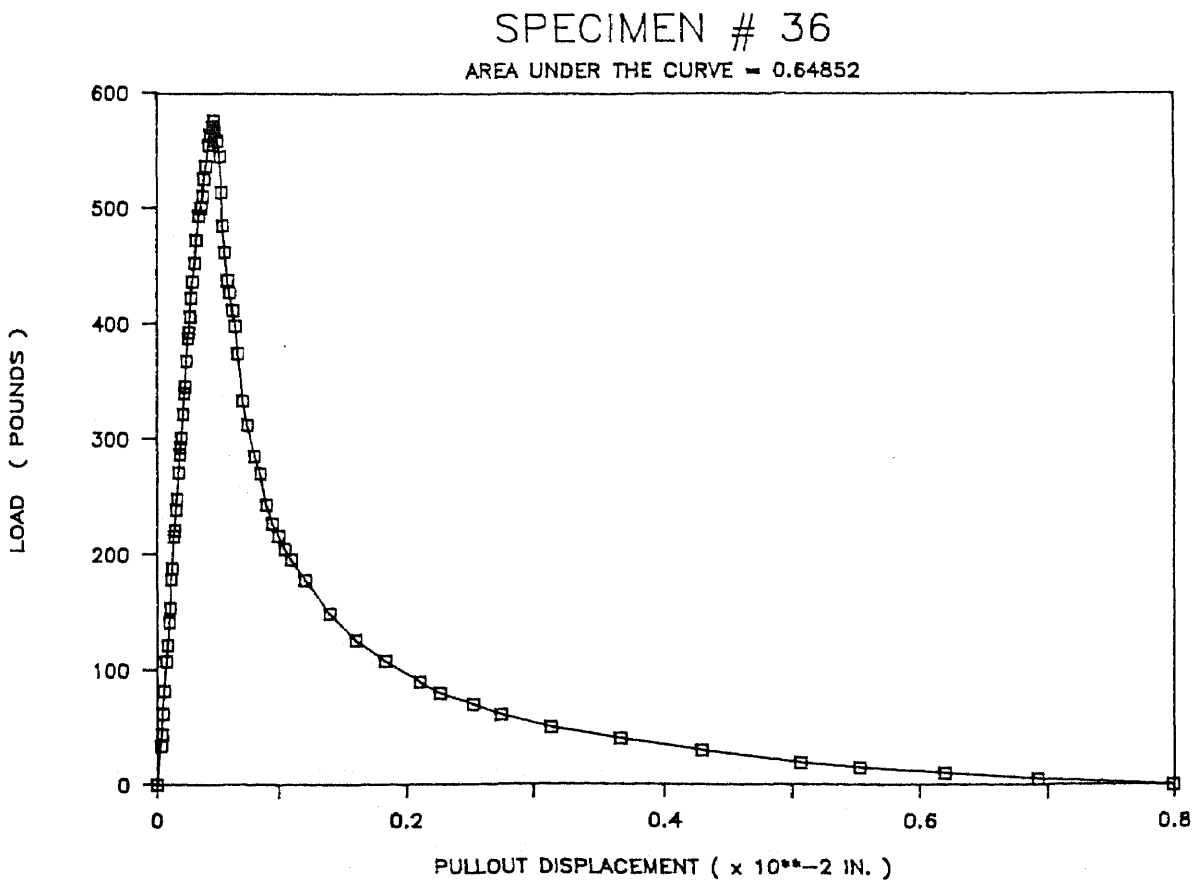
SPECIMEN # 36
AREA UNDER THE CURVE = 0.64852
LOAD (POUNDS)
600
500
400
300
200
100
0
0
0.2
0.4
0.6
0.8
PULLOUT DISPLACEMENT (x 10**-2 IN.)

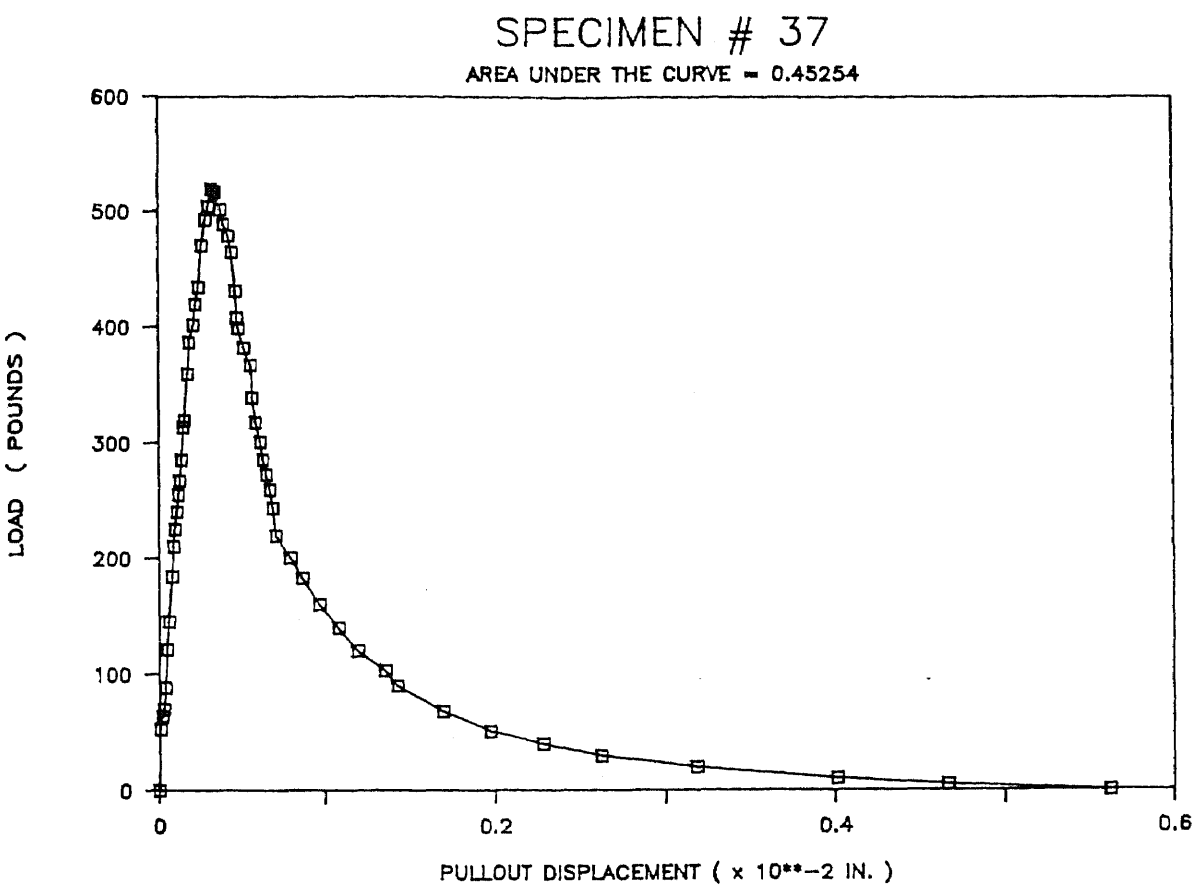
SPECIMEN # 37
AREA UNDER THE CURVE = 0.45254
LOAD (POUNDS)
600
500
400
300
200
100
0
0
0.2
0.4
0.6
PULLOUT DISPLACEMENT (x 10**-2 IN.)

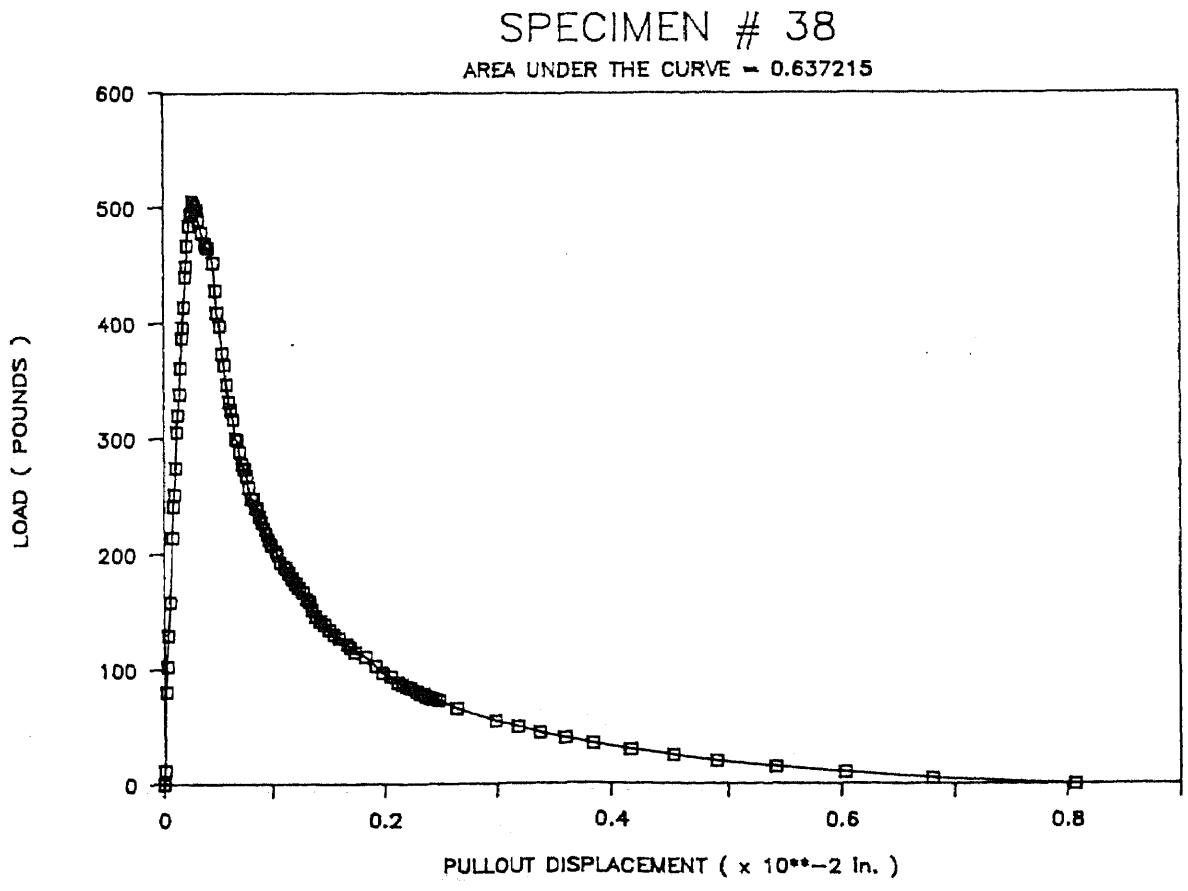
SPECIMEN # 38
AREA UNDER THE CURVE = 0.637215
LOAD (POUNDS)
600
500
400
300
200
100
0
0
0.2
0.4
0.6
0.8
PULLOUT DISPLACEMENT (x 10**-2 In.)

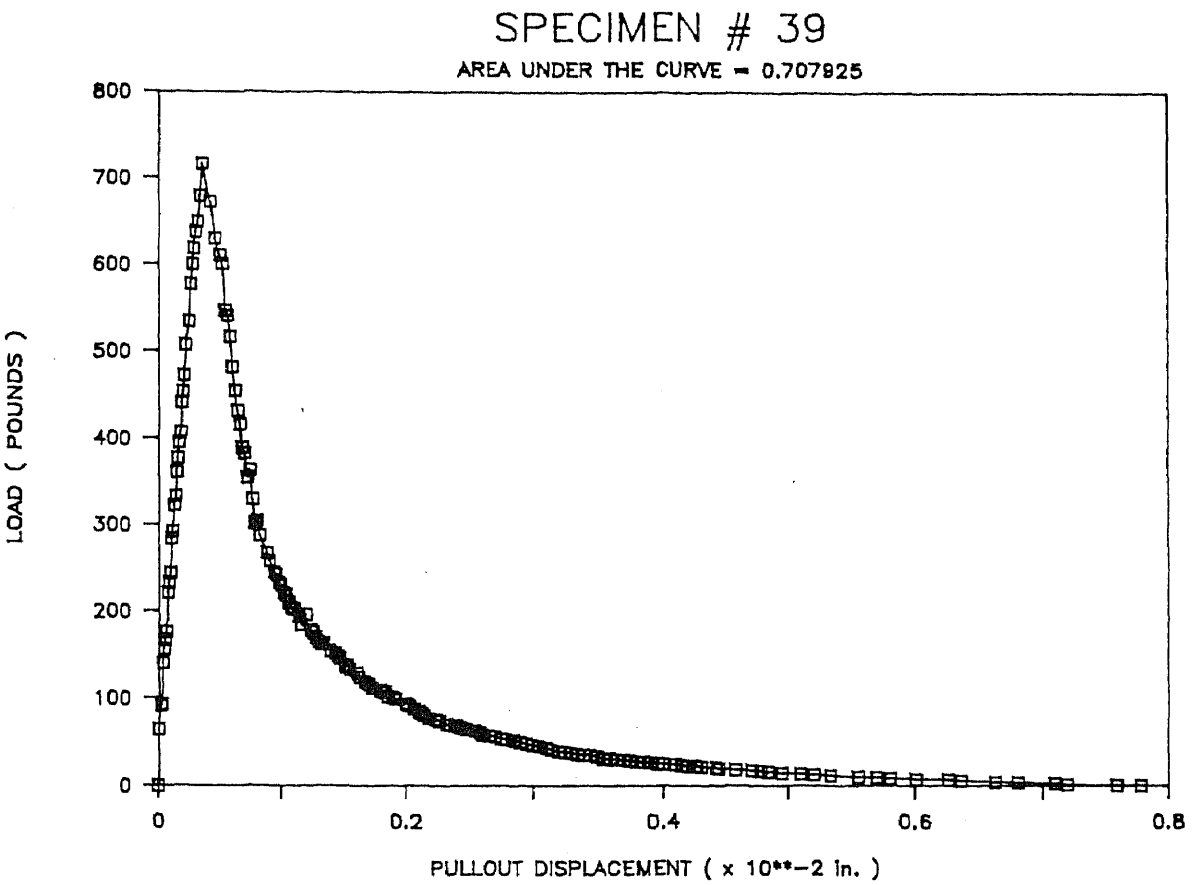
SPECIMEN # 39
AREA UNDER THE CURVE = 0.707825
LOAD (POUNDS)
800
700
600
500
400
300
200
100
0
0
0.2
0.4
0.6
0.8
PULLOUT DISPLACEMENT (x 10**-2 in.)

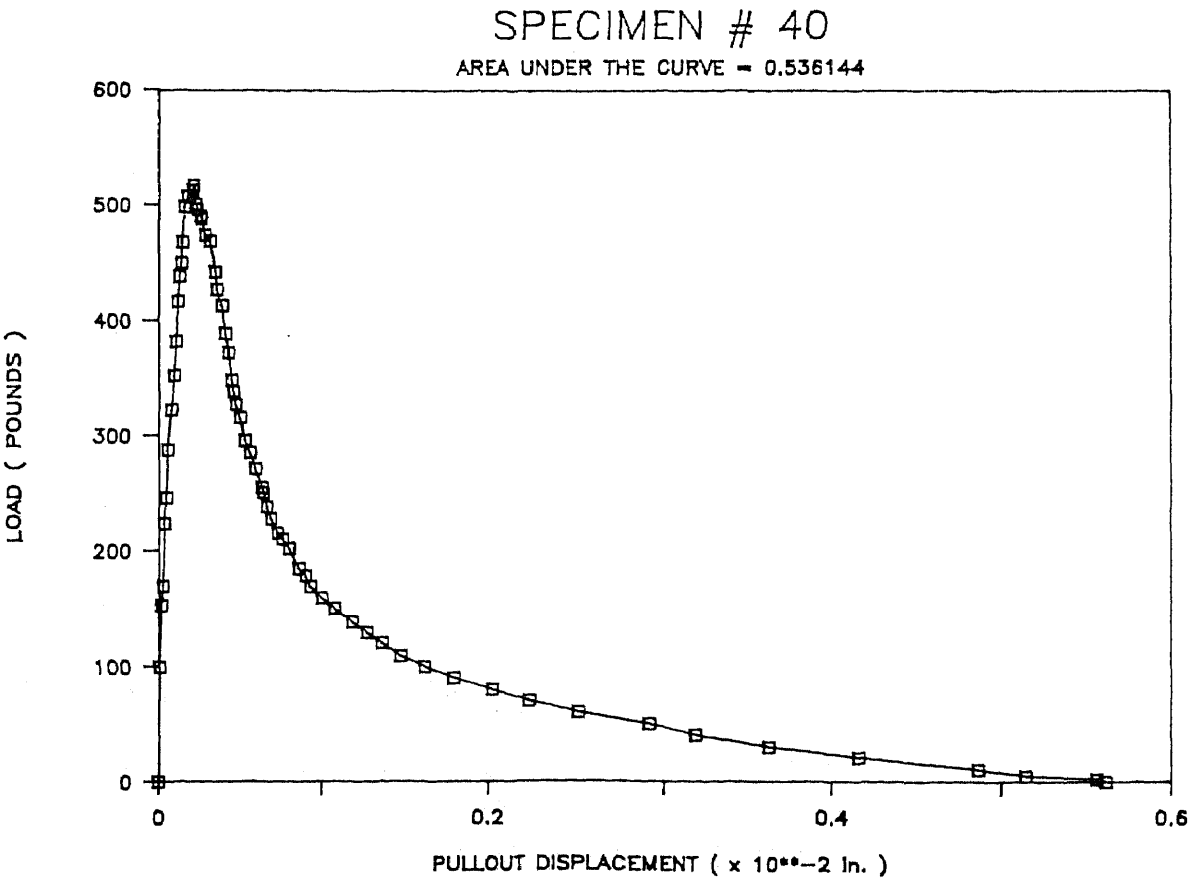
SPECIMEN # 40
AREA UNDER THE CURVE = 0.536144
LOAD (POUNDS)
600
500
400
300
200
100
0
0
0.2
0.4
0.6
PULLOUT DISPLACEMENT (x 10**-2 in.)

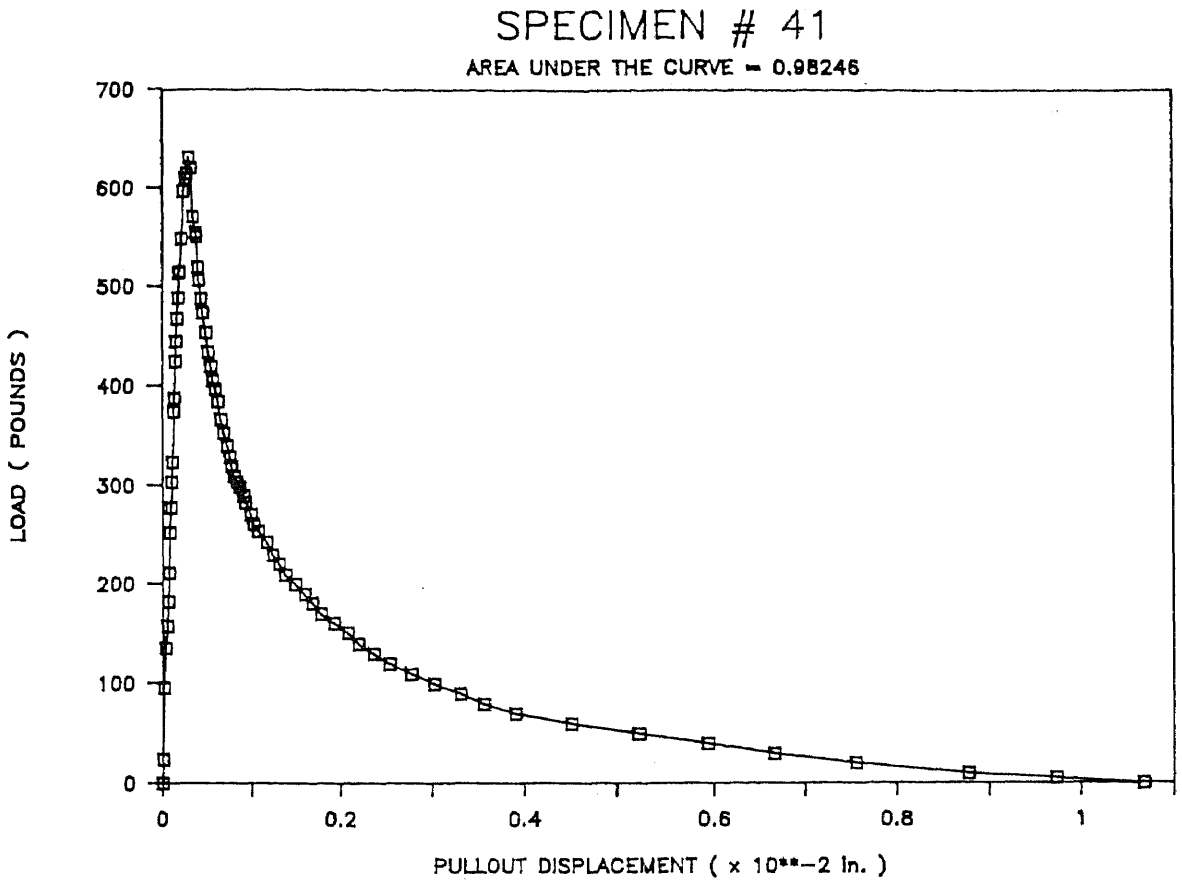
SPECIMEN # 41
AREA UNDER THE CURVE = 0.98246
LOAD (POUNDS)
700
600
500
400
300
200
100
0
0
0.2
0.4
0.6
0.8
1
PULLOUT DISPLACEMENT (x 10**-2 in.)

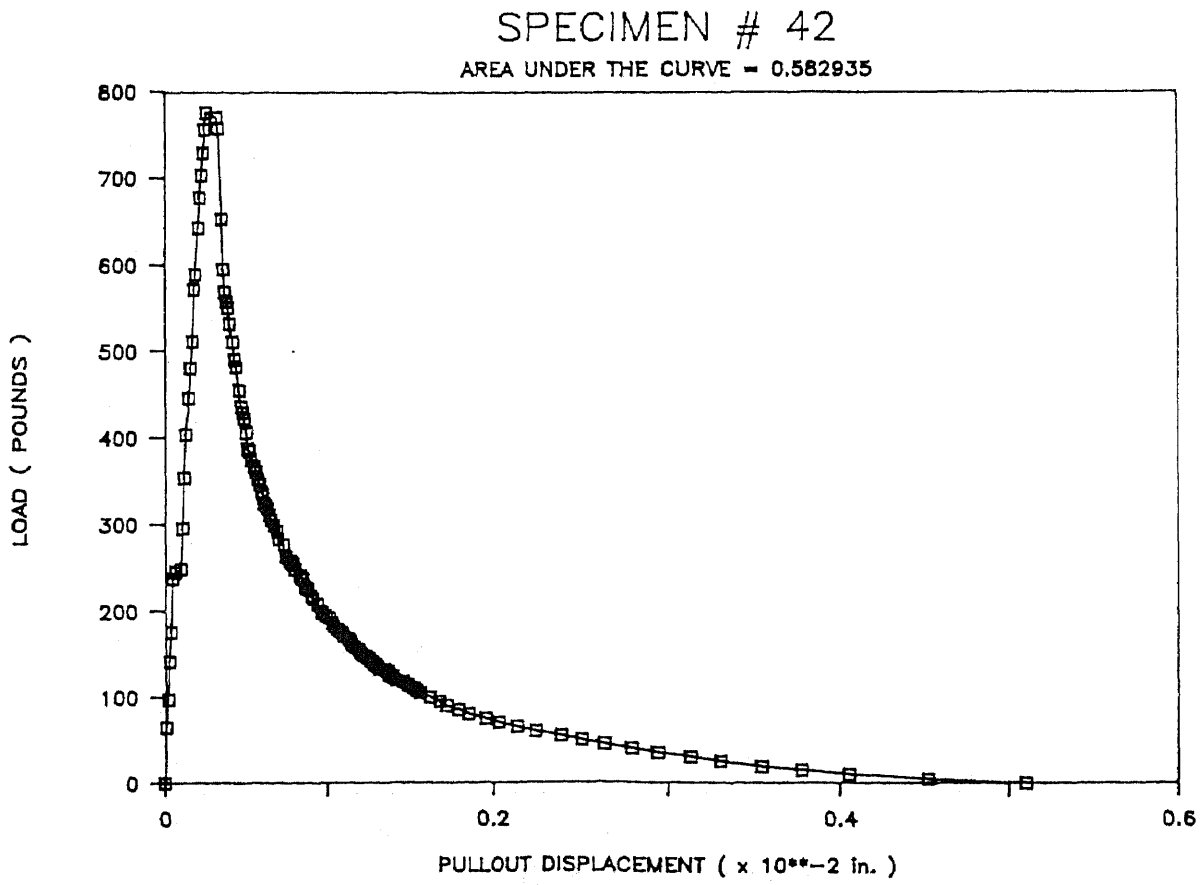
SPECIMEN # 42
AREA UNDER THE CURVE = 0.582935
LOAD (POUNDS)
800
700
600
500
400
300
200
100
0
0
0.2
0.4
0.6
PULLOUT DISPLACEMENT (x 10**-2 in.)

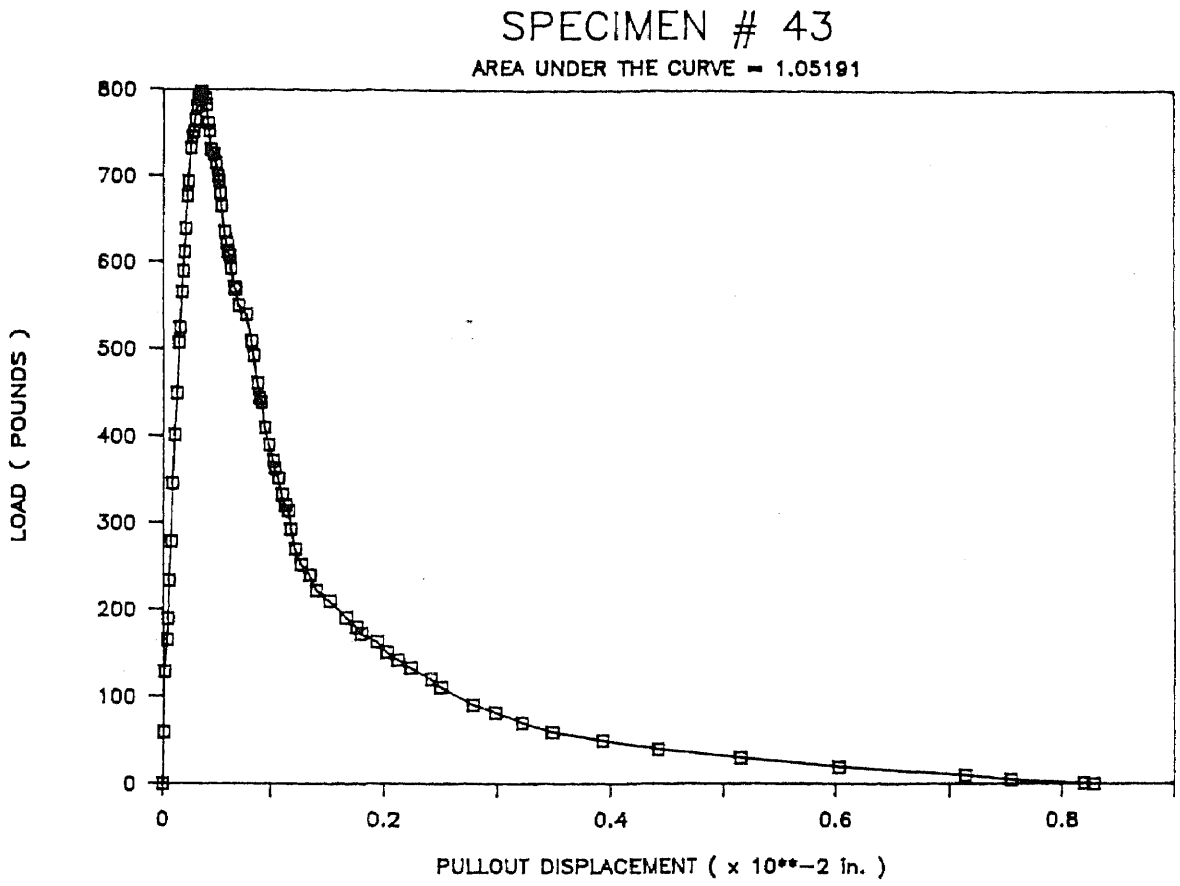
SPECIMEN # 43
AREA UNDER THE CURVE = 1.05191
LOAD (POUNDS)
800
700
600
500
400
300
200
100
0
0
0.2
0.4
0.6
0.8
PULLOUT DISPLACEMENT (x 10**-2 in.)

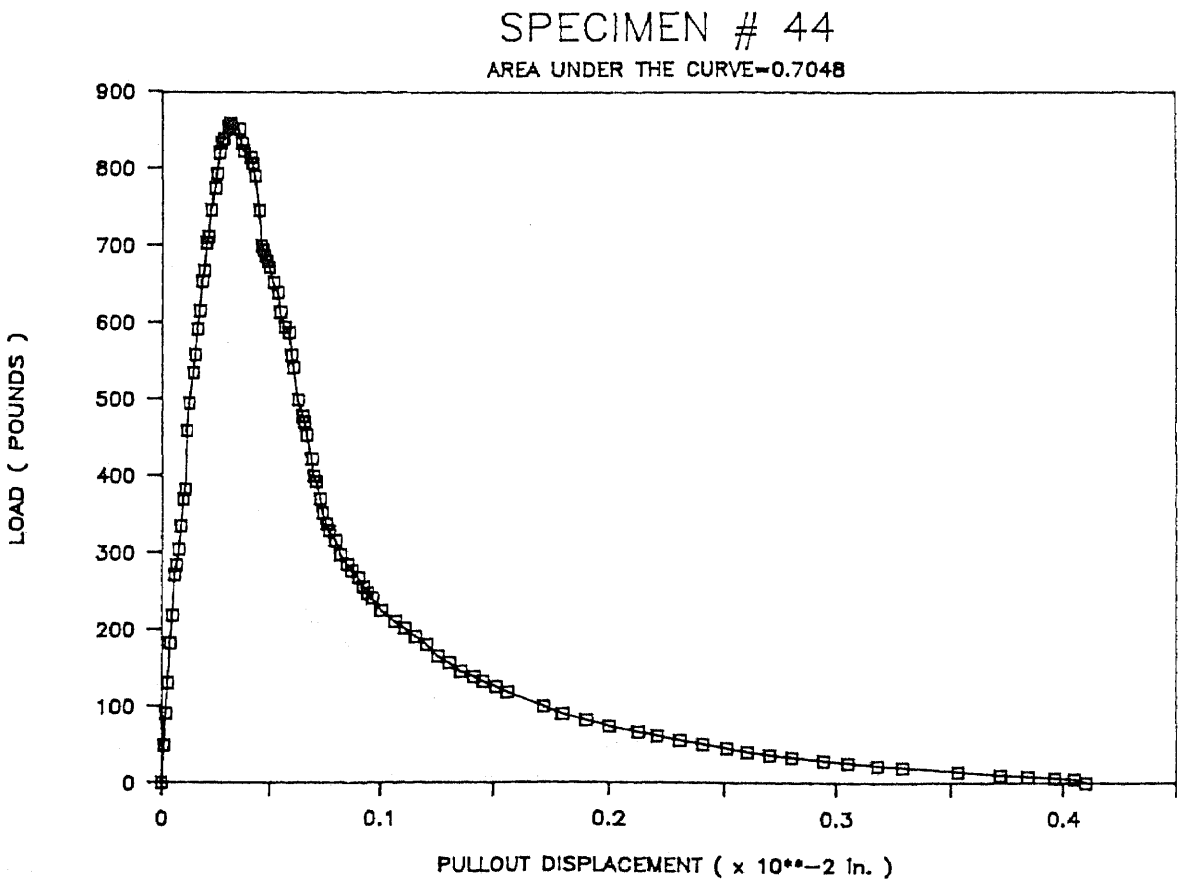
SPECIMEN # 44
AREA UNDER THE CURVE=0.7048
LOAD (POUNDS)
900
800
700
600
500
400
300
200
100
0
0
0.1
0.2
0.3
0.4
PULLOUT DISPLACEMENT (x 10**-2 in.)

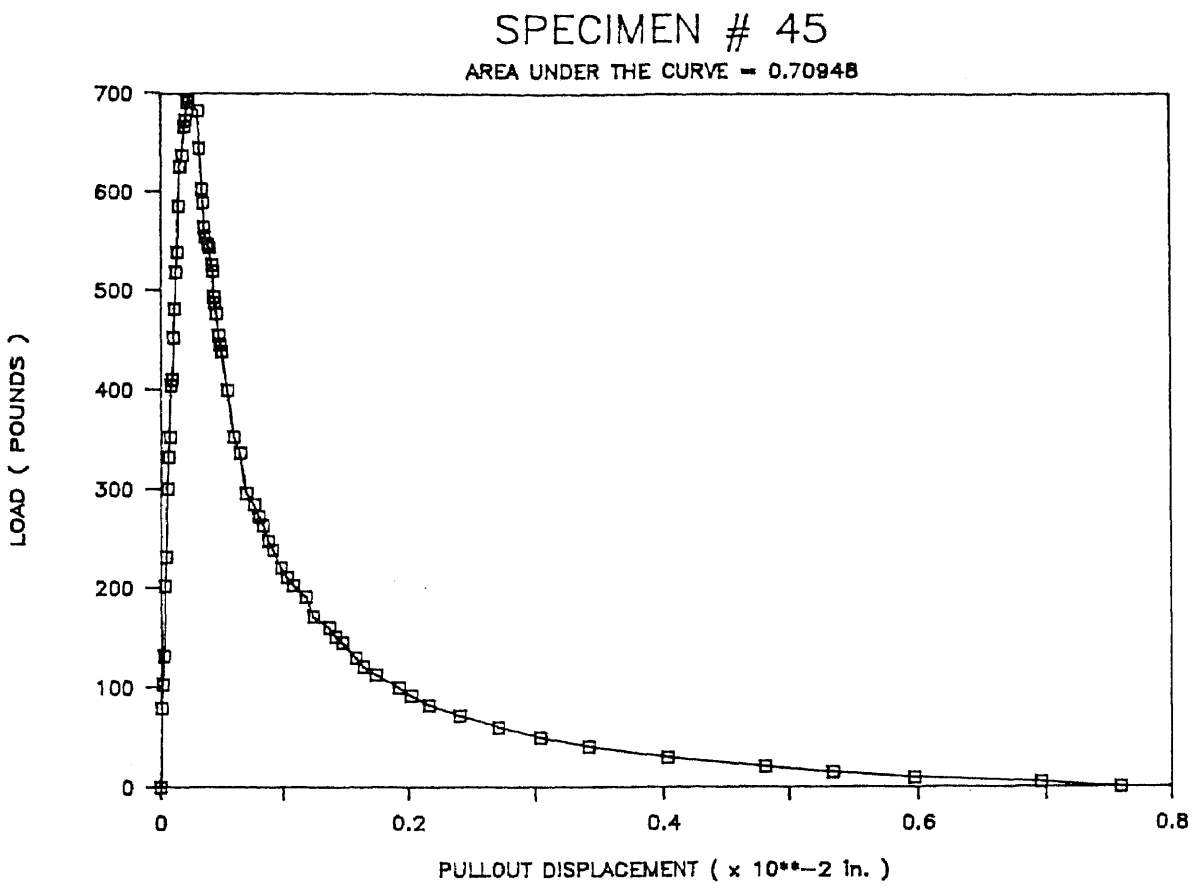
SPECIMEN # 45
AREA UNDER THE CURVE = 0.70948
LOAD (POUNDS)
700
600
500
400
300
200
100
0
0
0.2
0.4
0.6
0.8
PULLOUT DISPLACEMENT (x 10**-2 in.)

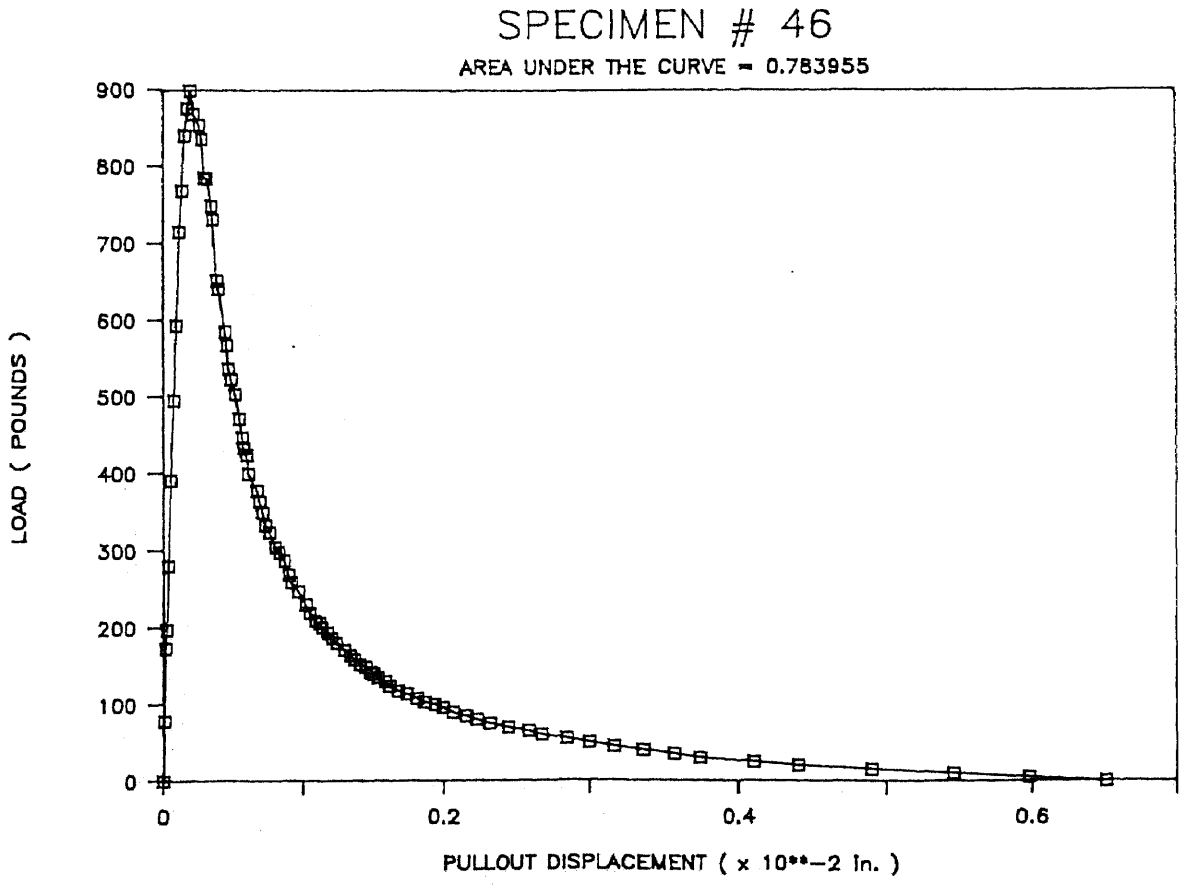
SPECIMEN # 46
AREA UNDER THE CURVE = 0.783955
LOAD (POUNDS)
900
800
700
600
500
400
300
200
100
0
0
0.2
0.4
0.6
PULLOUT DISPLACEMENT (x 10**-2 in.)

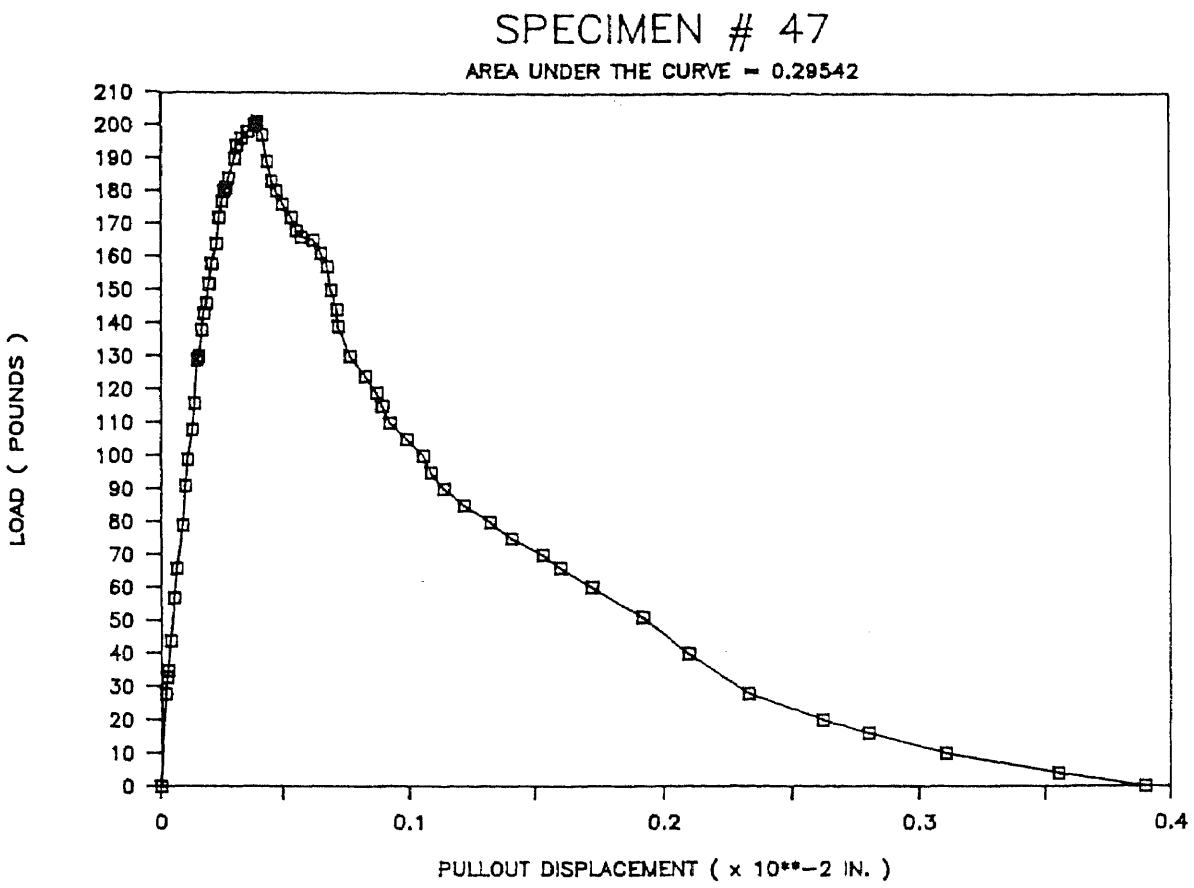
SPECIMEN # 47
AREA UNDER THE CURVE = 0.29542
LOAD (POUNDS)
210
200
190
180
170
160
150
140
130
120
110
100
90
80
70
60
50
40
30
20
10
0
0
0.1
0.2
0.3
0.4
PULLOUT DISPLACEMENT (x 10**-2 IN.)

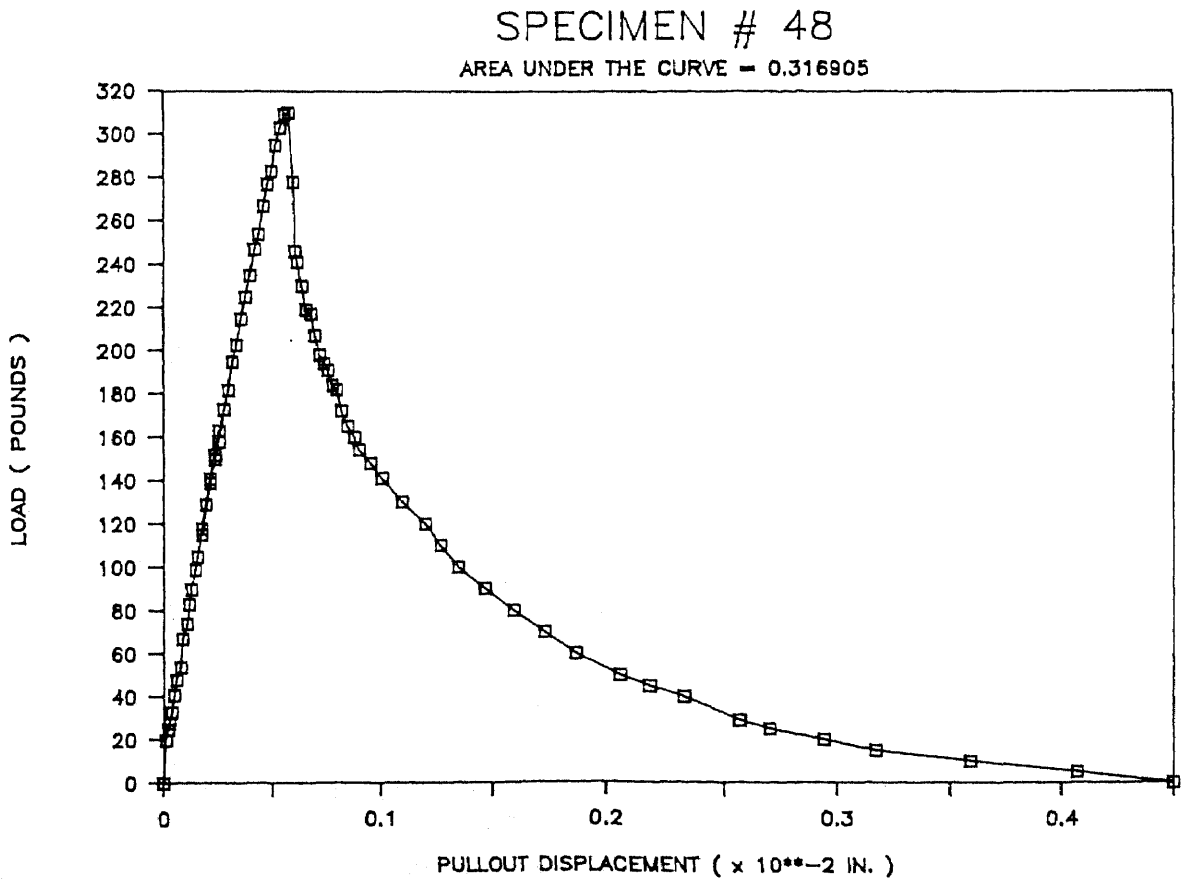
SPECIMEN # 48
AREA UNDER THE CURVE = 0.316905
LOAD (POUNDS)
320
300
280
260
240
220
200
180
160
140
120
100
80
60
40
20
0
0
0.1
0.2
0.3
0.4
PULLOUT DISPLACEMENT (x 10**-2 IN.)

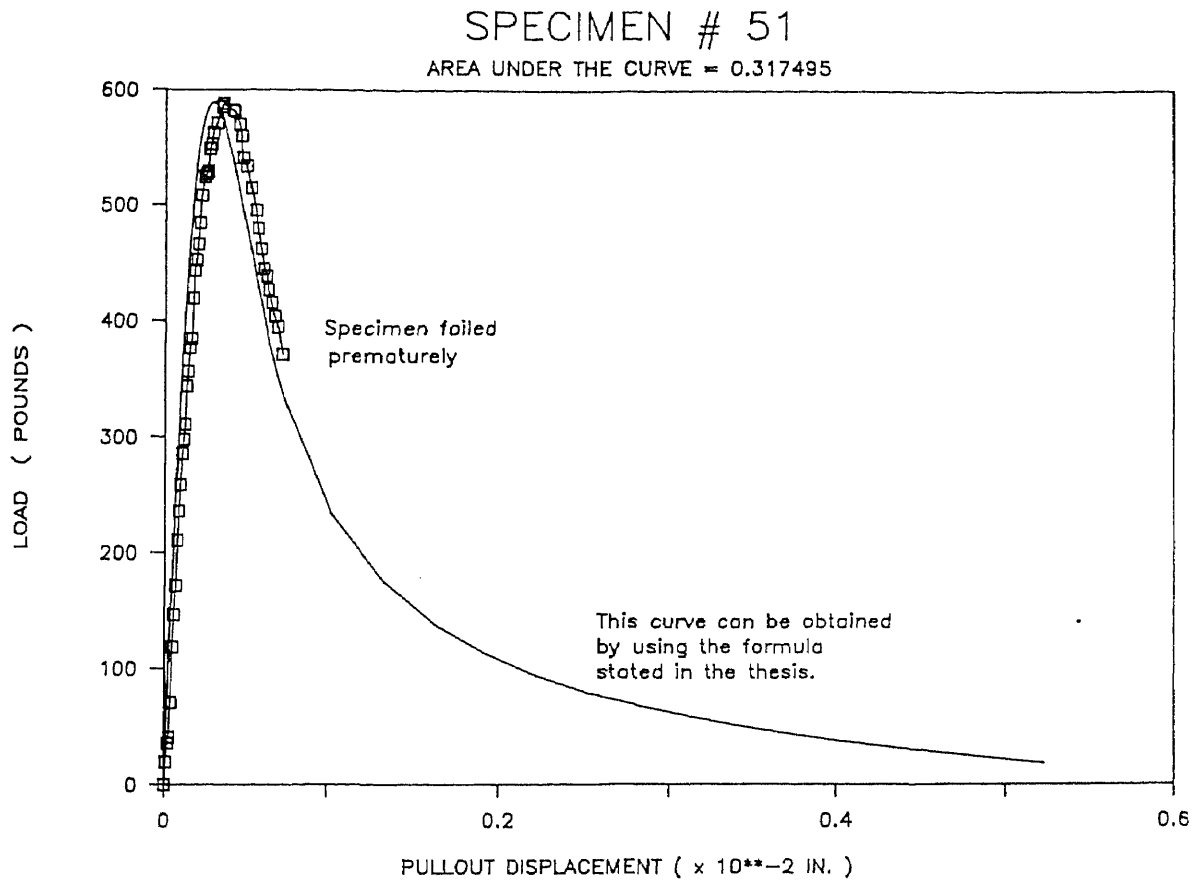
SPECIMEN # 51
AREA UNDER THE CURVE = 0.317495
LOAD (POUNDS)
600
500
400
300
200
100
0
Specimen failed prematurely
This curve can be obtained by using the formula stated in the thesis.
0
0.2
0.4
0.6
PULLOUT DISPLACEMENT (x 10**-2 IN.)

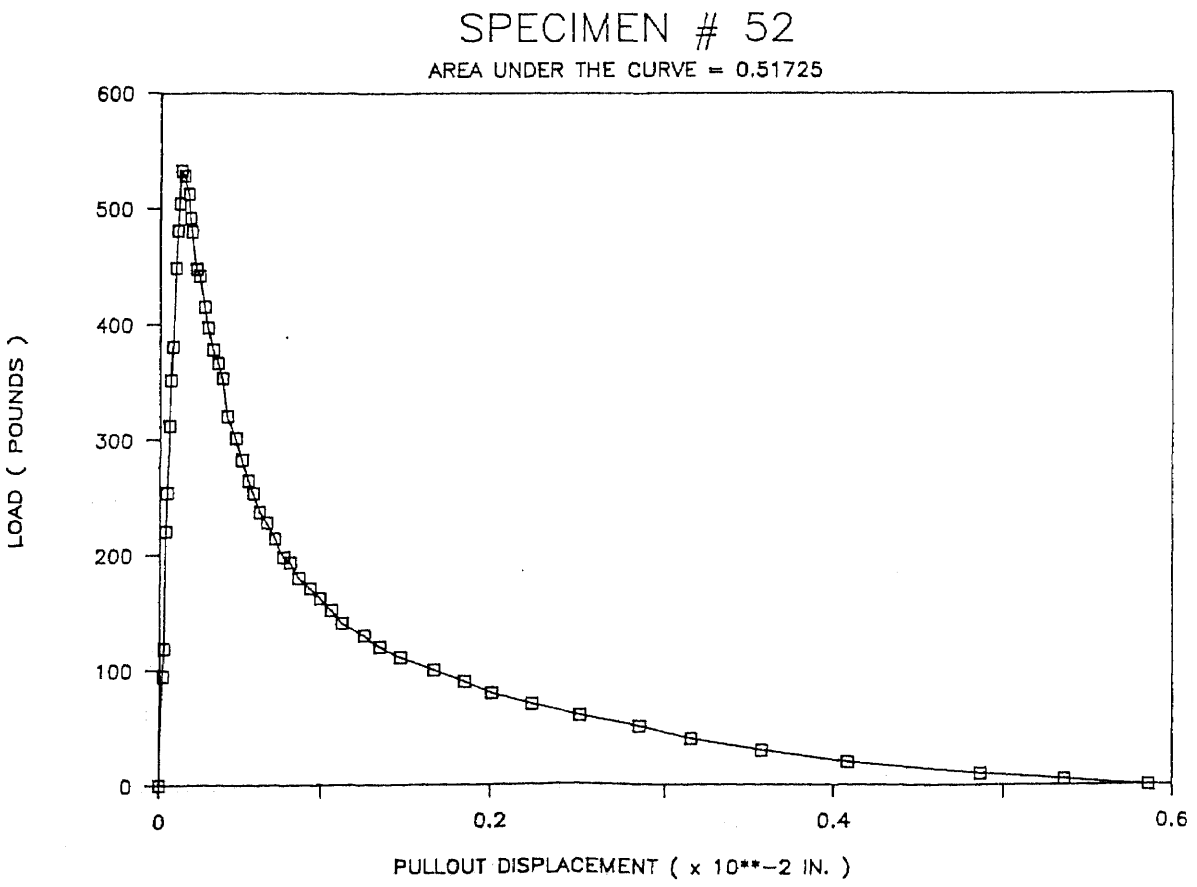
SPECIMEN # 52
AREA UNDER THE CURVE = 0.51725
LOAD (POUNDS)
600
500
400
300
200
100
0
0
0.2
0.4
0.6
PULLOUT DISPLACEMENT (x 10**-2 IN.)

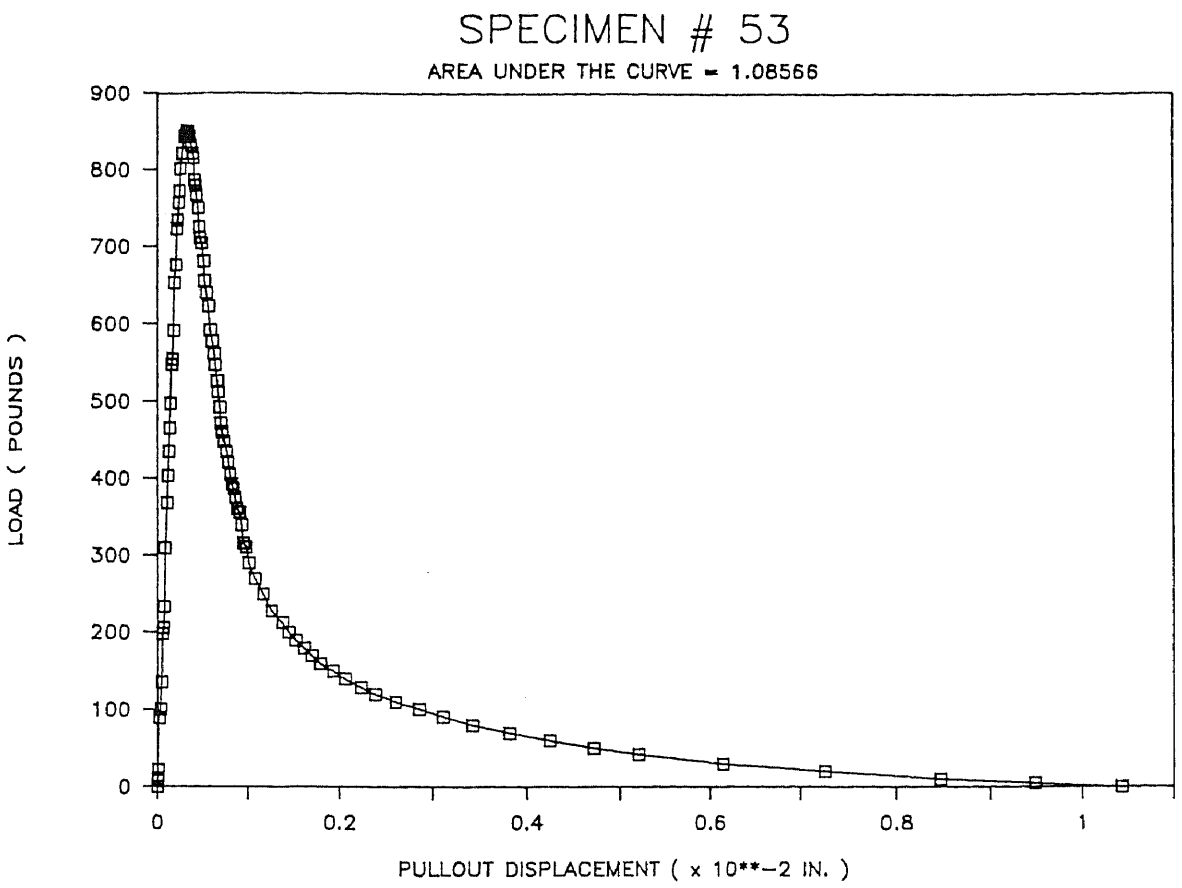
SPECIMEN # 53
AREA UNDER THE CURVE = 1.08566
LOAD (POUNDS)
900
800
700
600
500
400
300
200
100
0
0
0.2
0.4
0.6
0.8
1
PULLOUT DISPLACEMENT (x 10**-2 IN.)

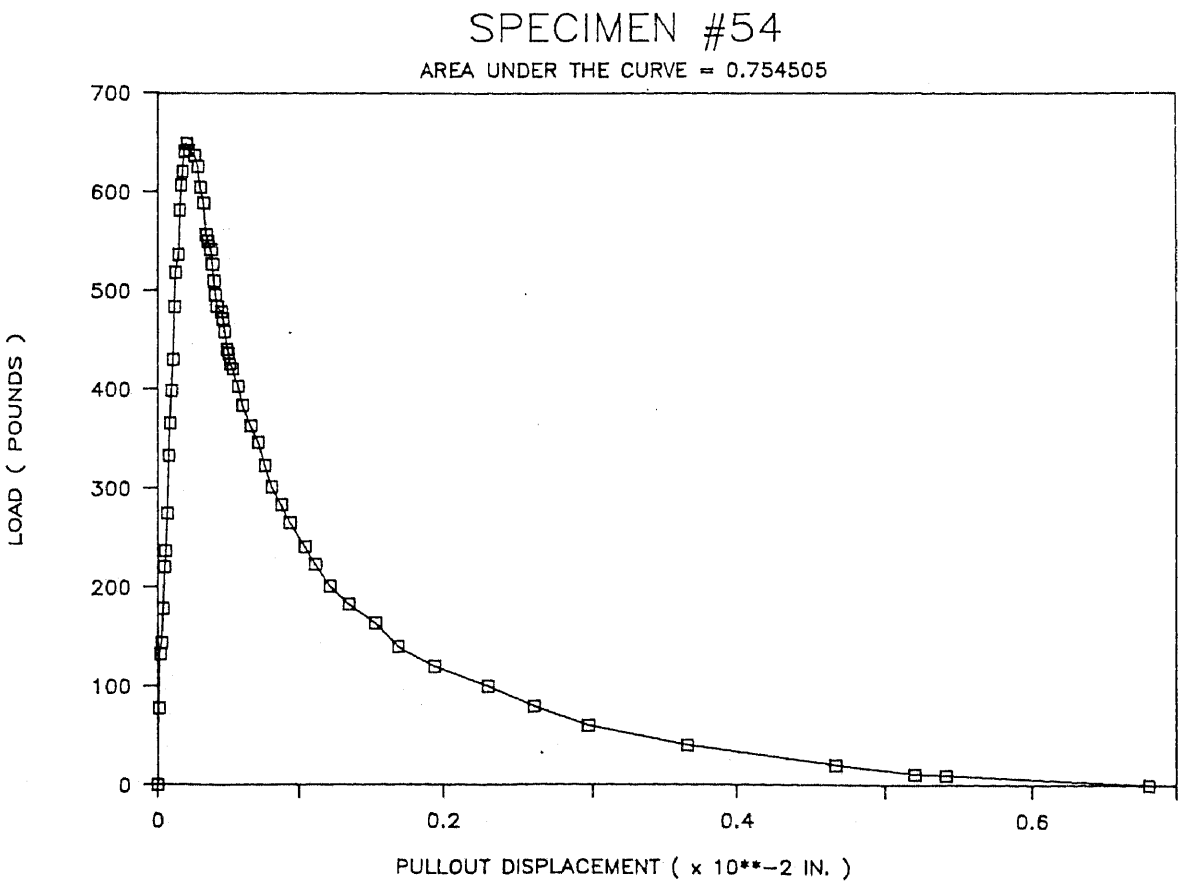
SPECIMEN #54
AREA UNDER THE CURVE = 0.754505
LOAD (POUNDS)
700
600
500
400
300
200
100
0
0
0.2
0.4
0.6
PULLOUT DISPLACEMENT (x 10**-2 IN.)

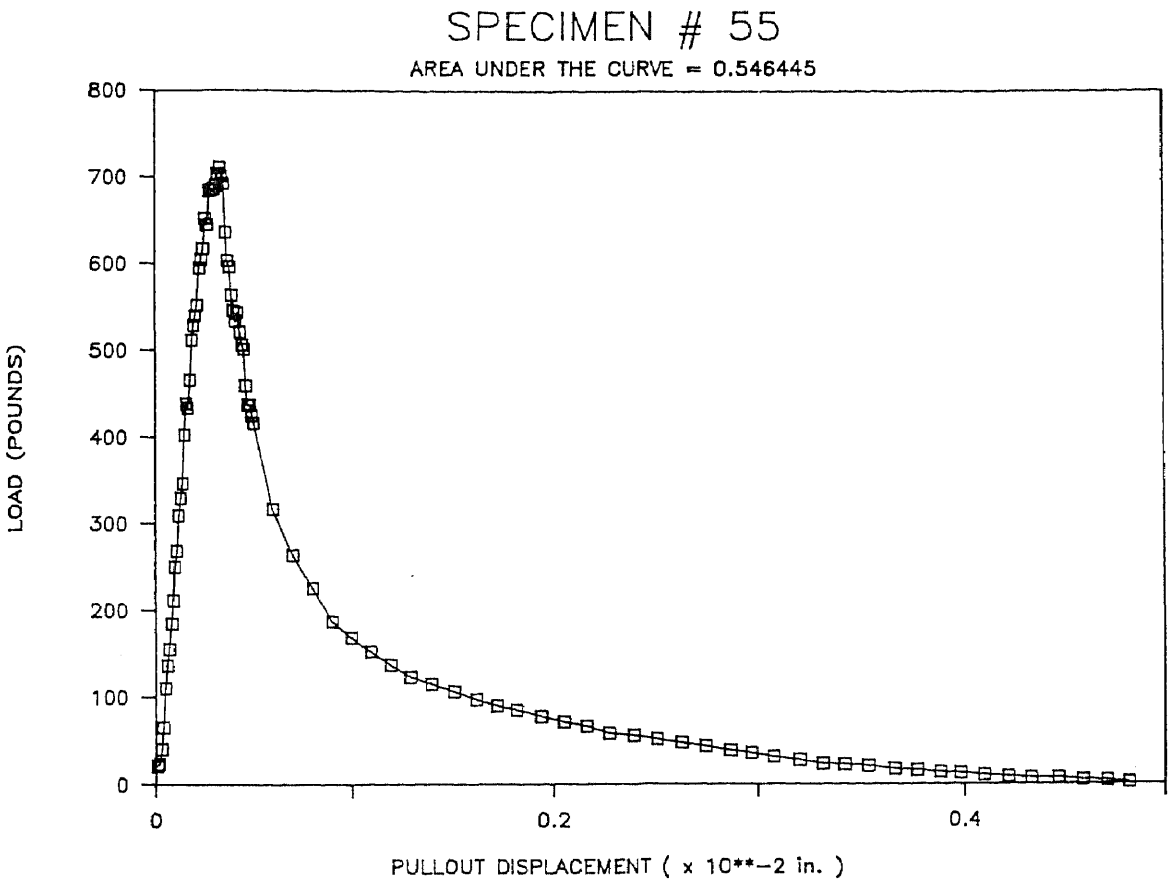
SPECIMEN # 55
AREA UNDER THE CURVE = 0.546445
LOAD (POUNDS)
800
700
600
500
400
300
200
100
0
0
0.2
0.4
PULLOUT DISPLACEMENT (x 10**-2 in.)

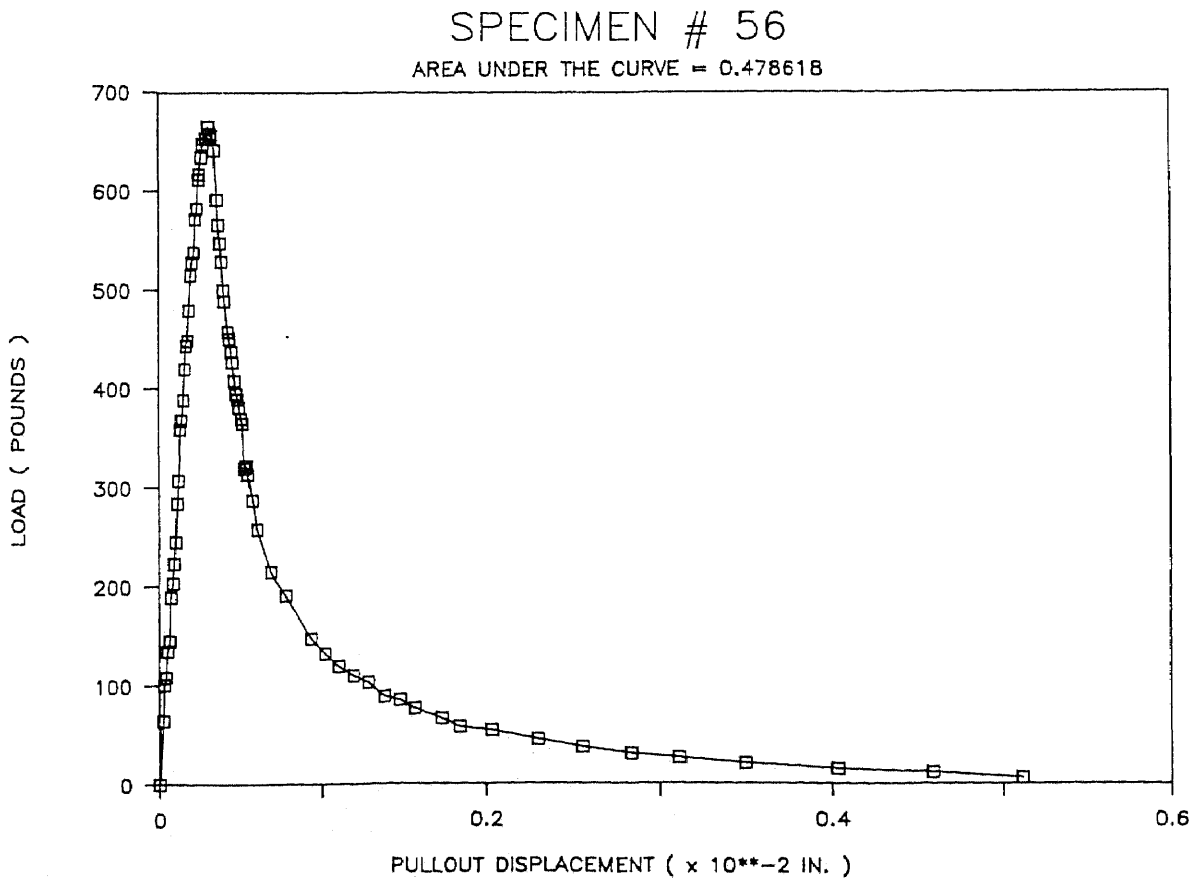
SPECIMEN # 56
AREA UNDER THE CURVE = 0.478618
LOAD (POUNDS)
700
600
500
400
300
200
100
0
0
0.2
0.4
0.6
PULLOUT DISPLACEMENT (x 10**-2 IN.)

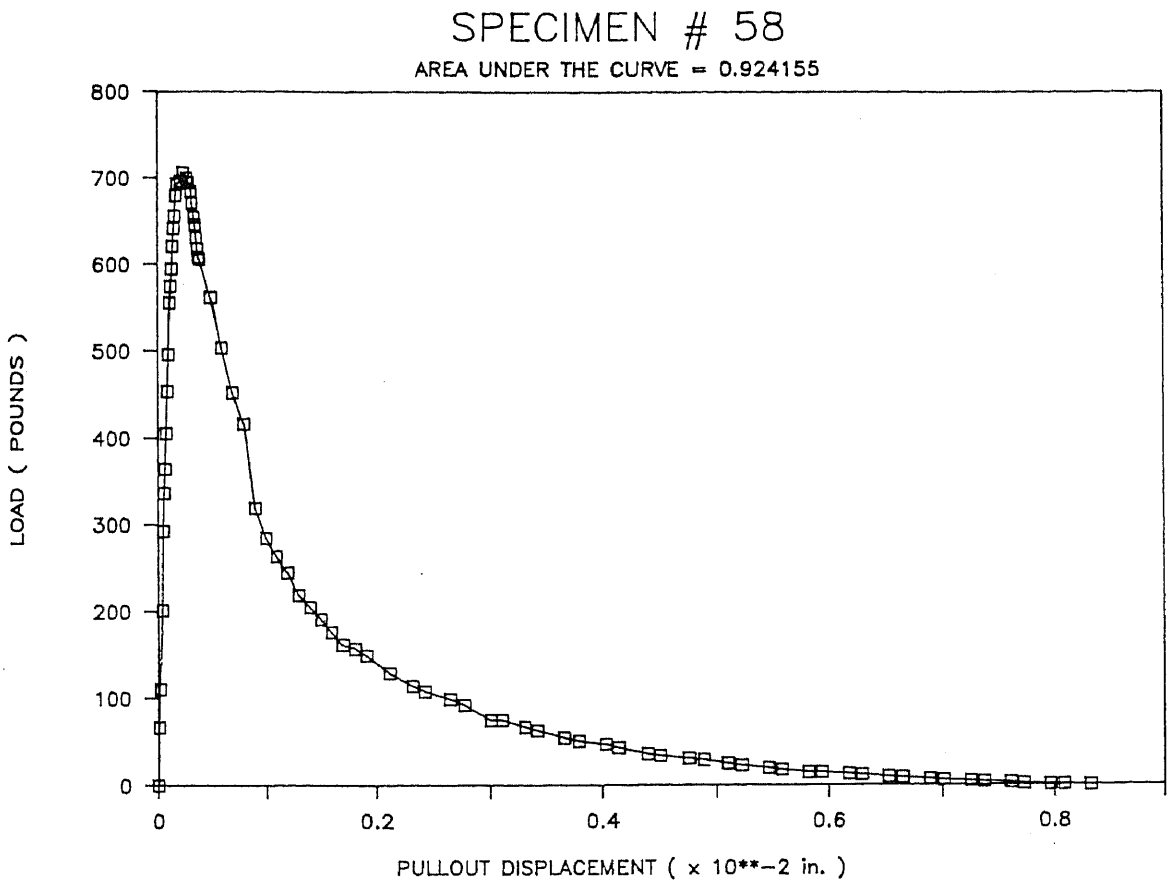
SPECIMEN # 58
AREA UNDER THE CURVE = 0.924155
LOAD (POUNDS)
800
700
600
500
400
300
200
100
0
0
0.2
0.4
0.6
0.8
PULLOUT DISPLACEMENT (x 10**-2 in.)

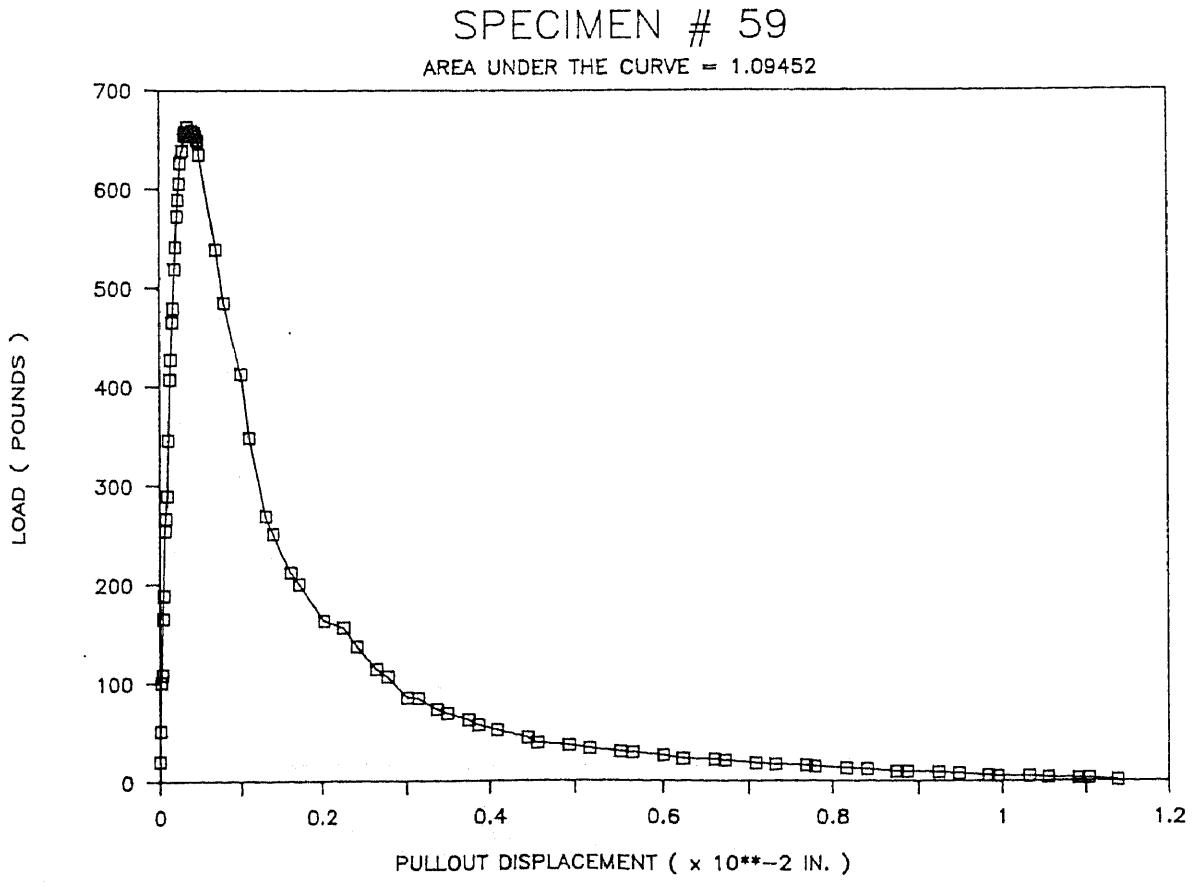
SPECIMEN # 59
AREA UNDER THE CURVE = 1.09452
LOAD (POUNDS)
700
600
500
400
300
200
100
0
0
0.2
0.4
0.6
0.8
1
1.2
PULLOUT DISPLACEMENT (x 10**-2 IN.)

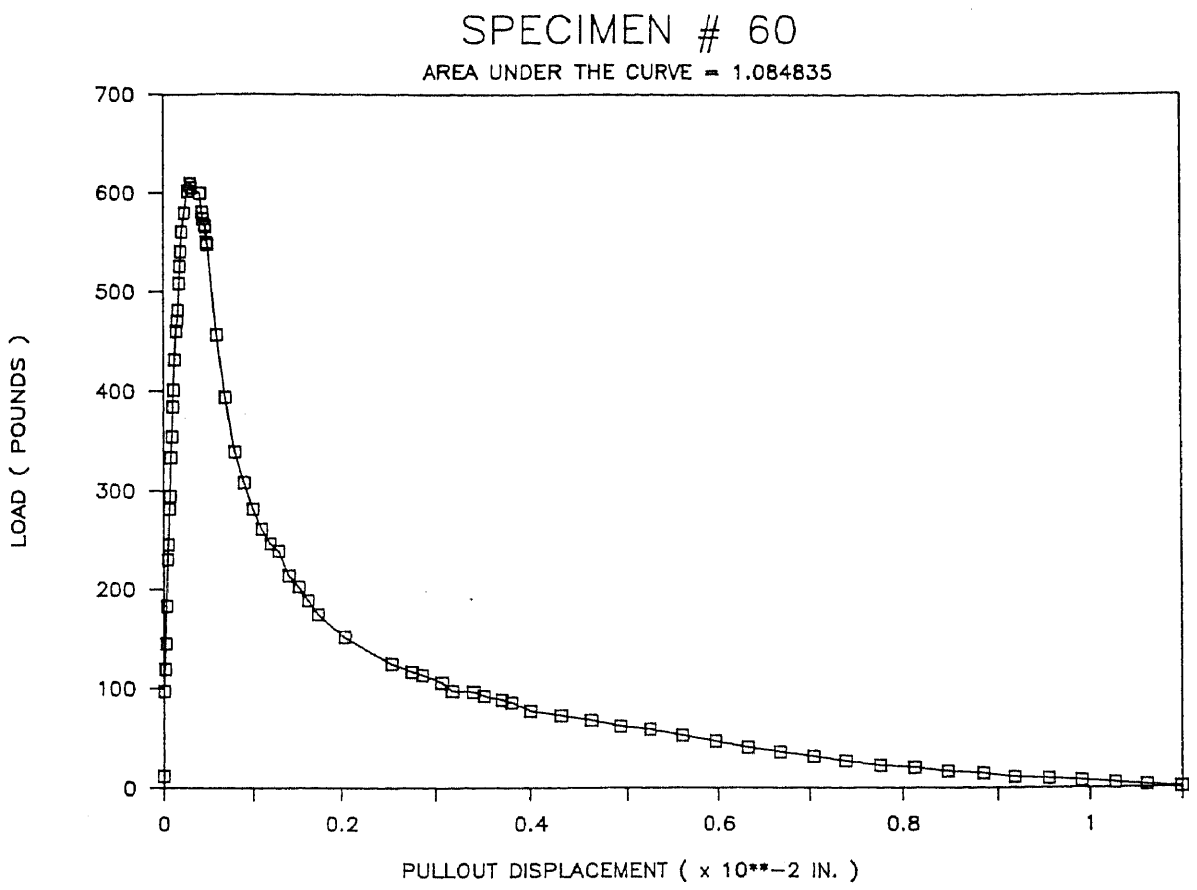
SPECIMEN # 60
AREA UNDER THE CURVE = 1.084835
LOAD (POUNDS)
700
600
500
400
300
200
100
0
0
0.2
0.4
0.6
0.8
1
PULLOUT DISPLACEMENT (x 10**-2 IN.)

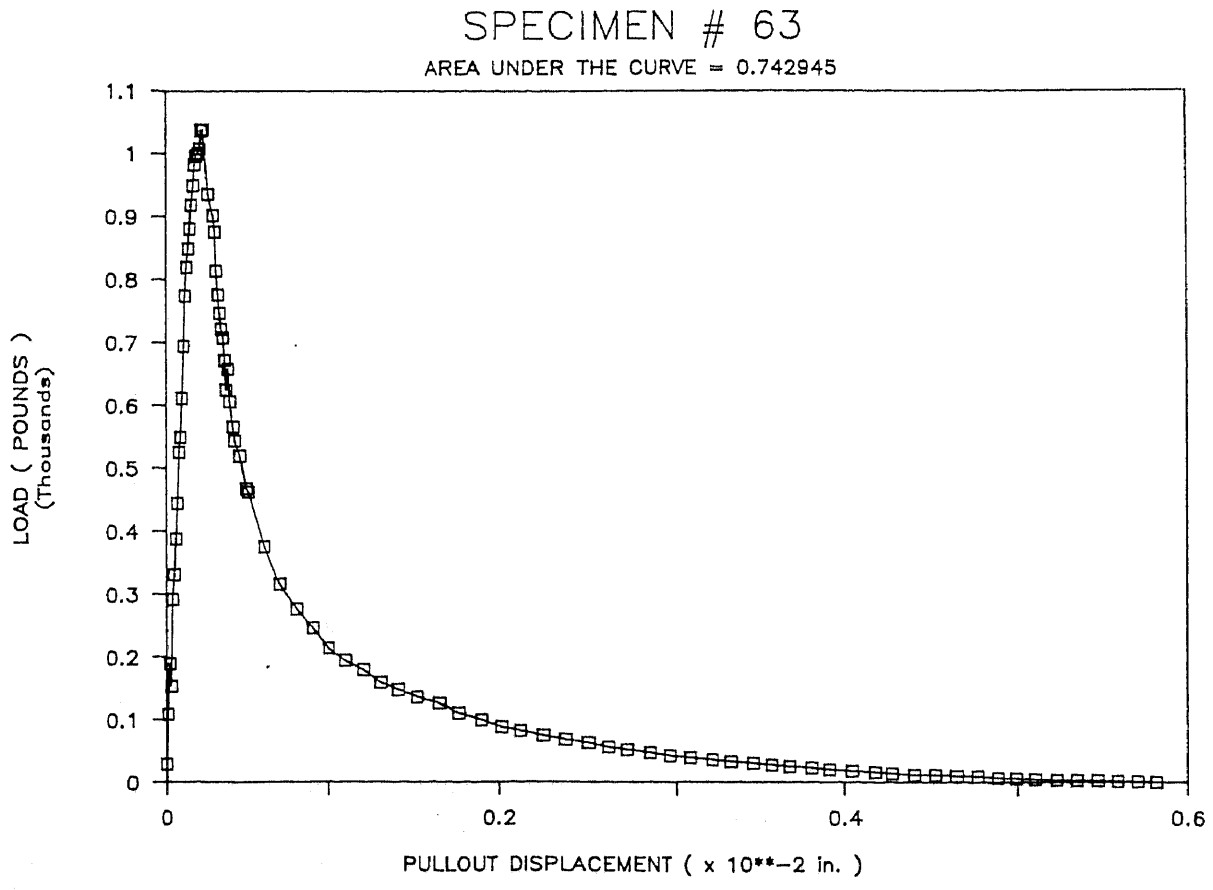
SPECIMEN # 63
AREA UNDER THE CURVE = 0.742945
LOAD (POUNDS)
(Thousands)
1.1
1
0.9
0.8
0.7
0.6
0.5
0.4
0.3
0.2
0.1
0
0
0.2
0.4
0.6
PULLOUT DISPLACEMENT (x 10**-2 in.)

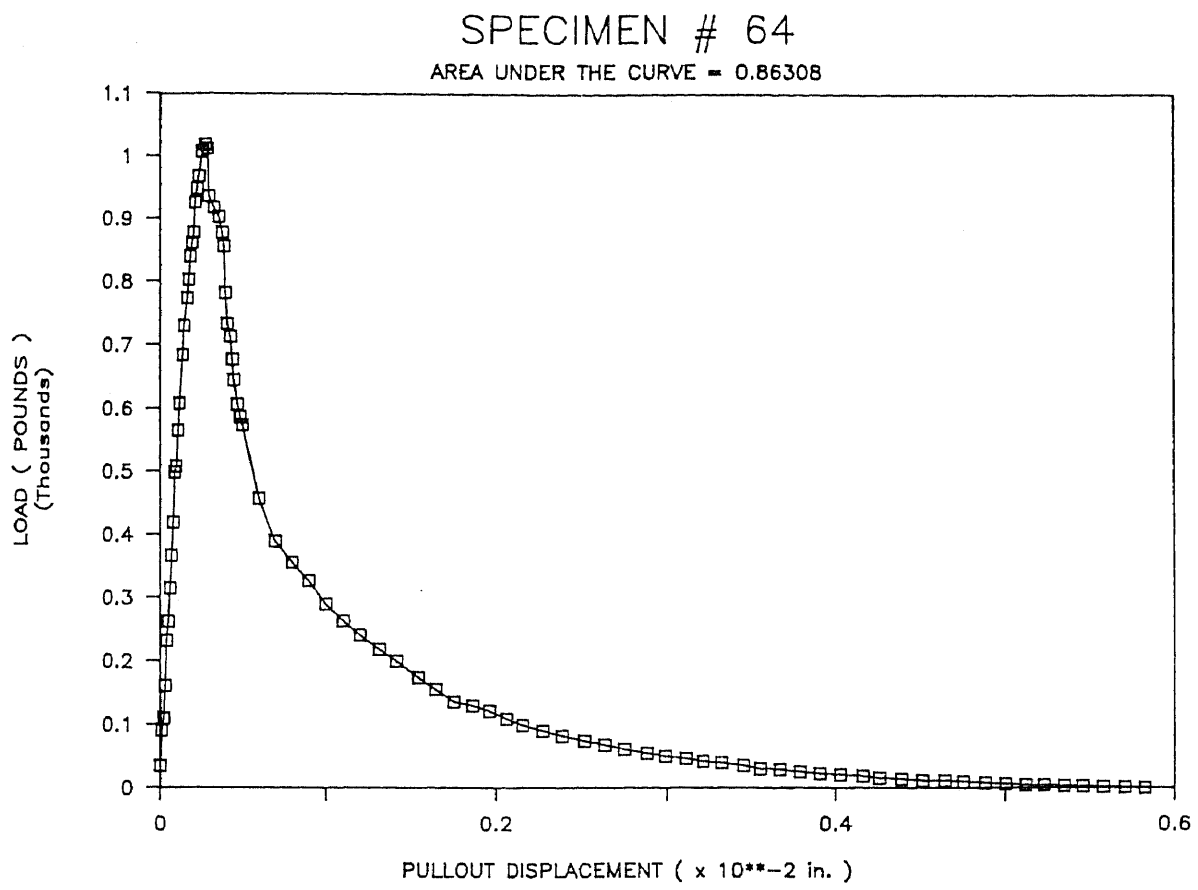
SPECIMEN # 64
AREA UNDER THE CURVE = 0.86308
LOAD (POUNDS)
(Thousands)
1.1
1
0.9
0.8
0.7
0.6
0.5
0.4
0.3
0.2
0.1
0
0
0.2
0.4
0.6
PULLOUT DISPLACEMENT (x 10**-2 in.)

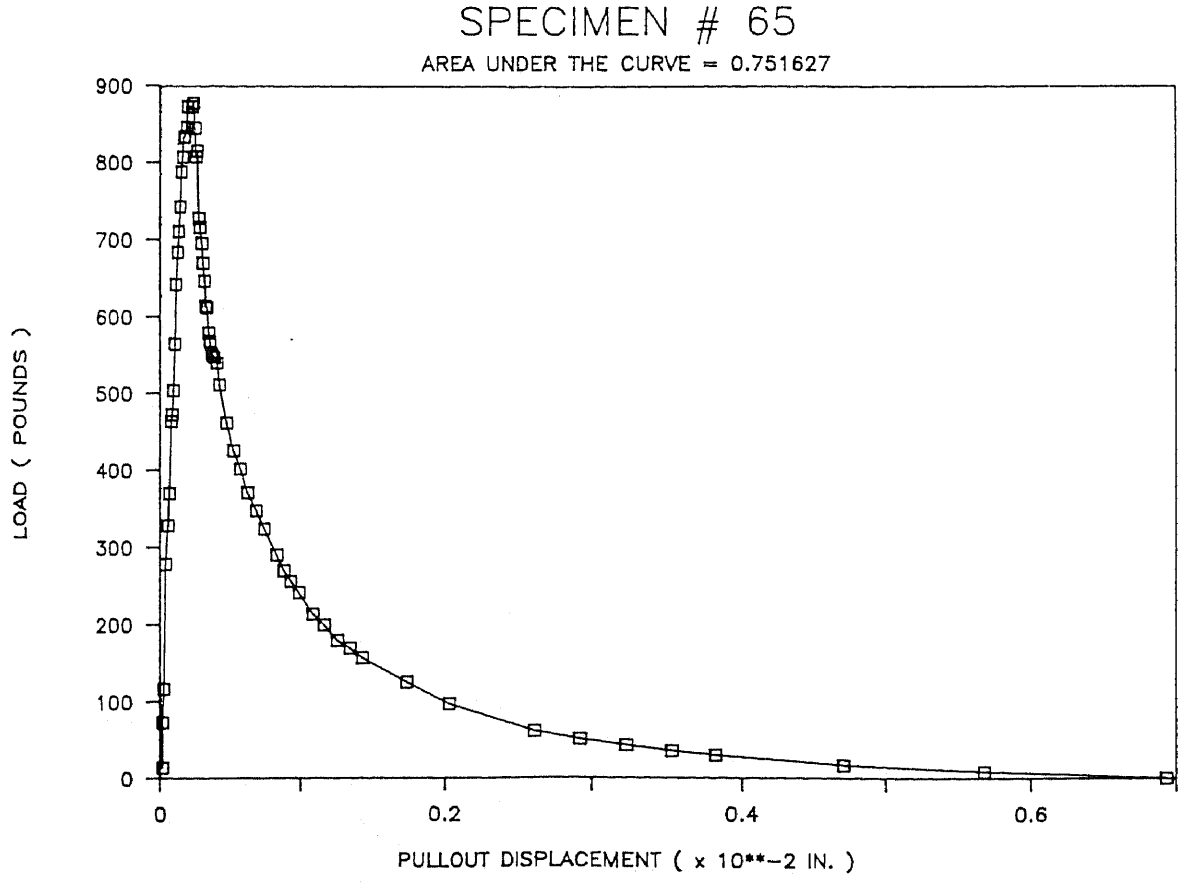
SPECIMEN # 65
AREA UNDER THE CURVE = 0.751627
LOAD (POUNDS)
900
800
700
600
500
400
300
200
100
0
0
0.2
0.4
0.6
PULLOUT DISPLACEMENT (x 10**-2 IN.)

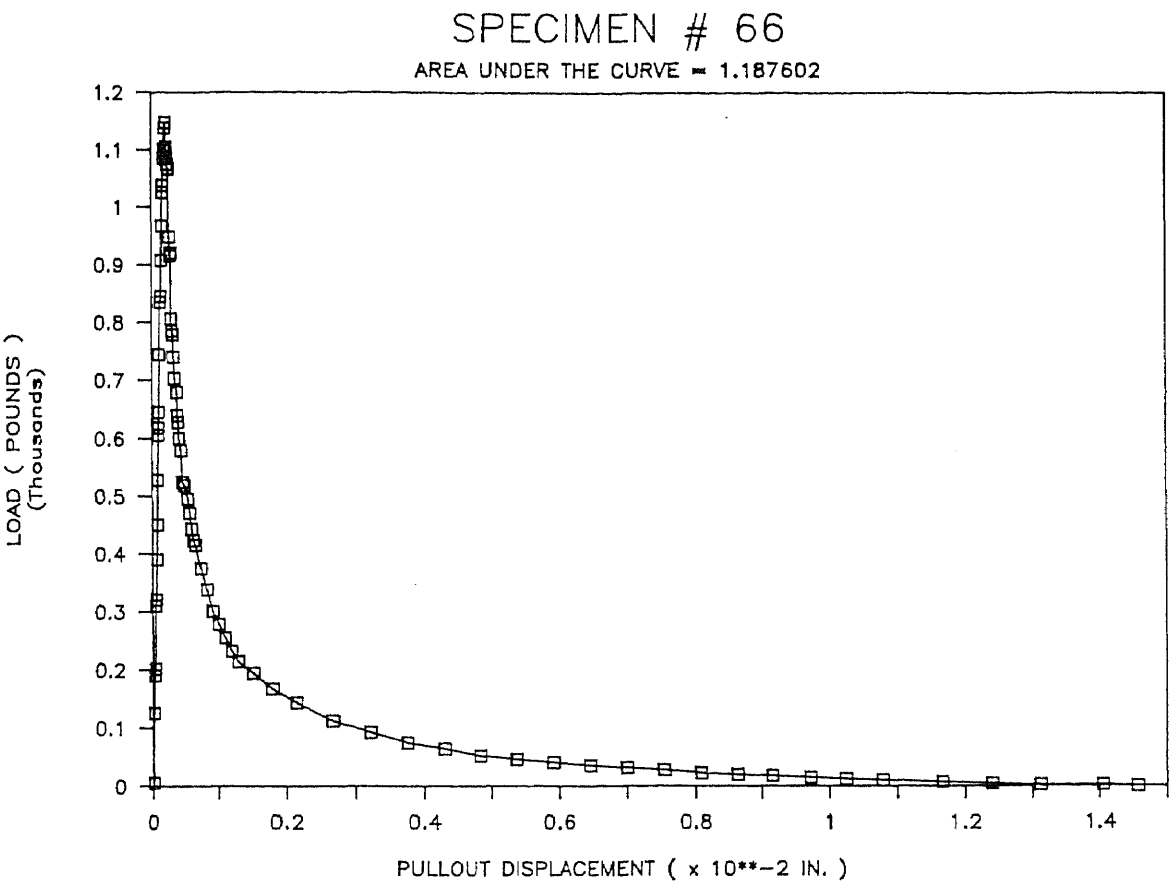
SPECIMEN # 66
AREA UNDER THE CURVE = 1.187602
LOAD (POUNDS)
(Thousands)
1.2
1.1
1
0.9
0.8
0.7
0.6
0.5
0.4
0.3
0.2
0.1
0
0
0.2
0.4
0.6
0.8
1
1.2
1.4
PULLOUT DISPLACEMENT (x 10**-2 IN.)

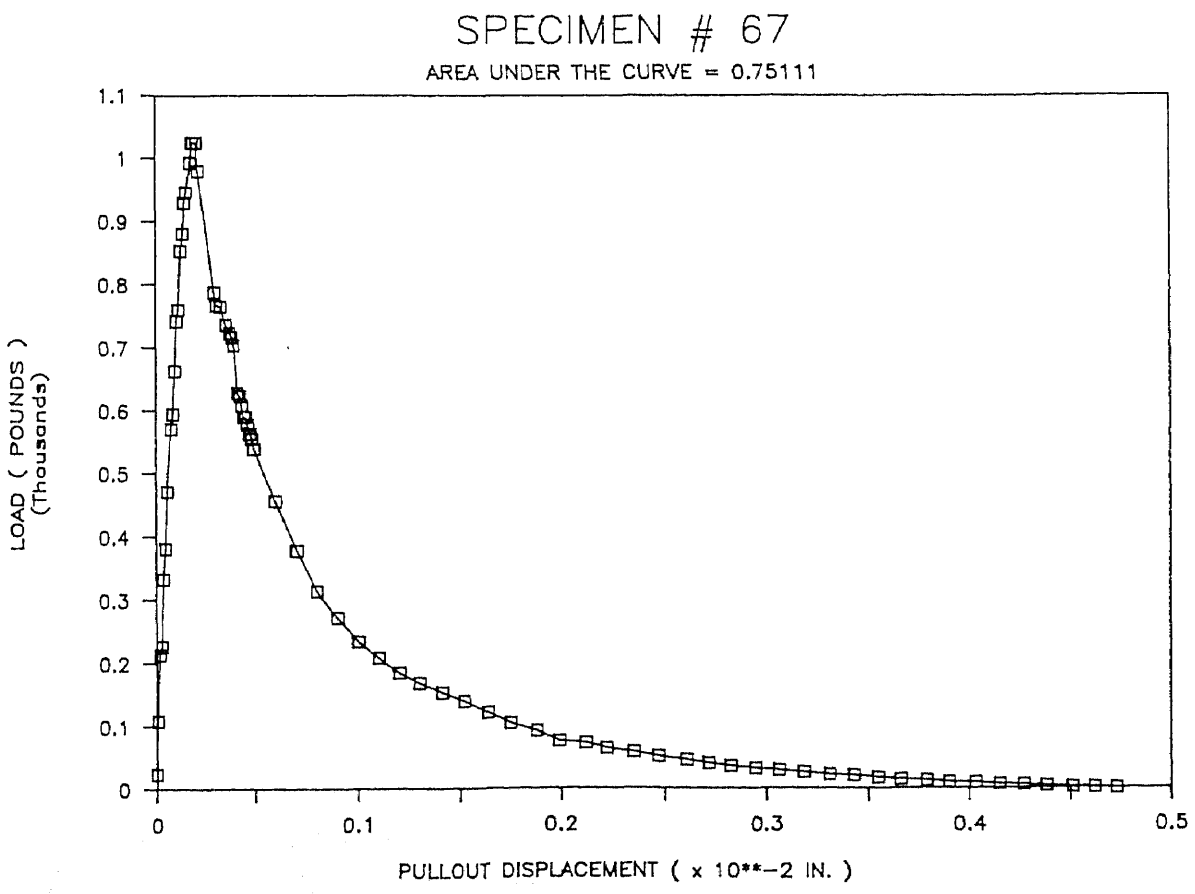
SPECIMEN # 67
AREA UNDER THE CURVE = 0.75111
LOAD (POUNDS)
(Thousands)
1.1
1
0.9
0.8
0.7
0.6
0.5
0.4
0.3
0.2
0.1
0
0
0.1
0.2
0.3
0.4
0.5
PULLOUT DISPLACEMENT (x 10**-2 IN.)

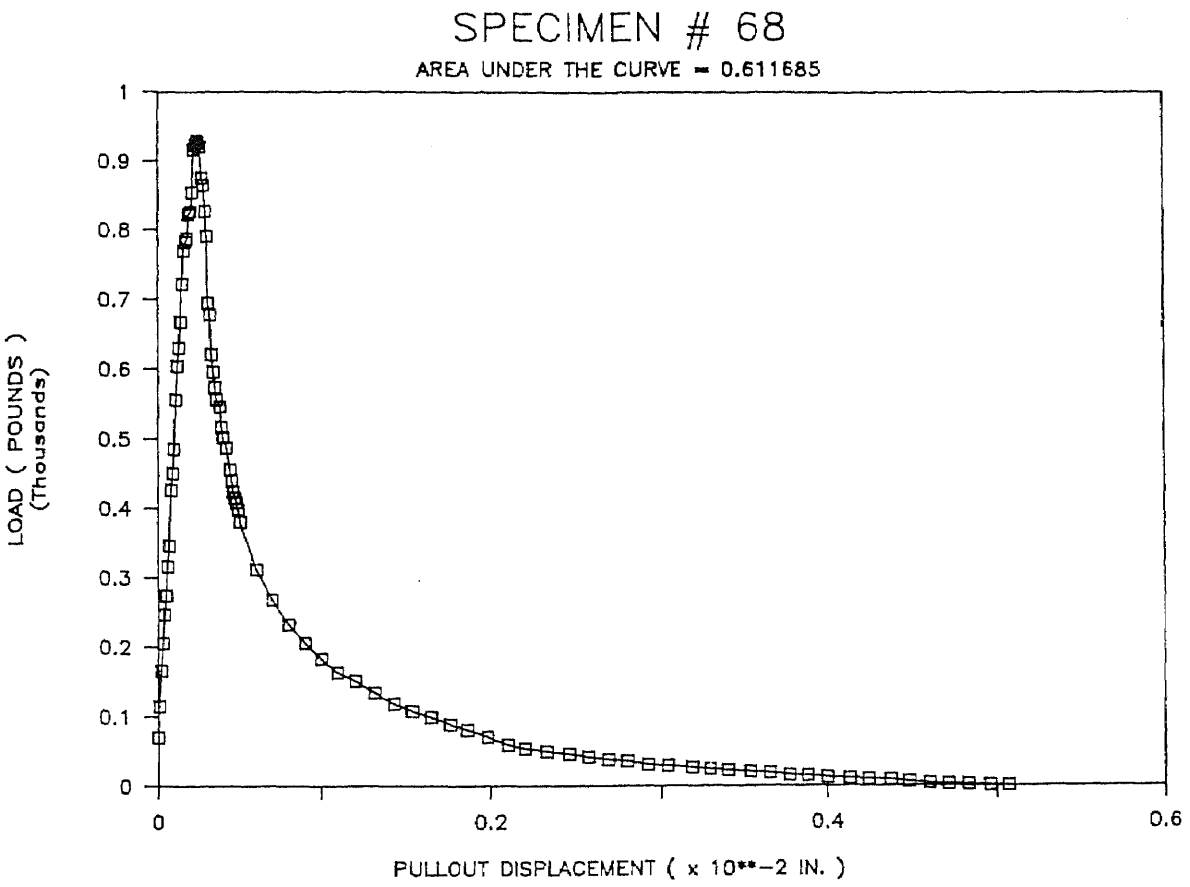
SPECIMEN # 68
AREA UNDER THE CURVE = 0.611685
LOAD (POUNDS)
(Thousands)
1
0.9
0.8
0.7
0.6
0.5
0.4
0.3
0.2
0.1
0
0
0.2
0.4
0.6
PULLOUT DISPLACEMENT (x 10**-2 IN.)

APPENDIX B

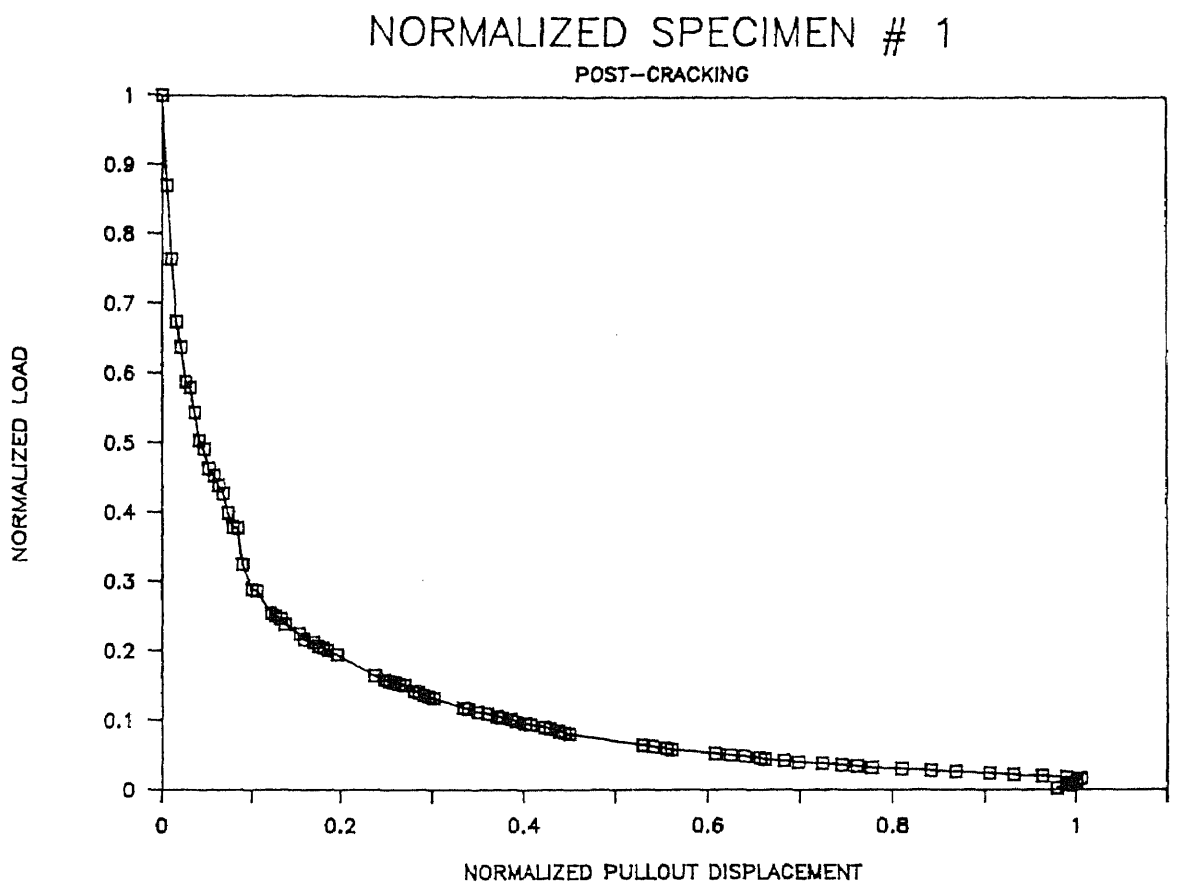
NORMALIZED SPECIMEN # 1
POST-CRACKING
NORMALIZED LOAD
NORMALIZED PULLOUT DISPLACEMENT
0
0.1
0.2
0.3
0.4
0.5
0.6
0.7
0.8
0.9
1
0
0.2
0.4
0.6
0.8
1

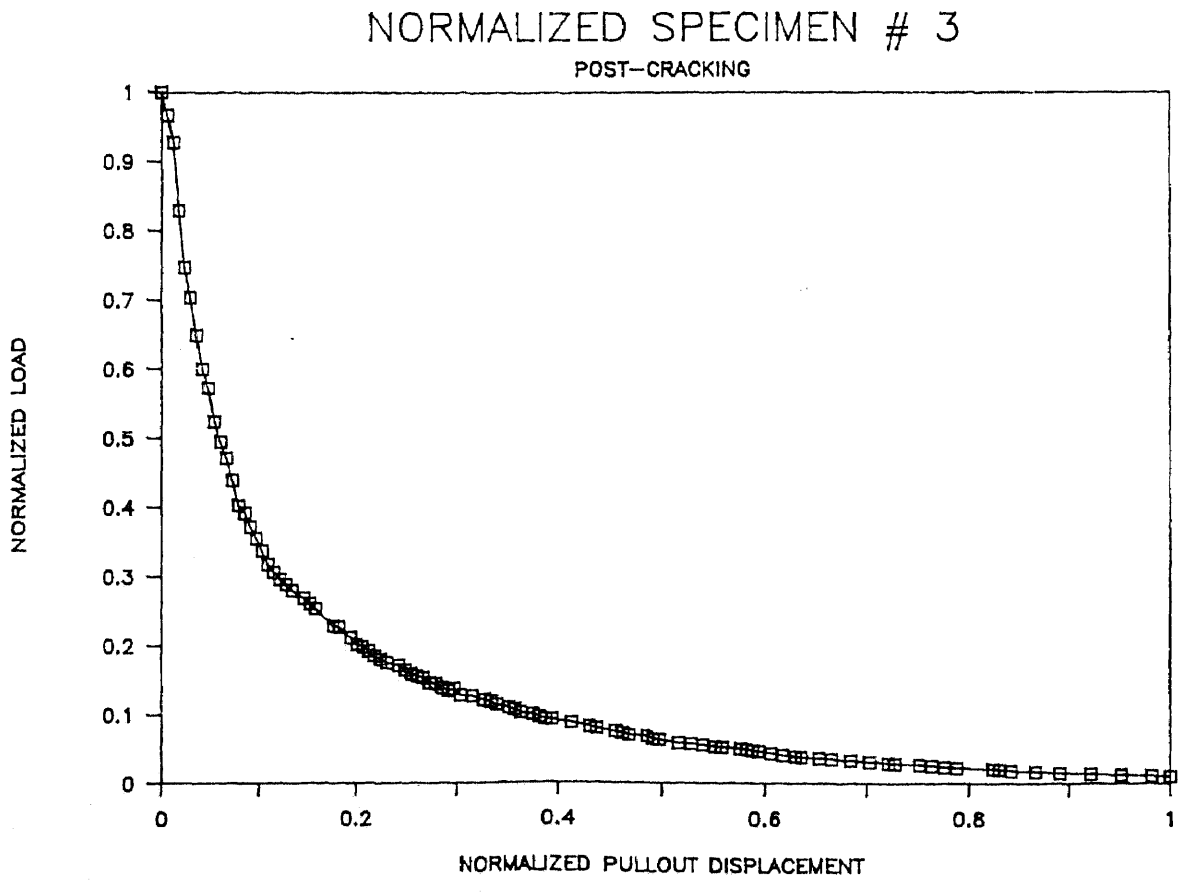
NORMALIZED SPECIMEN # 3
POST-CRACKING
NORMALIZED LOAD
NORMALIZED PULLOUT DISPLACEMENT
0
0.1
0.2
0.3
0.4
0.5
0.6
0.7
0.8
0.9
1
0
0.2
0.4
0.6
0.8
1

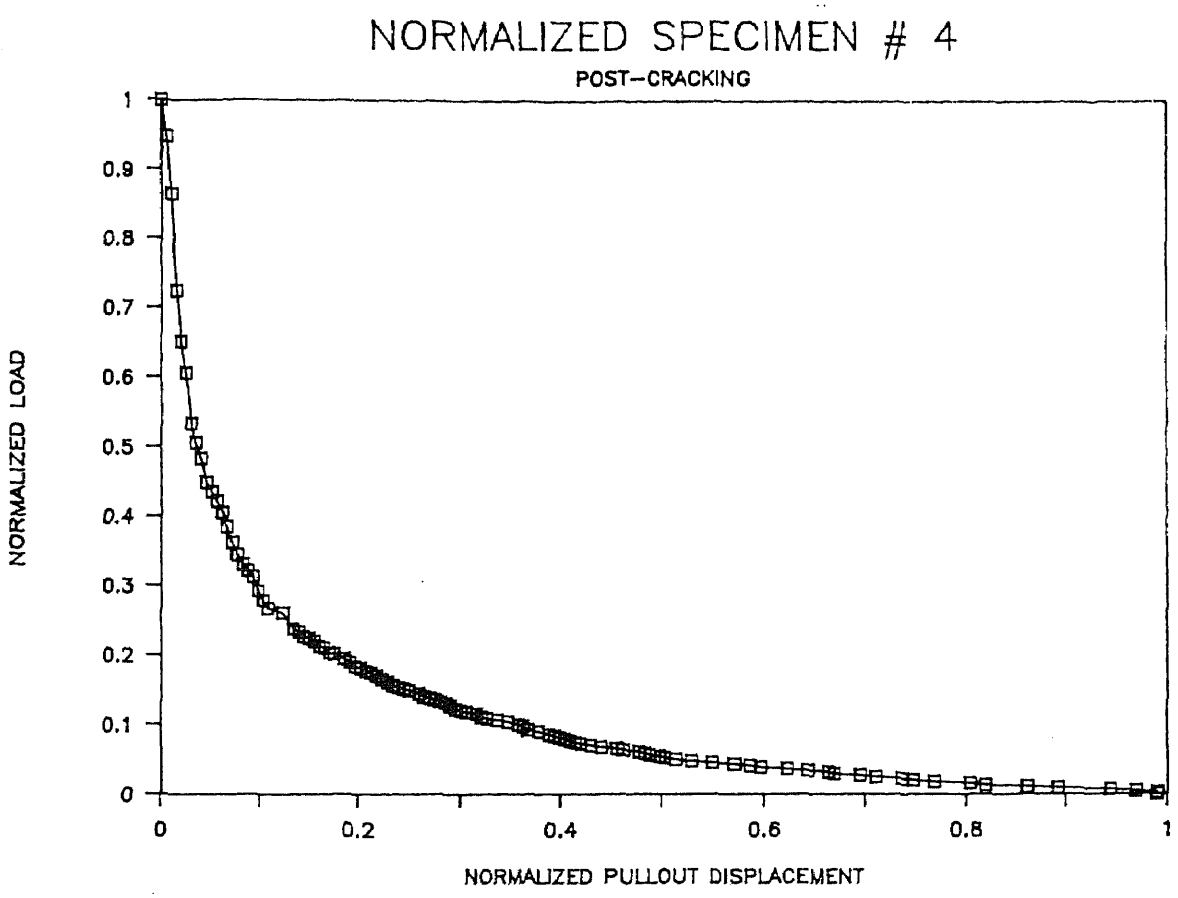
NORMALIZED SPECIMEN # 4
POST-CRACKING
NORMALIZED LOAD
NORMALIZED PULLOUT DISPLACEMENT
0
0.1
0.2
0.3
0.4
0.5
0.6
0.7
0.8
0.9
1
0
0.2
0.4
0.6
0.8
1

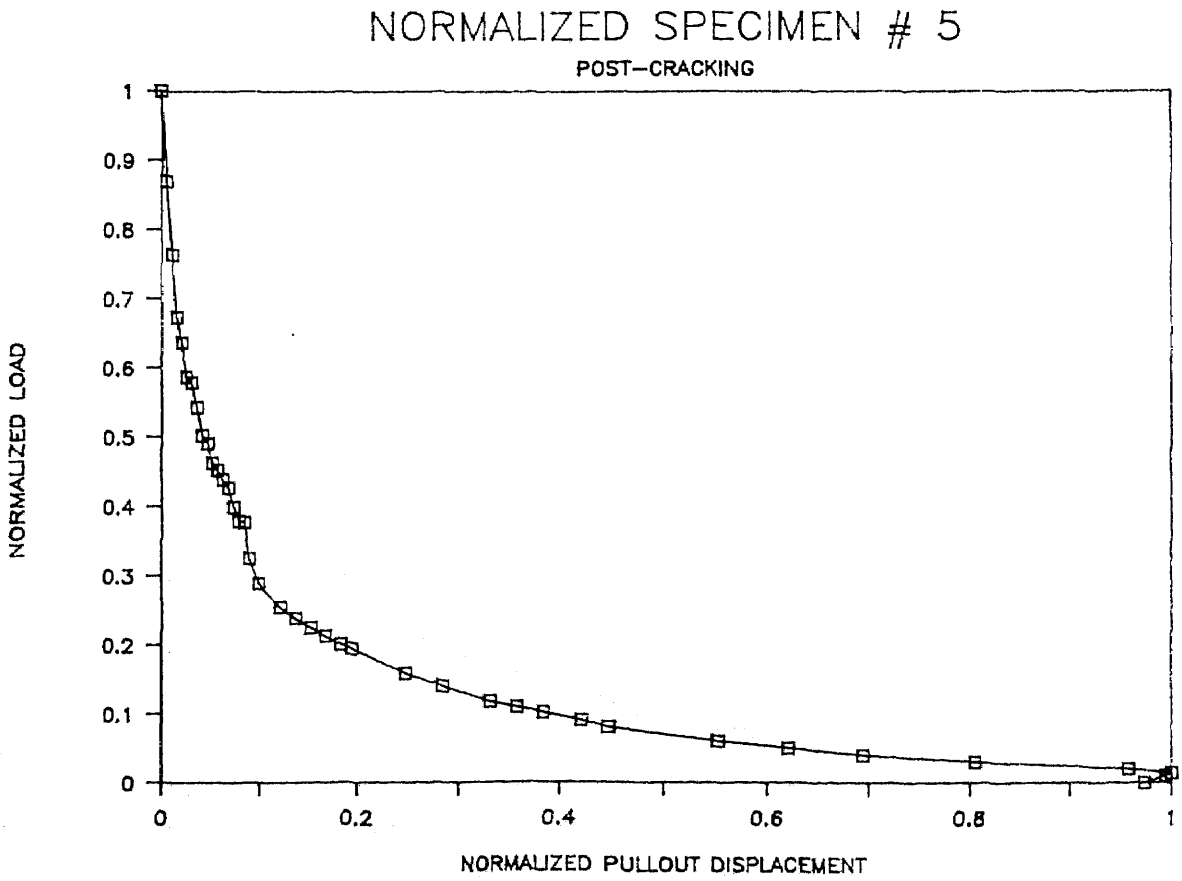
NORMALIZED SPECIMEN # 5
POST-CRACKING
NORMALIZED LOAD
NORMALIZED PULLOUT DISPLACEMENT
0
0.1
0.2
0.3
0.4
0.5
0.6
0.7
0.8
0.9
1
0
0.2
0.4
0.6
0.8
1

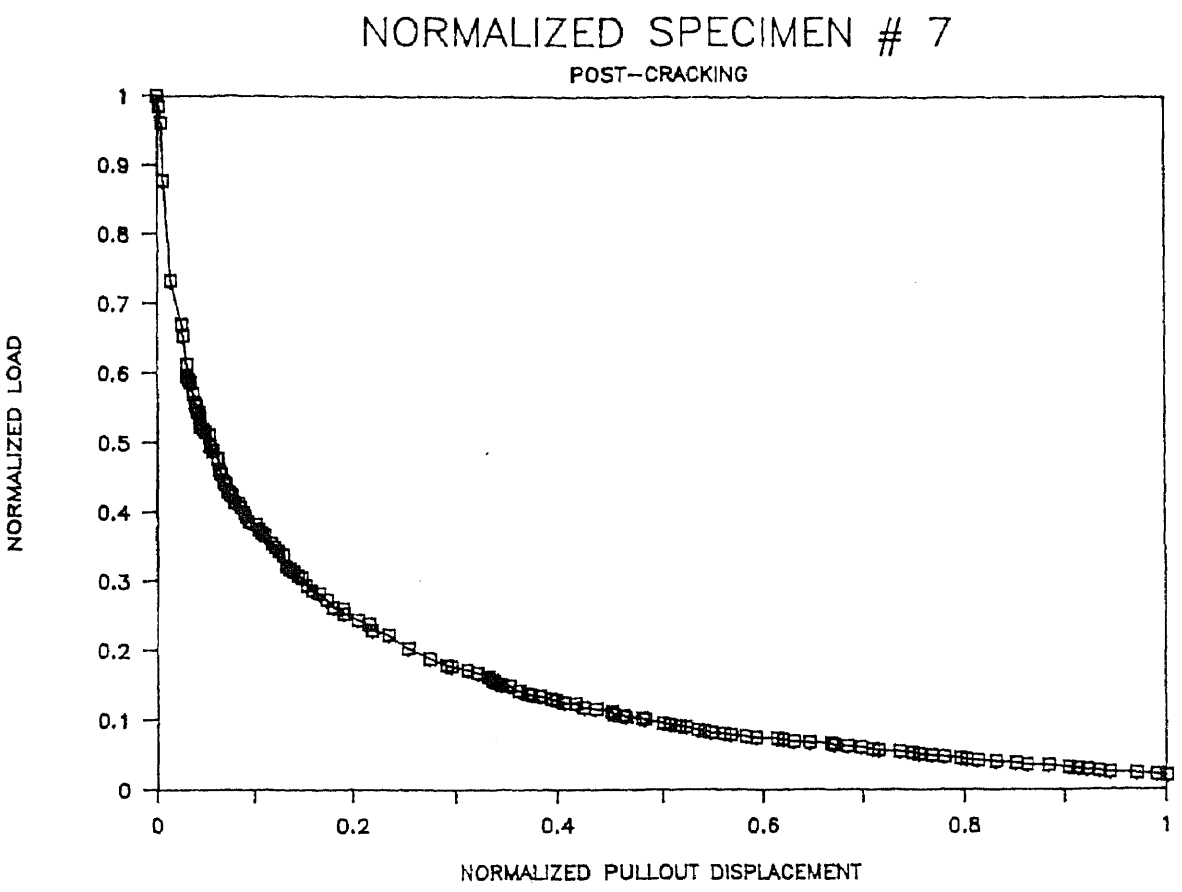
NORMALIZED SPECIMEN # 7
POST-CRACKING
NORMALIZED LOAD
NORMALIZED PULLOUT DISPLACEMENT
0
0.1
0.2
0.3
0.4
0.5
0.6
0.7
0.8
0.9
1
0
0.2
0.4
0.6
0.8
1

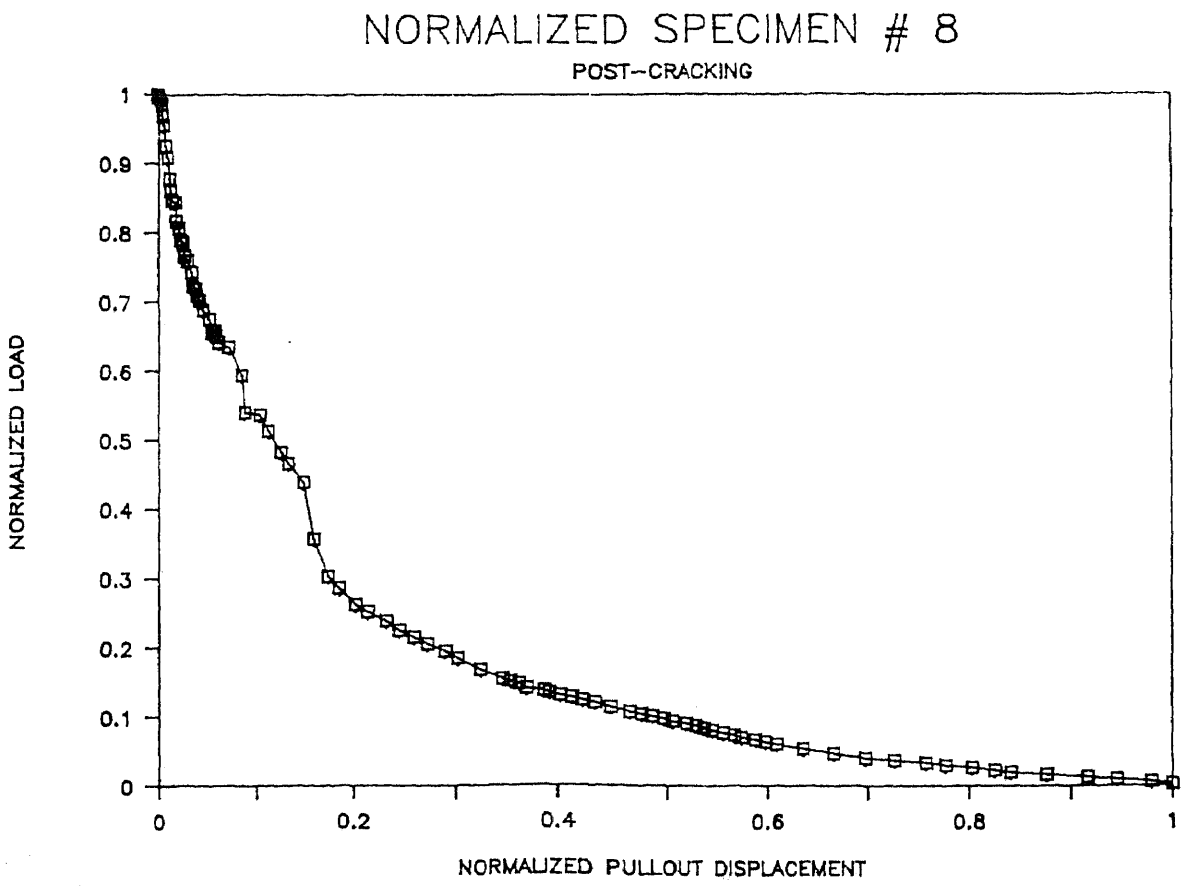
NORMALIZED SPECIMEN # 8
POST-CRACKING
NORMALIZED LOAD
NORMALIZED PULLOUT DISPLACEMENT
0
0.1
0.2
0.3
0.4
0.5
0.6
0.7
0.8
0.9
1
0
0.2
0.4
0.6
0.8
1

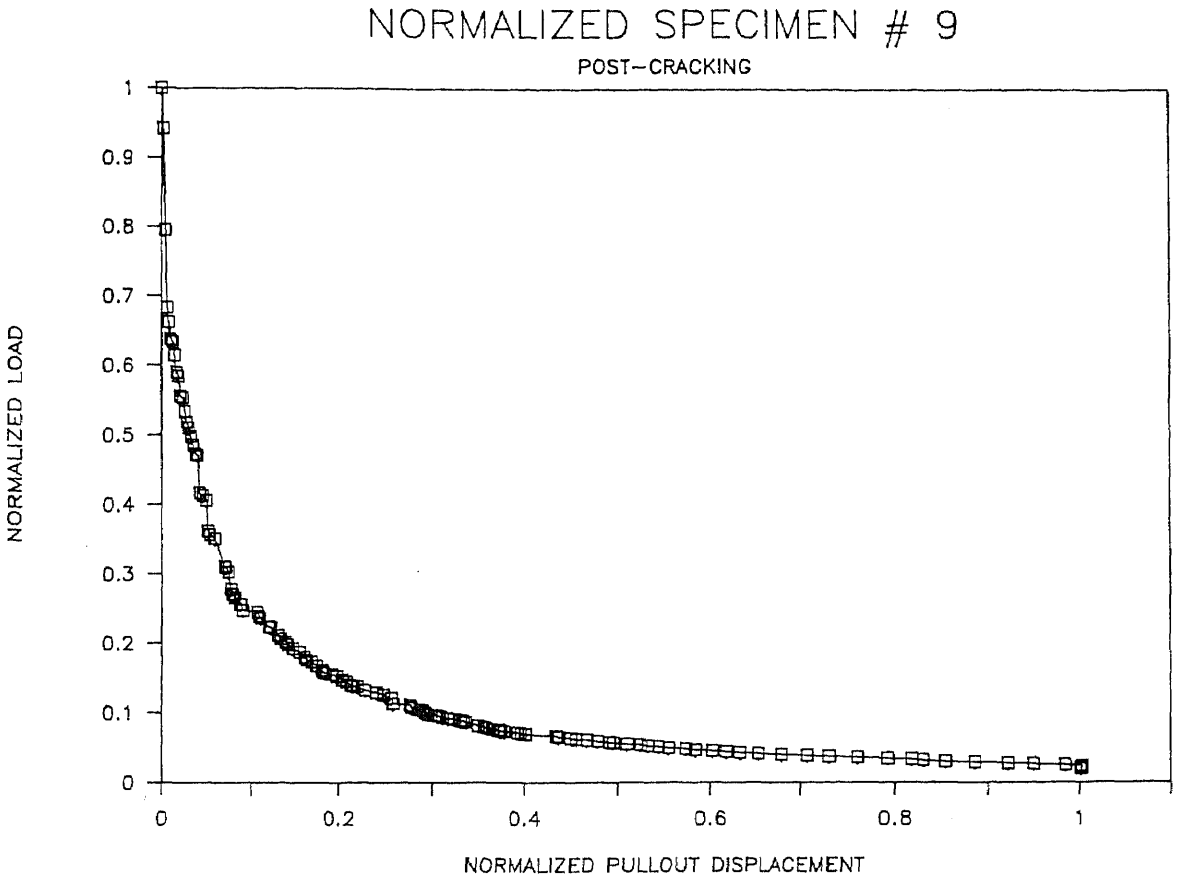
NORMALIZED SPECIMEN # 9
POST-CRACKING
NORMALIZED LOAD
NORMALIZED PULLOUT DISPLACEMENT
0
0.1
0.2
0.3
0.4
0.5
0.6
0.7
0.8
0.9
1
0
0.2
0.4
0.6
0.8
1

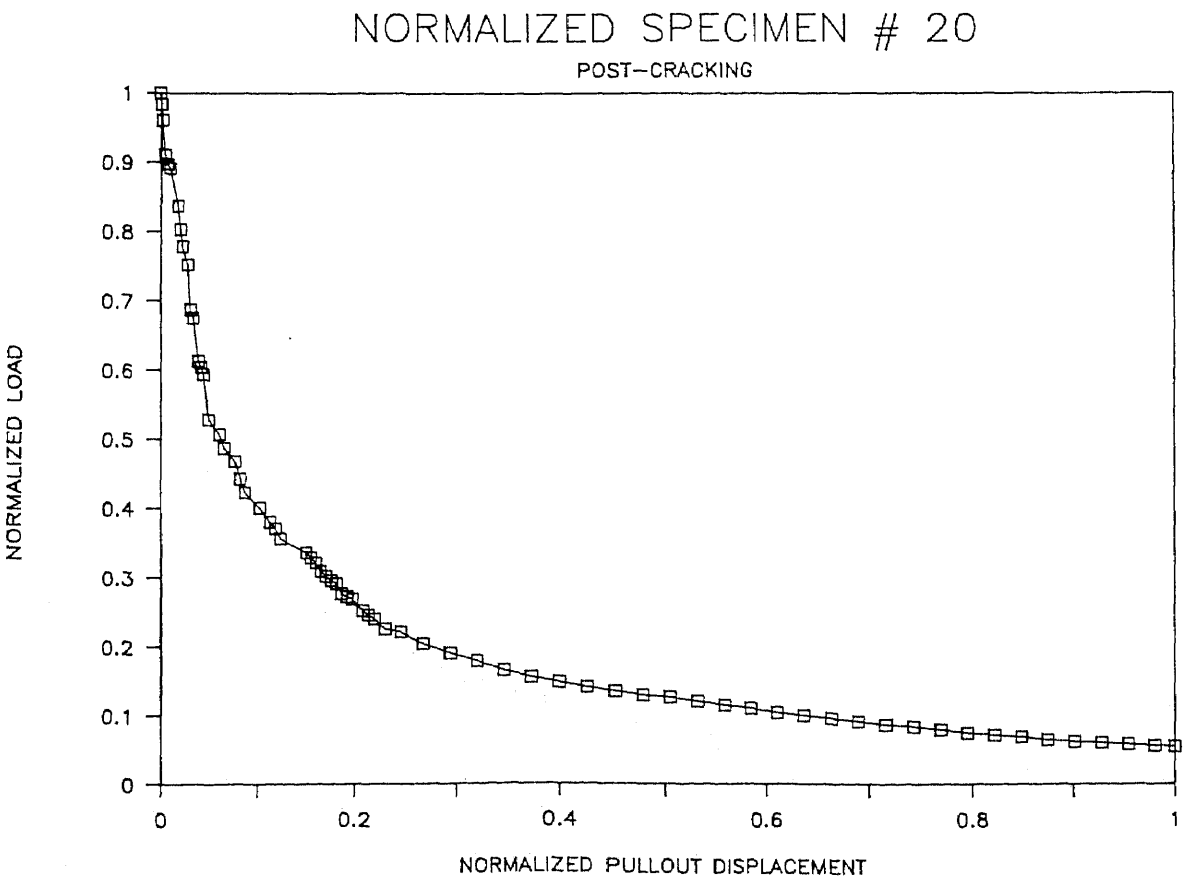
NORMALIZED SPECIMEN # 20
POST-CRACKING
NORMALIZED LOAD
NORMALIZED PULLOUT DISPLACEMENT
0
0.1
0.2
0.3
0.4
0.5
0.6
0.7
0.8
0.9
1
0
0.2
0.4
0.6
0.8
1

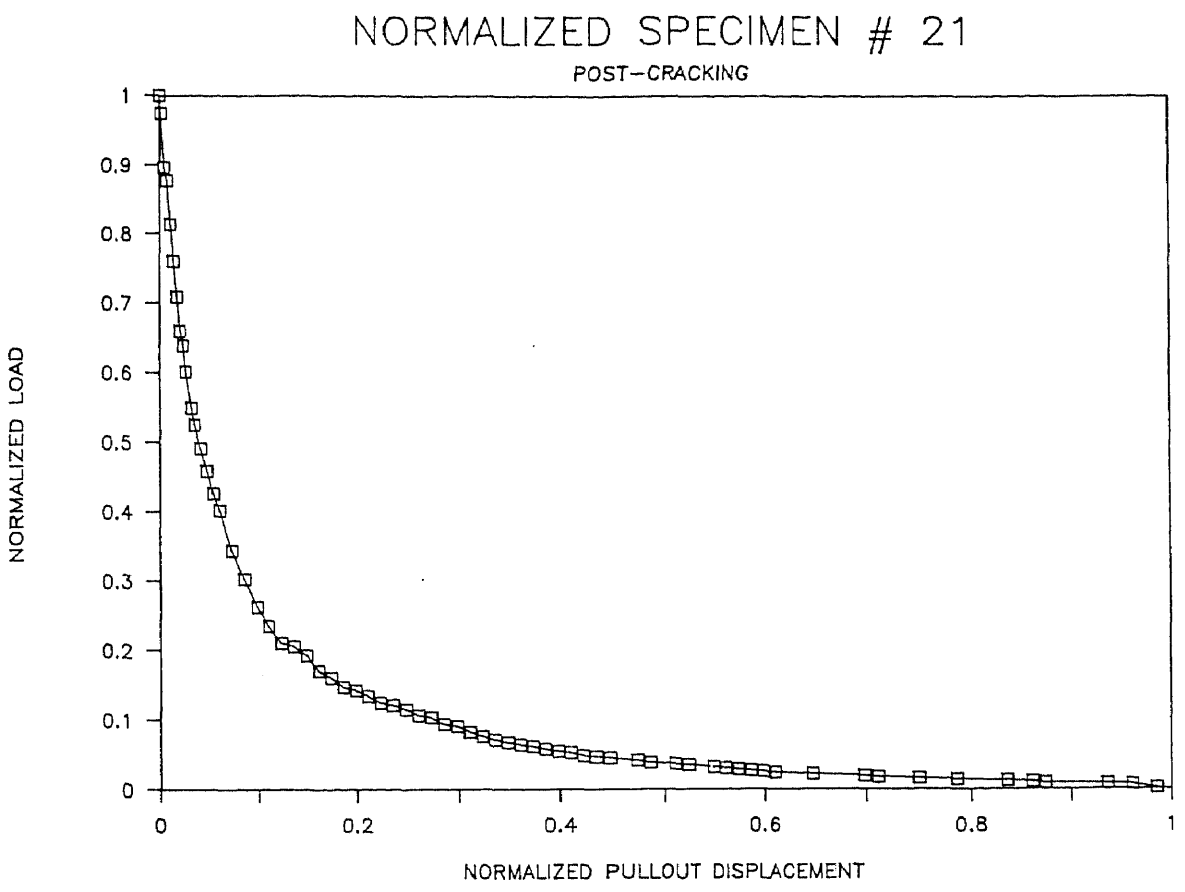
NORMALIZED SPECIMEN # 21
POST-CRACKING
NORMALIZED LOAD
NORMALIZED PULLOUT DISPLACEMENT
0
0.1
0.2
0.3
0.4
0.5
0.6
0.7
0.8
0.9
1
0
0.2
0.4
0.6
0.8
1

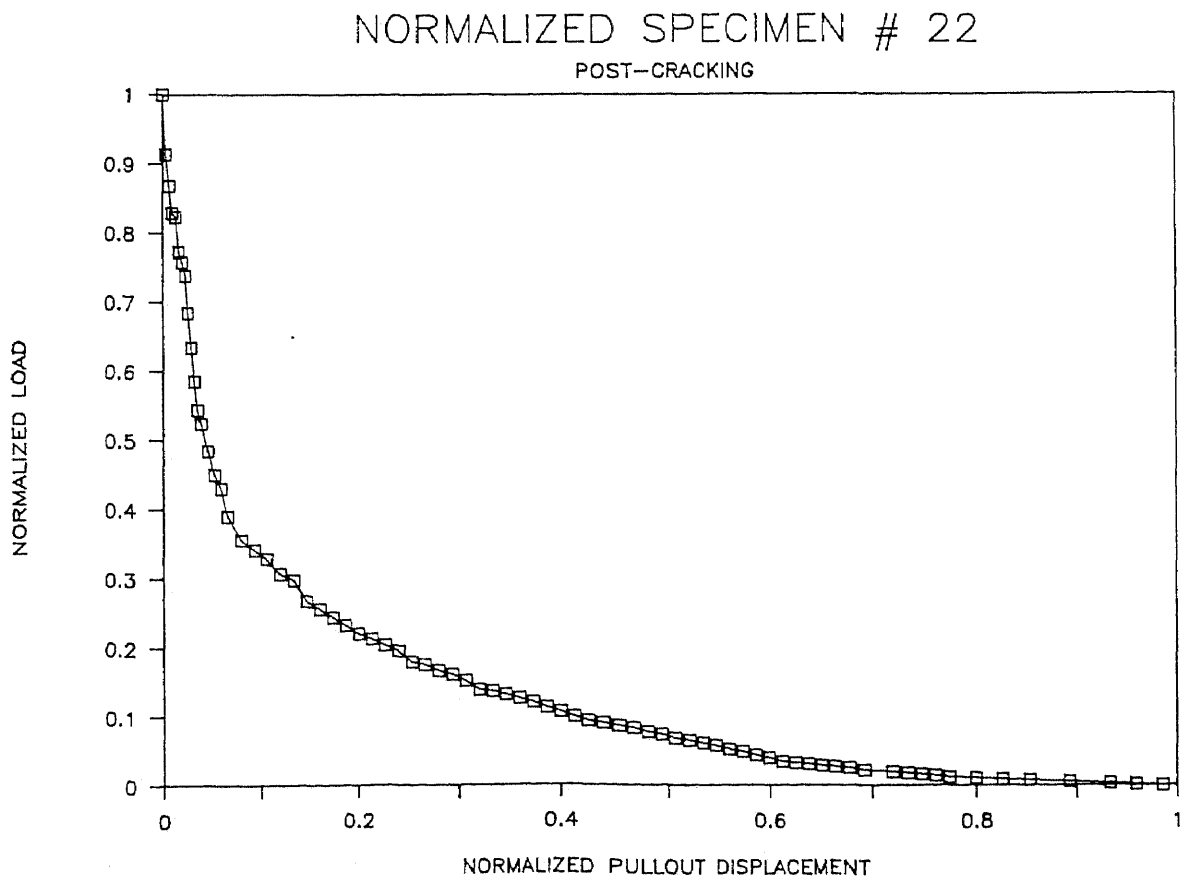
NORMALIZED SPECIMEN # 22
POST-CRACKING
NORMALIZED LOAD
NORMALIZED PULLOUT DISPLACEMENT
0
0.1
0.2
0.3
0.4
0.5
0.6
0.7
0.8
0.9
1
0
0.2
0.4
0.6
0.8
1

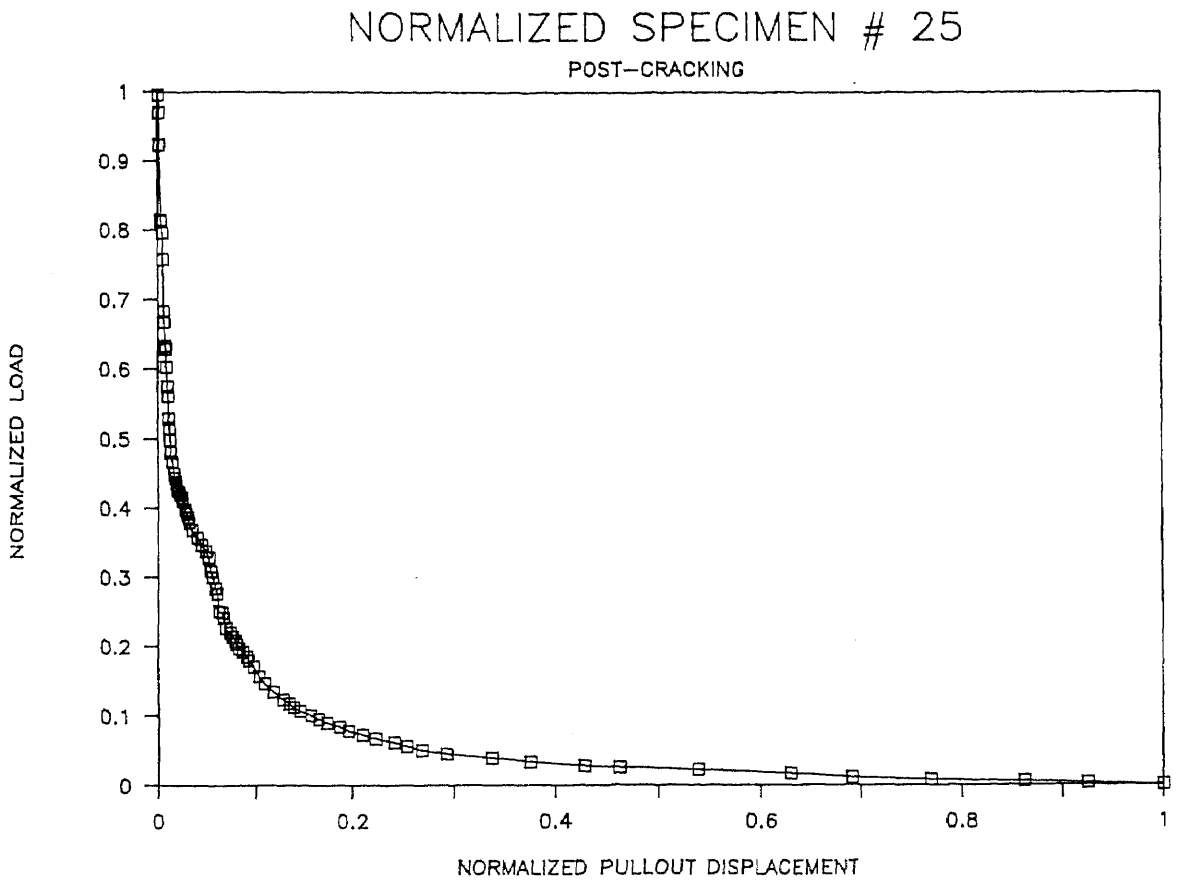
NORMALIZED SPECIMEN # 25
POST-CRACKING
NORMALIZED LOAD
NORMALIZED PULLOUT DISPLACEMENT
0
0.1
0.2
0.3
0.4
0.5
0.6
0.7
0.8
0.9
1
0
0.2
0.4
0.6
0.8
1

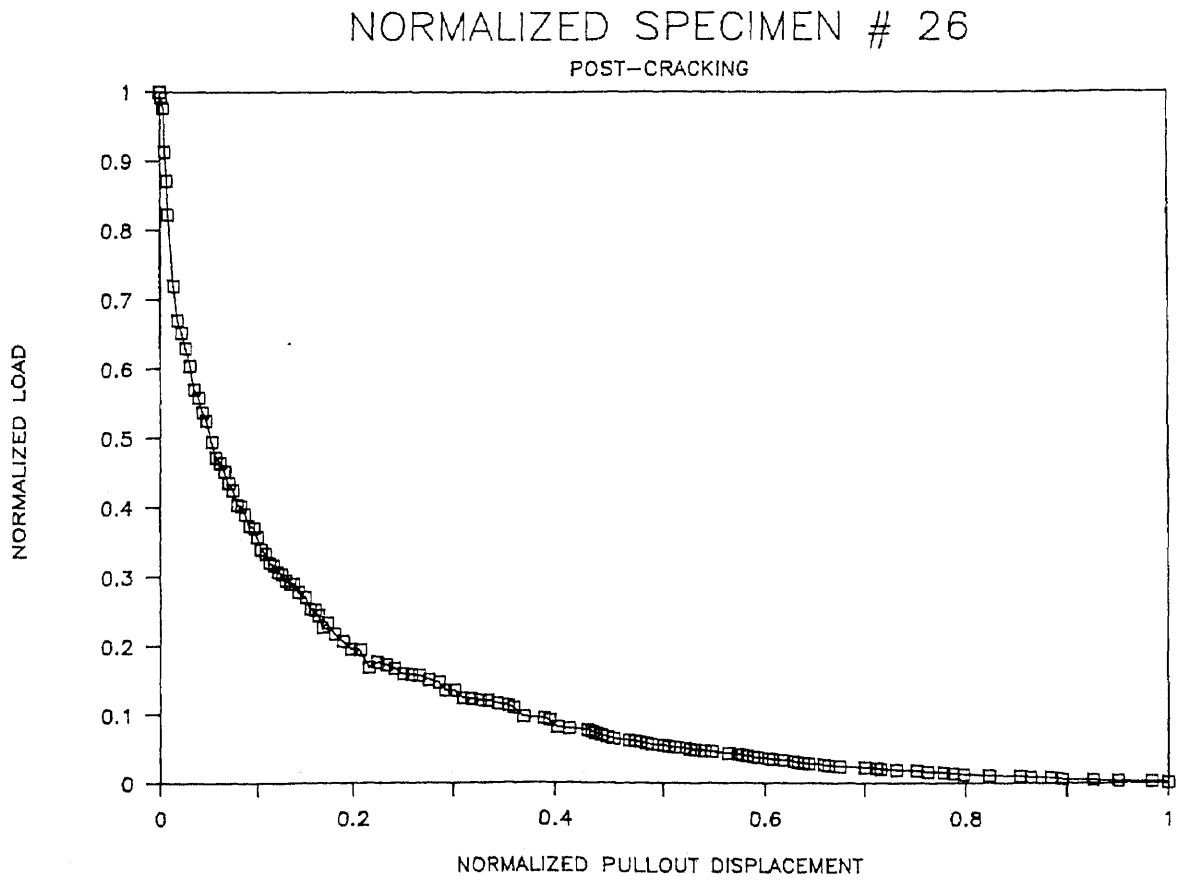
NORMALIZED SPECIMEN # 26
POST-CRACKING
NORMALIZED LOAD
NORMALIZED PULLOUT DISPLACEMENT
0
0.1
0.2
0.3
0.4
0.5
0.6
0.7
0.8
0.9
1
0
0.2
0.4
0.6
0.8
1

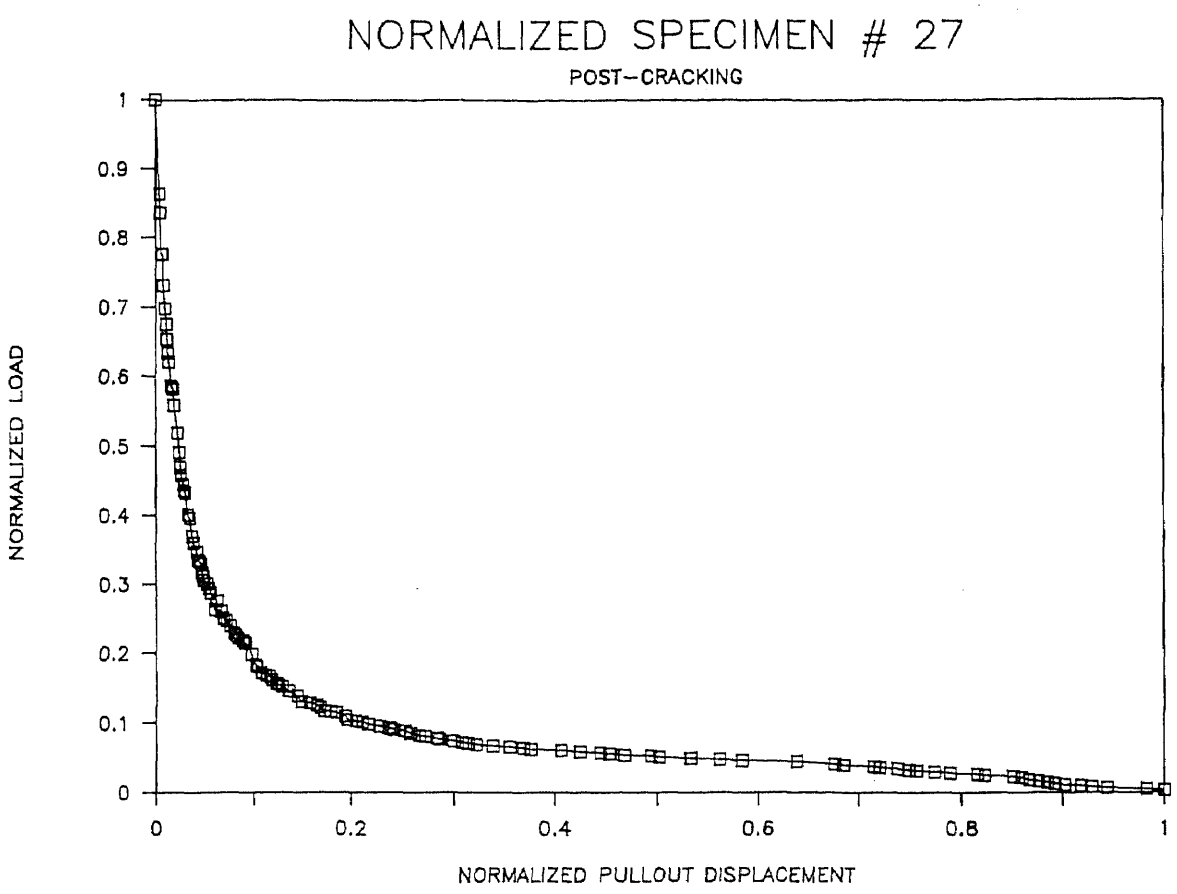
NORMALIZED SPECIMEN # 27
POST-CRACKING
NORMALIZED LOAD
0
0.1
0.2
0.3
0.4
0.5
0.6
0.7
0.8
0.9
1
0
0.2
0.4
0.6
0.8
1
NORMALIZED PULLOUT DISPLACEMENT

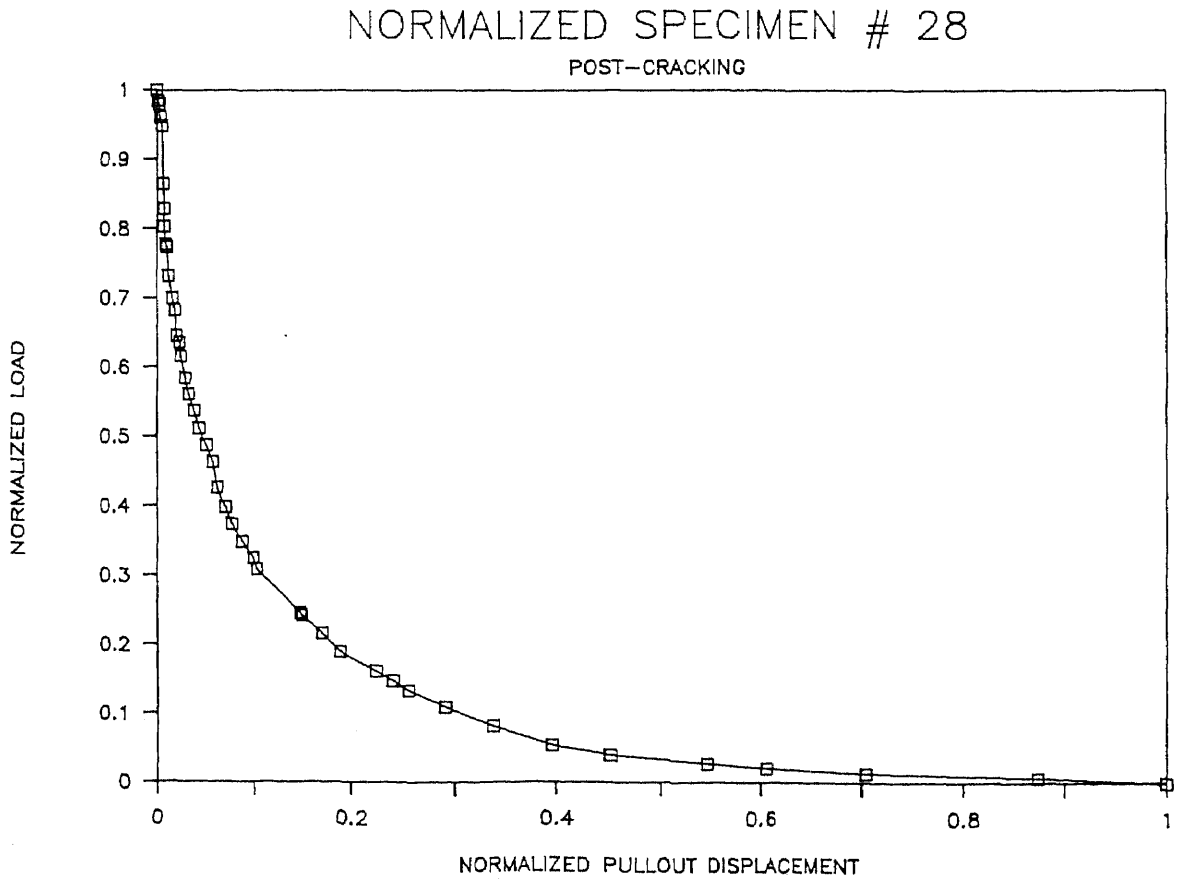
NORMALIZED SPECIMEN # 28
POST-CRACKING
NORMALIZED LOAD
0
0.1
0.2
0.3
0.4
0.5
0.6
0.7
0.8
0.9
1
0
0.2
0.4
0.6
0.8
1
NORMALIZED PULLOUT DISPLACEMENT

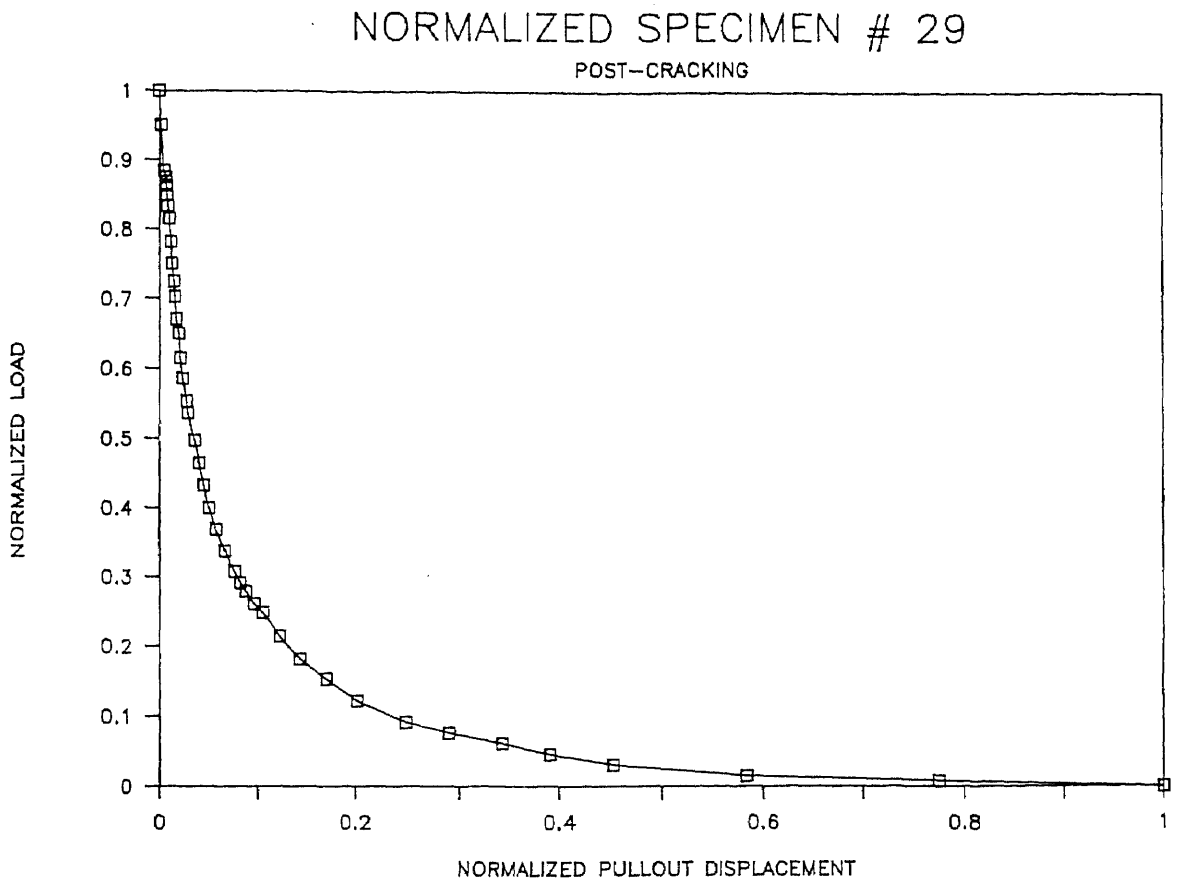
NORMALIZED SPECIMEN # 29
POST-CRACKING
NORMALIZED LOAD
0
0.1
0.2
0.3
0.4
0.5
0.6
0.7
0.8
0.9
1
0
0.2
0.4
0.6
0.8
1
NORMALIZED PULLOUT DISPLACEMENT

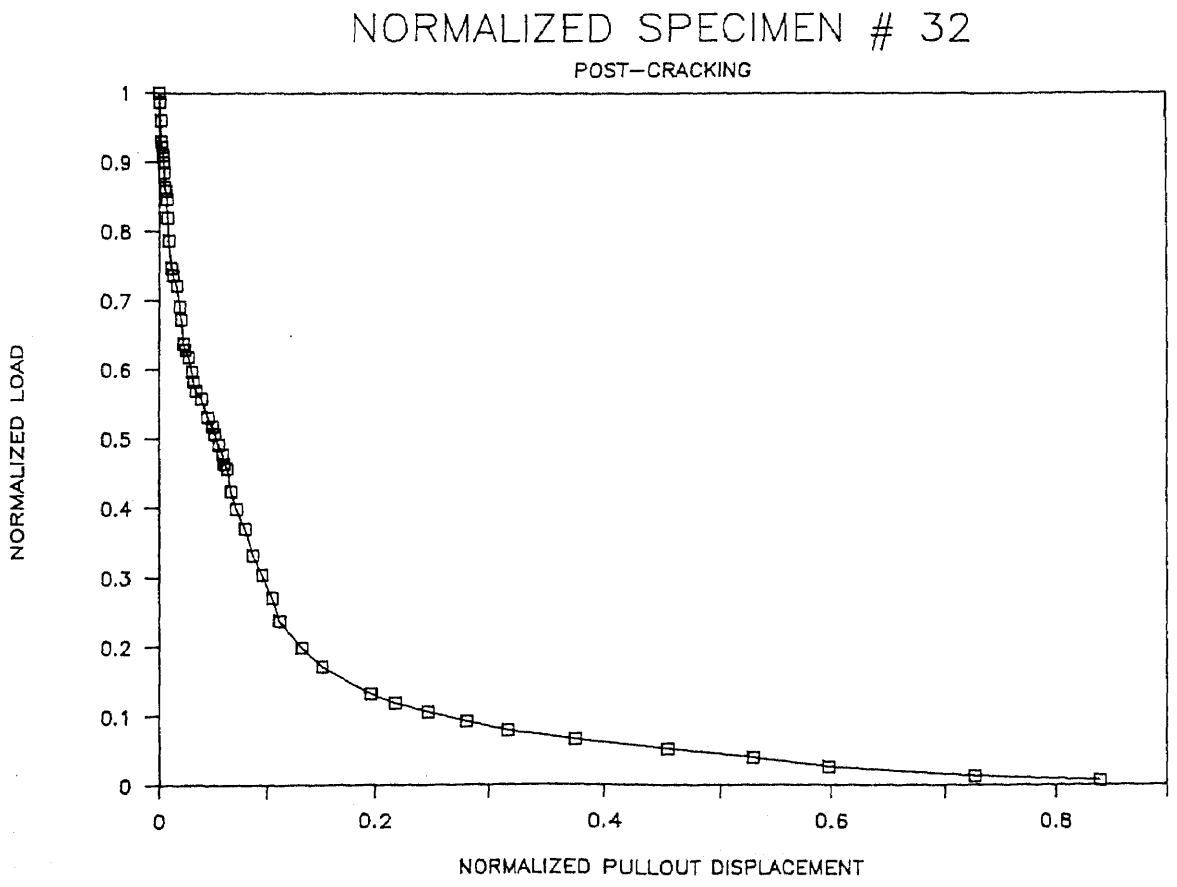
NORMALIZED SPECIMEN # 32
POST-CRACKING
NORMALIZED LOAD
0
0.1
0.2
0.3
0.4
0.5
0.6
0.7
0.8
0.9
1
0
0.2
0.4
0.6
0.8
NORMALIZED PULLOUT DISPLACEMENT

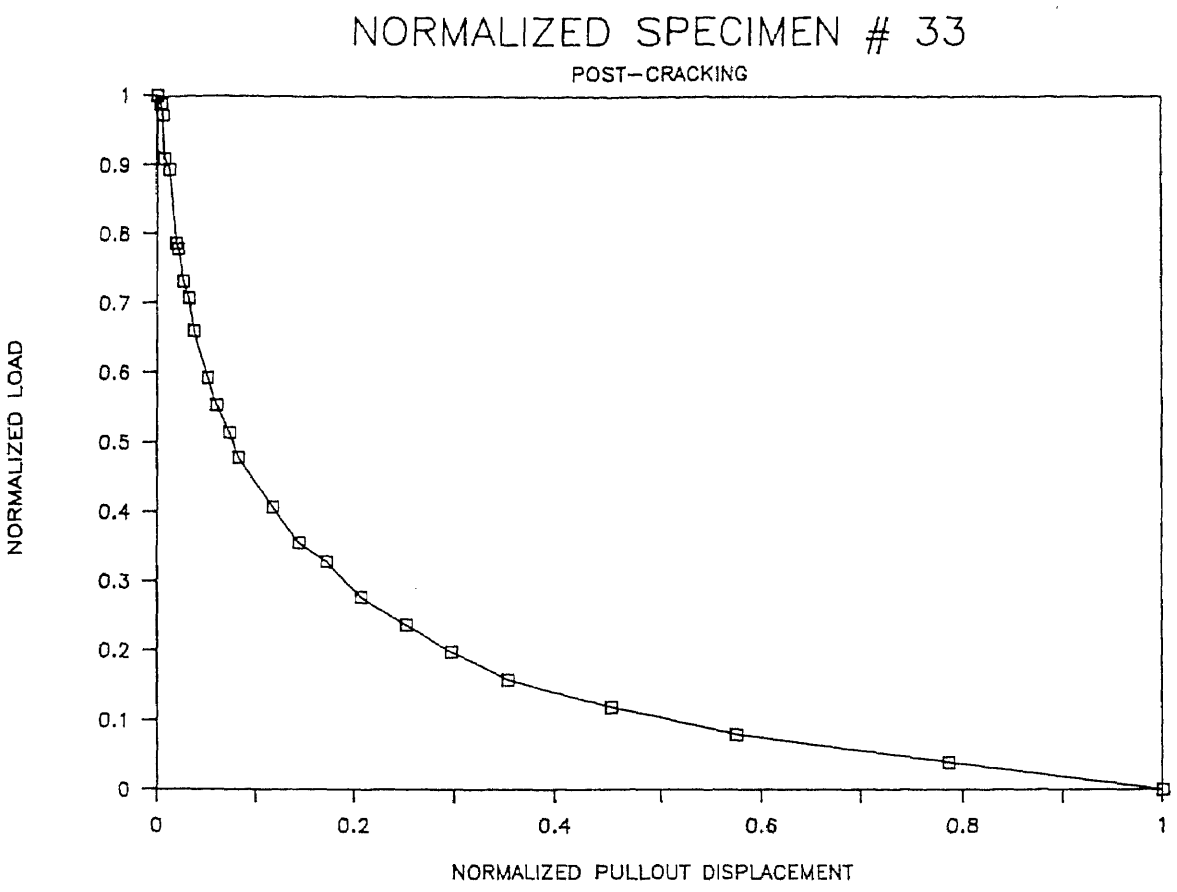
NORMALIZED SPECIMEN # 33
POST-CRACKING
NORMALIZED LOAD
0
0.1
0.2
0.3
0.4
0.5
0.6
0.7
0.8
0.9
1
0
0.2
0.4
0.6
0.8
1
NORMALIZED PULLOUT DISPLACEMENT

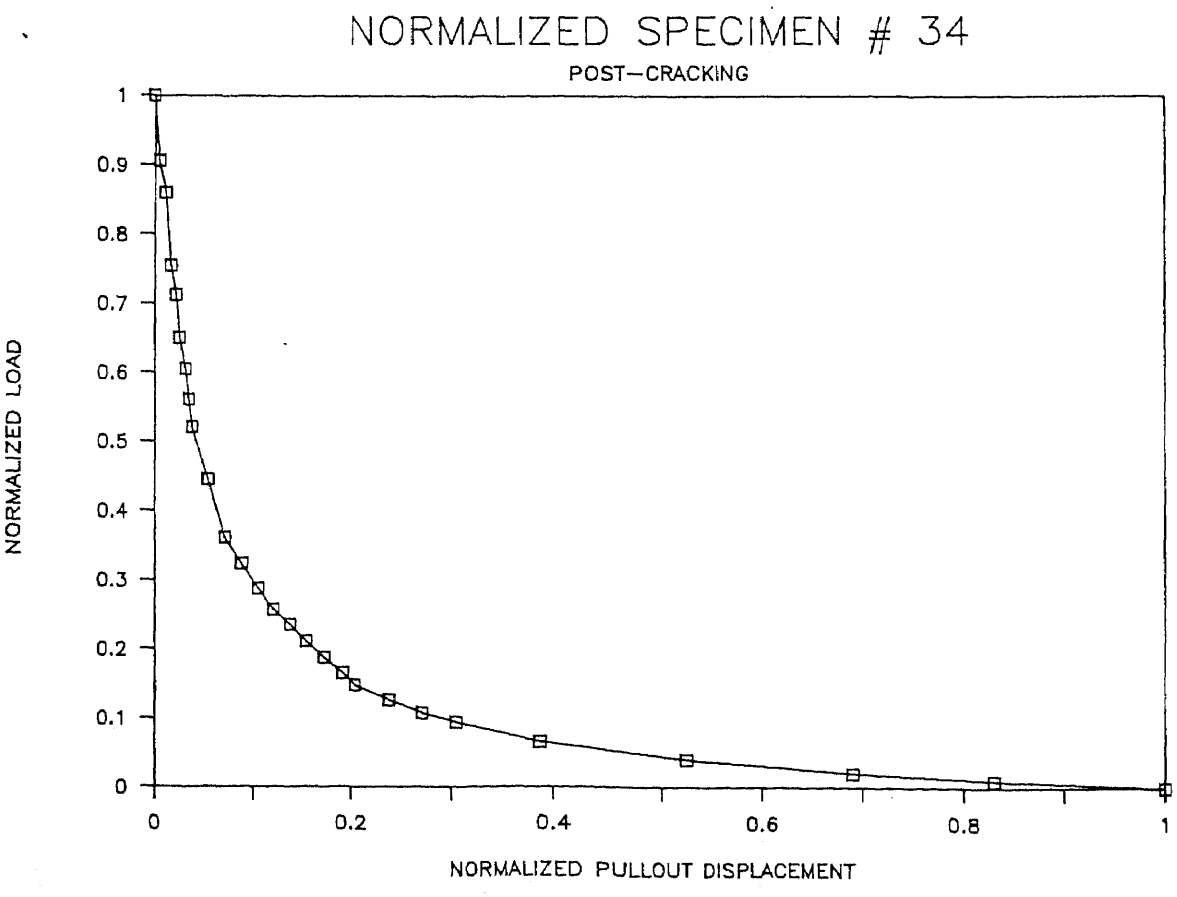
NORMALIZED SPECIMEN # 34
POST-CRACKING
NORMALIZED LOAD
0
0.1
0.2
0.3
0.4
0.5
0.6
0.7
0.8
0.9
1
0
0.2
0.4
0.6
0.8
1
NORMALIZED PULLOUT DISPLACEMENT

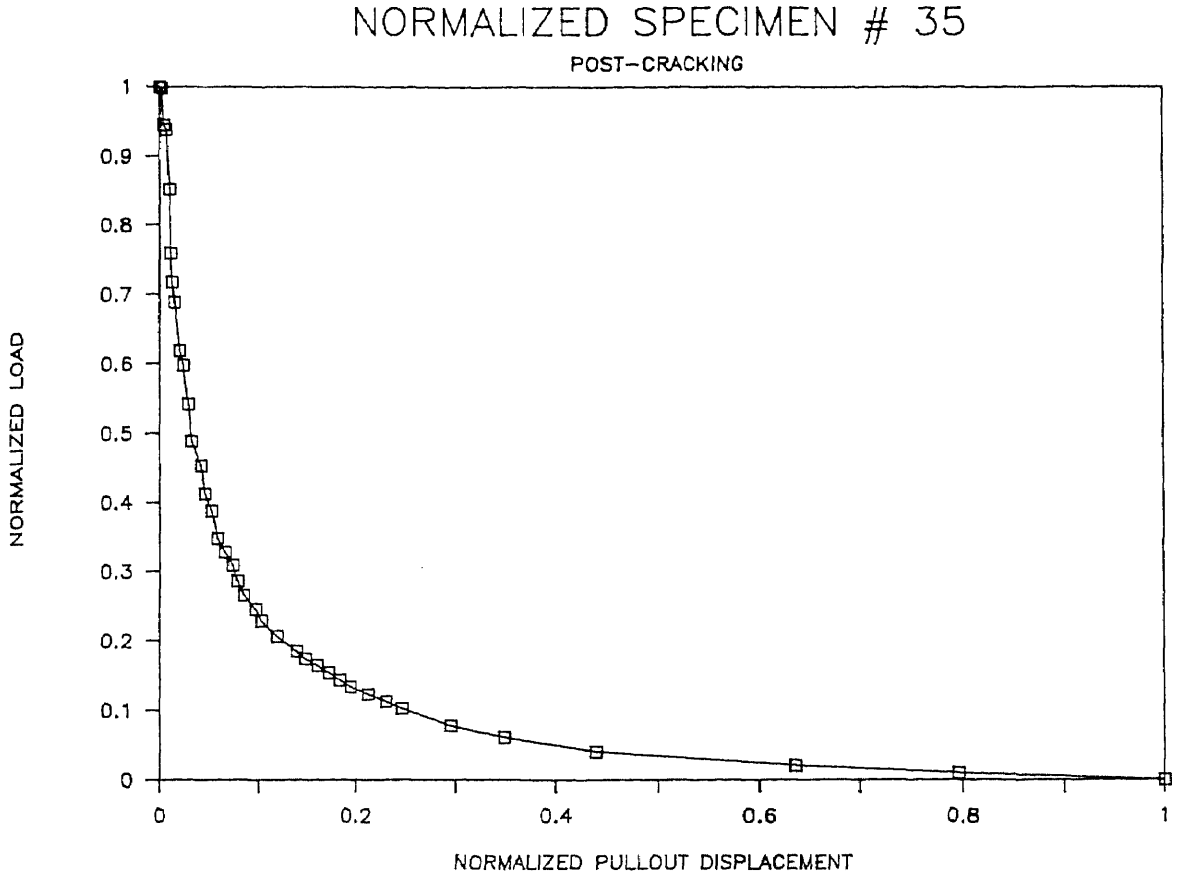
NORMALIZED SPECIMEN # 35
POST-CRACKING
NORMALIZED LOAD
0
0.1
0.2
0.3
0.4
0.5
0.6
0.7
0.8
0.9
1
0
0.2
0.4
0.6
0.8
1
NORMALIZED PULLOUT DISPLACEMENT

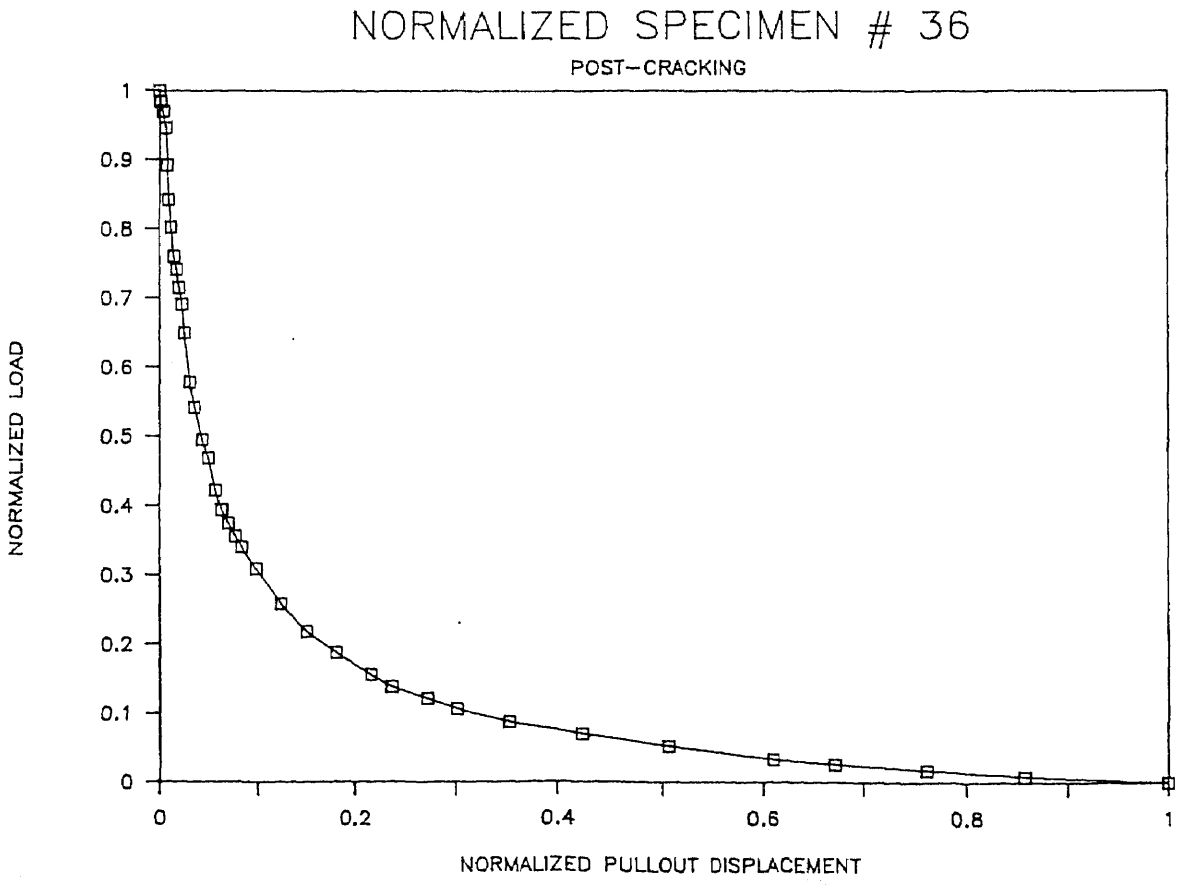
NORMALIZED SPECIMEN # 36
POST-CRACKING
NORMALIZED LOAD
0
0.1
0.2
0.3
0.4
0.5
0.6
0.7
0.8
0.9
1
0
0.2
0.4
0.6
0.8
1
NORMALIZED PULLOUT DISPLACEMENT

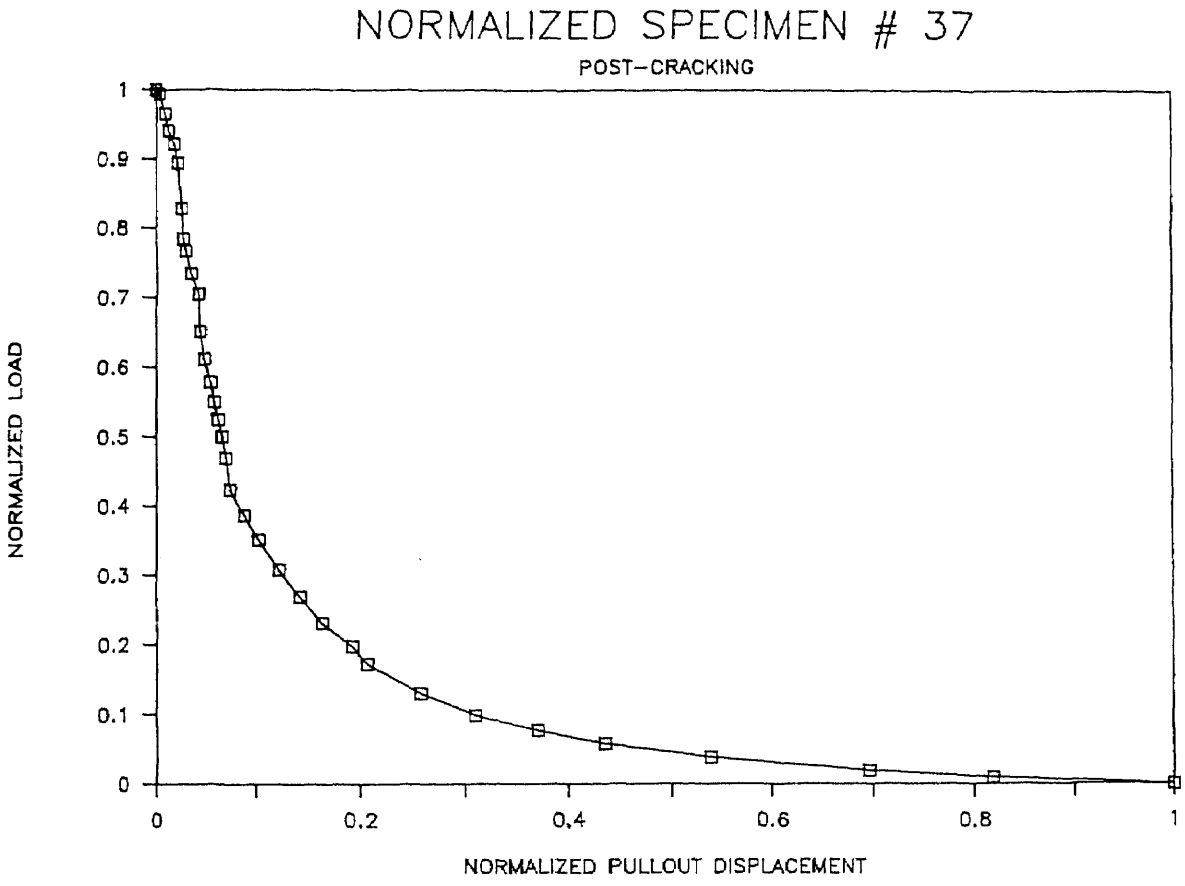
NORMALIZED SPECIMEN # 37
POST-CRACKING
NORMALIZED LOAD
NORMALIZED PULLOUT DISPLACEMENT
0
0.1
0.2
0.3
0.4
0.5
0.6
0.7
0.8
0.9
1
0
0.2
0.4
0.6
0.8
1

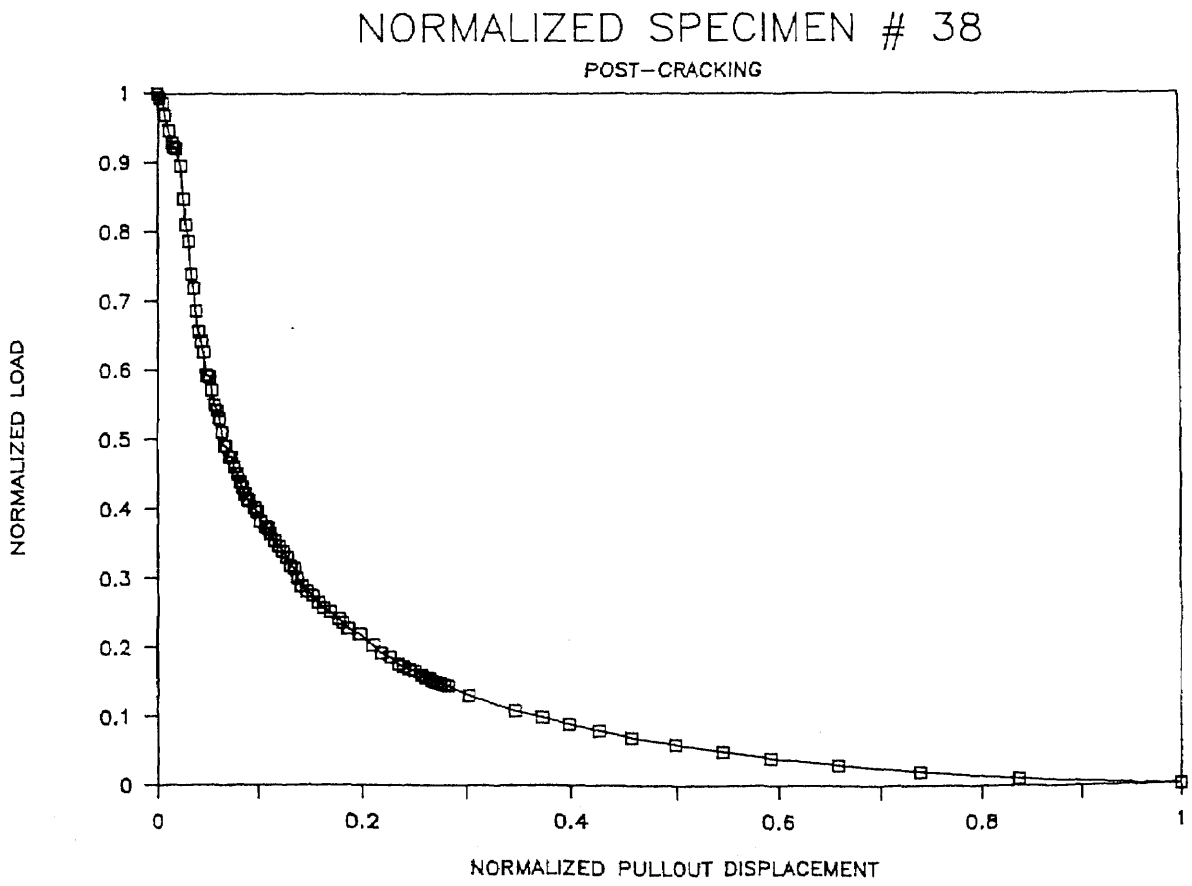
NORMALIZED SPECIMEN # 38
POST-CRACKING
NORMALIZED LOAD
NORMALIZED PULLOUT DISPLACEMENT
0
0.1
0.2
0.3
0.4
0.5
0.6
0.7
0.8
0.9
1
0
0.2
0.4
0.6
0.8
1

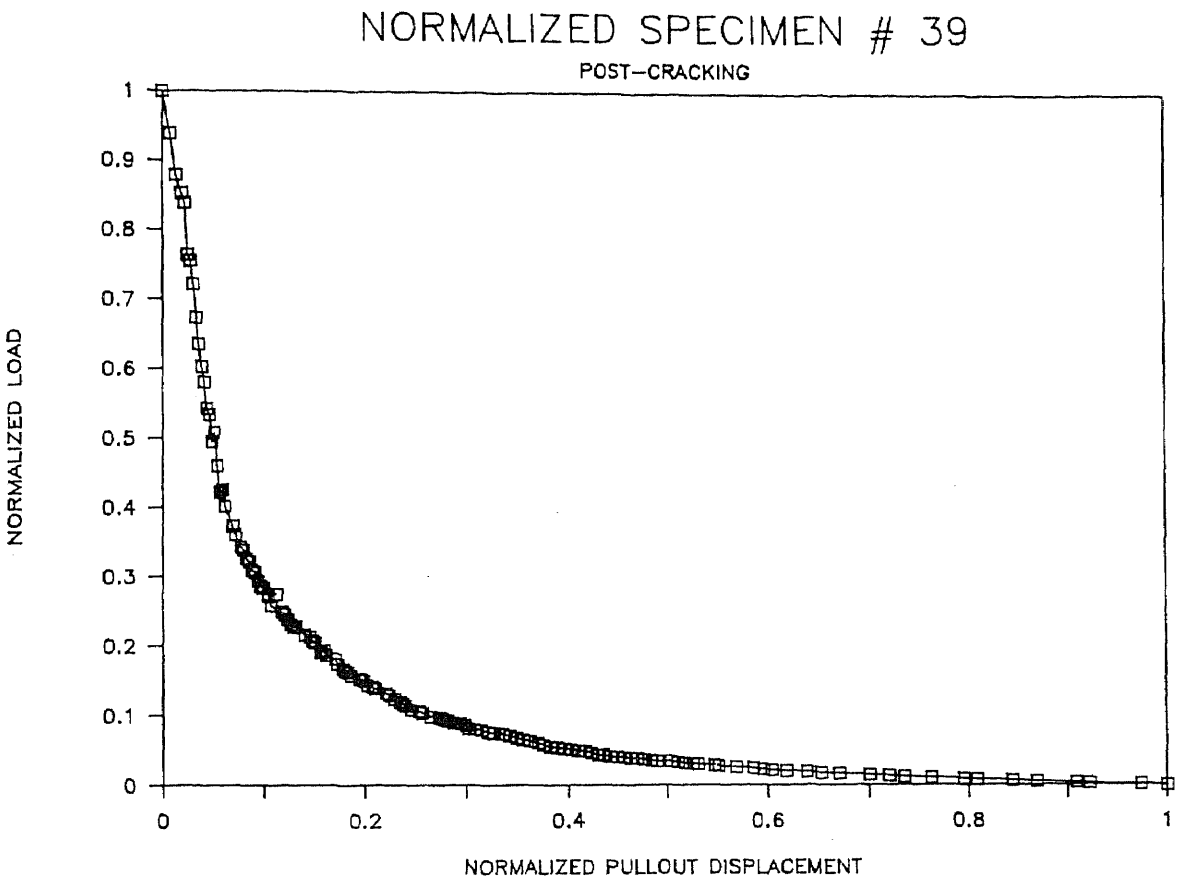
NORMALIZED SPECIMEN # 39
POST-CRACKING
NORMALIZED LOAD
NORMALIZED PULLOUT DISPLACEMENT
0
0.1
0.2
0.3
0.4
0.5
0.6
0.7
0.8
0.9
1
0
0.2
0.4
0.6
0.8
1

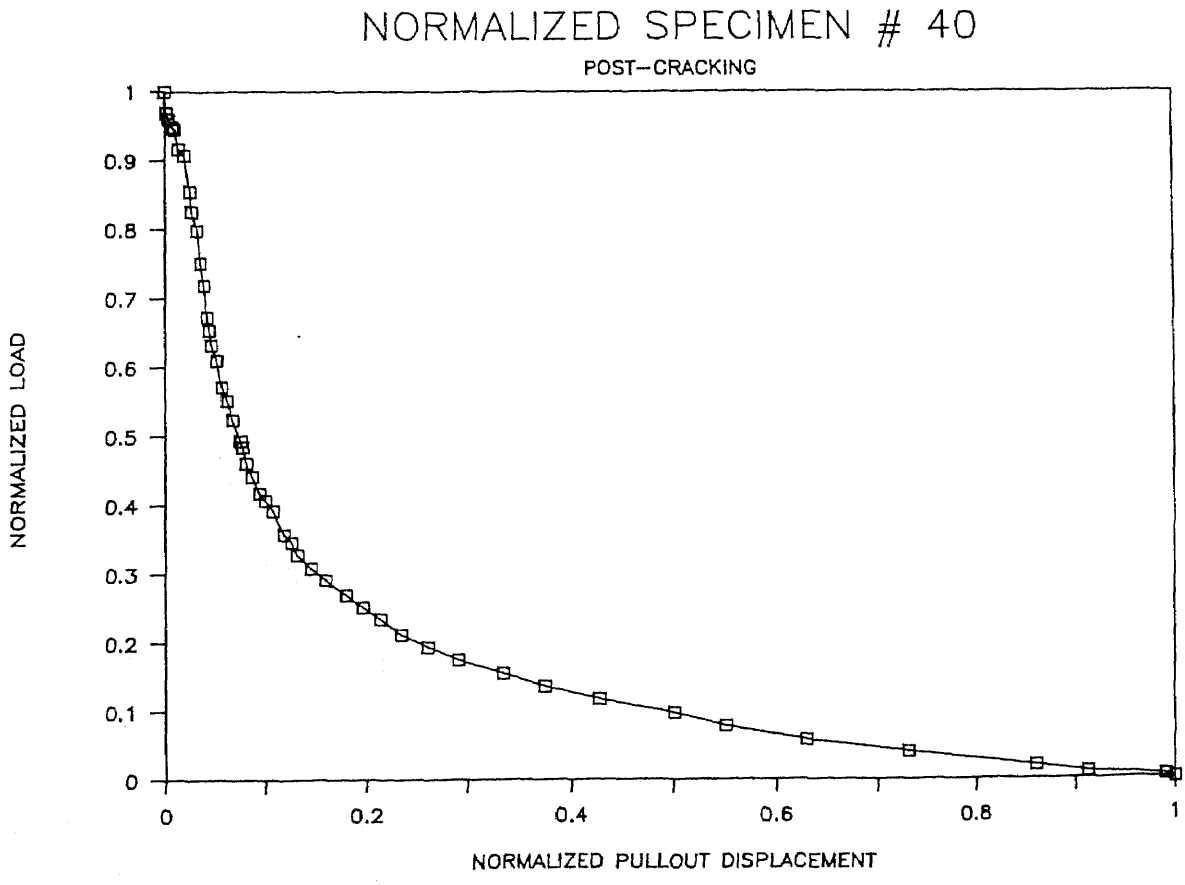
NORMALIZED SPECIMEN # 40
POST-CRACKING
NORMALIZED LOAD
NORMALIZED PULLOUT DISPLACEMENT
0
0.1
0.2
0.3
0.4
0.5
0.6
0.7
0.8
0.9
1
0
0.2
0.4
0.6
0.8
1

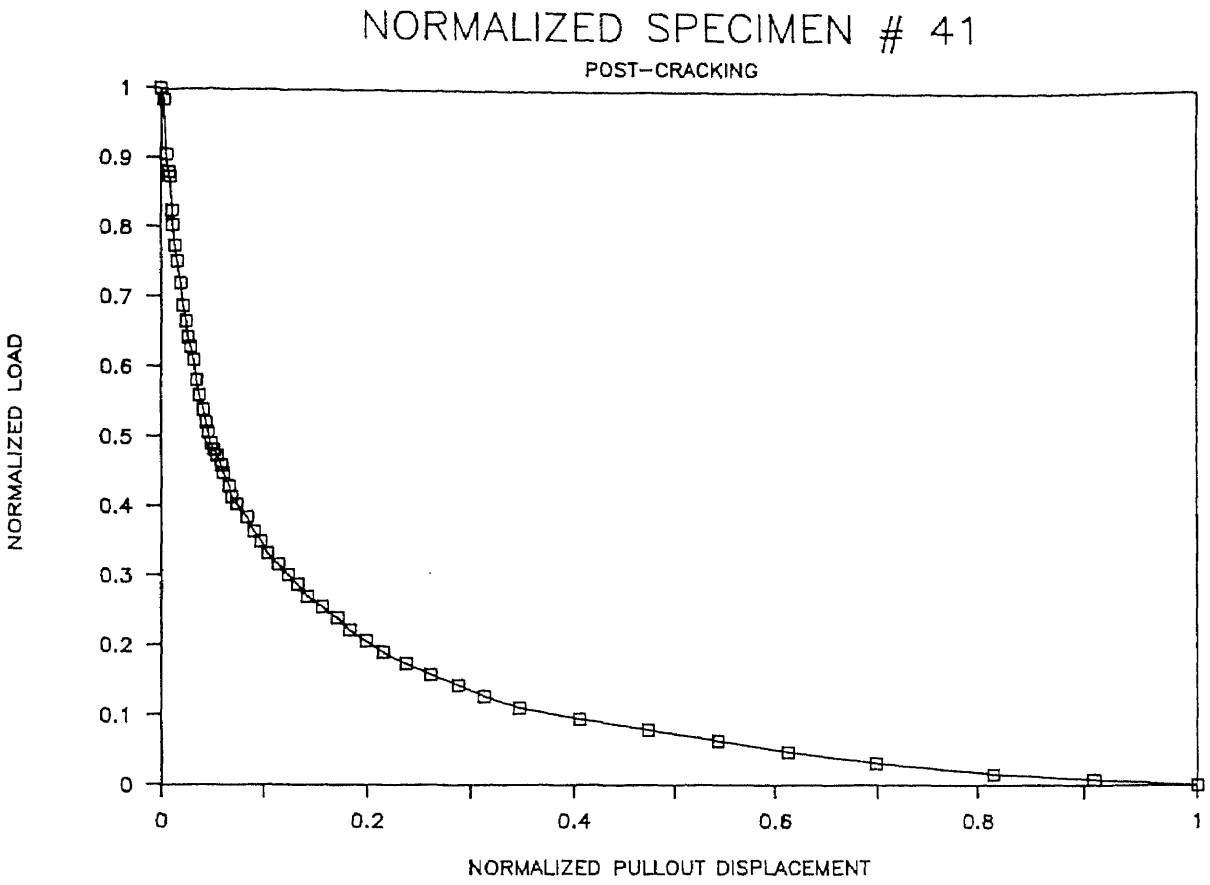
NORMALIZED SPECIMEN # 41
POST-CRACKING
NORMALIZED LOAD
NORMALIZED PULLOUT DISPLACEMENT
0
0.1
0.2
0.3
0.4
0.5
0.6
0.7
0.8
0.9
1
0
0.2
0.4
0.6
0.8
1

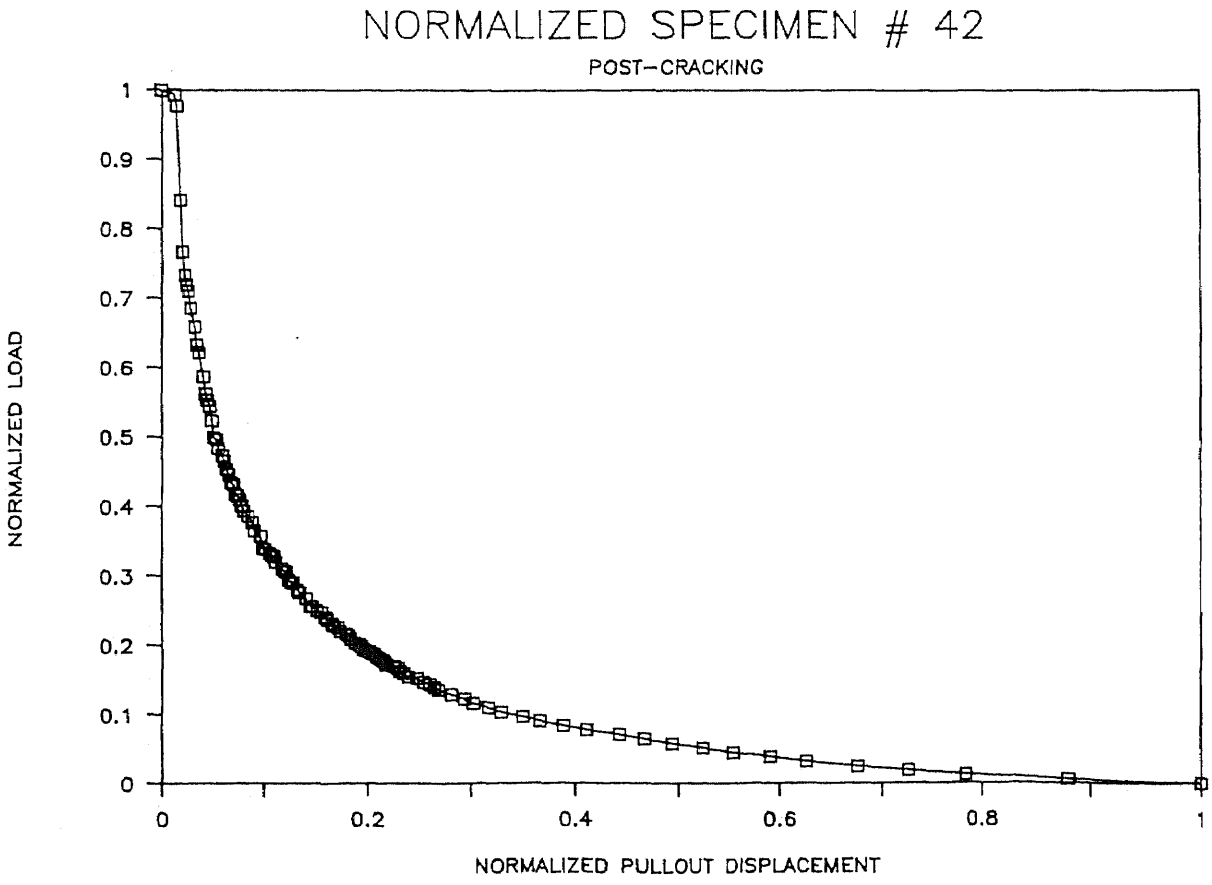
NORMALIZED SPECIMEN # 42
POST-CRACKING
NORMALIZED LOAD
NORMALIZED PULLOUT DISPLACEMENT
0
0.1
0.2
0.3
0.4
0.5
0.6
0.7
0.8
0.9
1
0
0.2
0.4
0.6
0.8
1

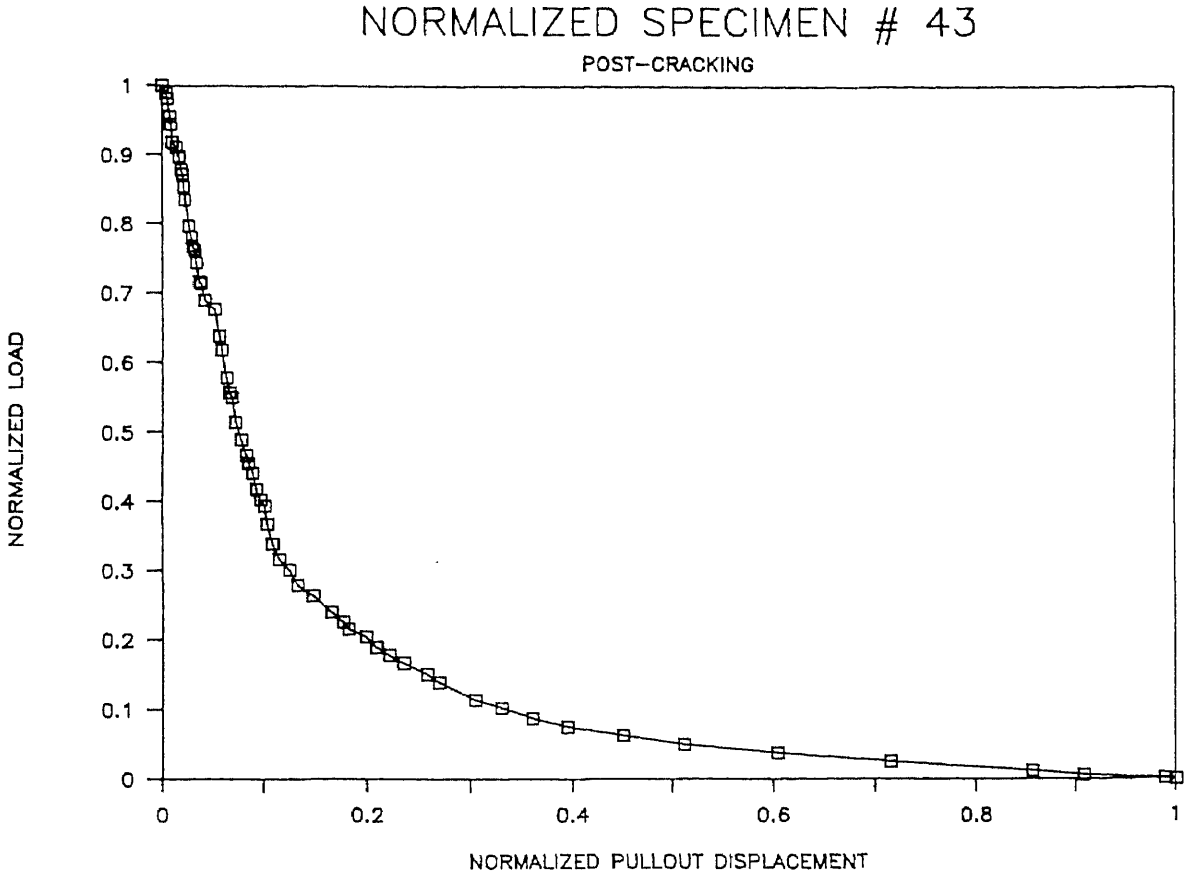
NORMALIZED SPECIMEN # 43
POST-CRACKING
NORMALIZED LOAD
NORMALIZED PULLOUT DISPLACEMENT
0
0.1
0.2
0.3
0.4
0.5
0.6
0.7
0.8
0.9
1
0
0.2
0.4
0.6
0.8
1

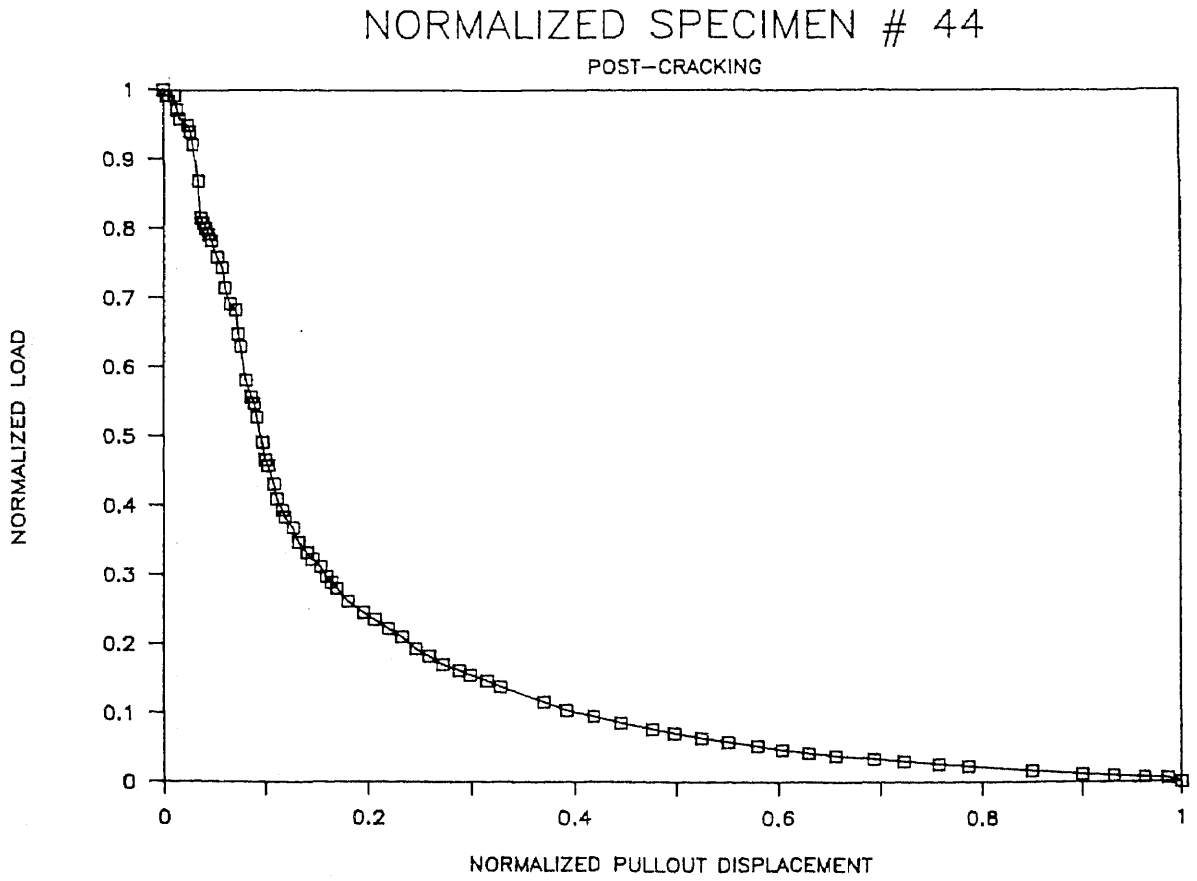
NORMALIZED SPECIMEN # 44
POST-CRACKING
NORMALIZED LOAD
NORMALIZED PULLOUT DISPLACEMENT
0
0.1
0.2
0.3
0.4
0.5
0.6
0.7
0.8
0.9
1
0
0.2
0.4
0.6
0.8
1

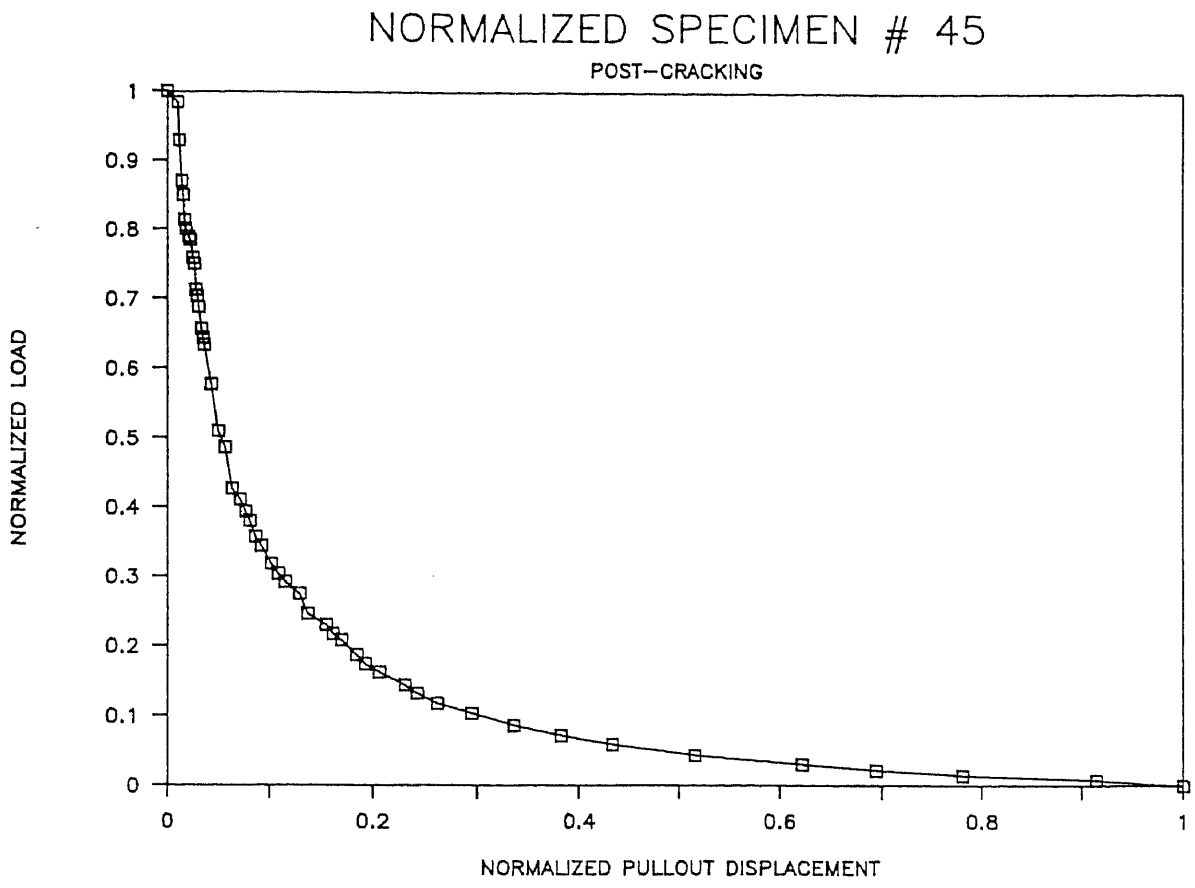
NORMALIZED SPECIMEN # 45
POST-CRACKING
NORMALIZED LOAD
NORMALIZED PULLOUT DISPLACEMENT
0
0.1
0.2
0.3
0.4
0.5
0.6
0.7
0.8
0.9
1
0
0.2
0.4
0.6
0.8
1

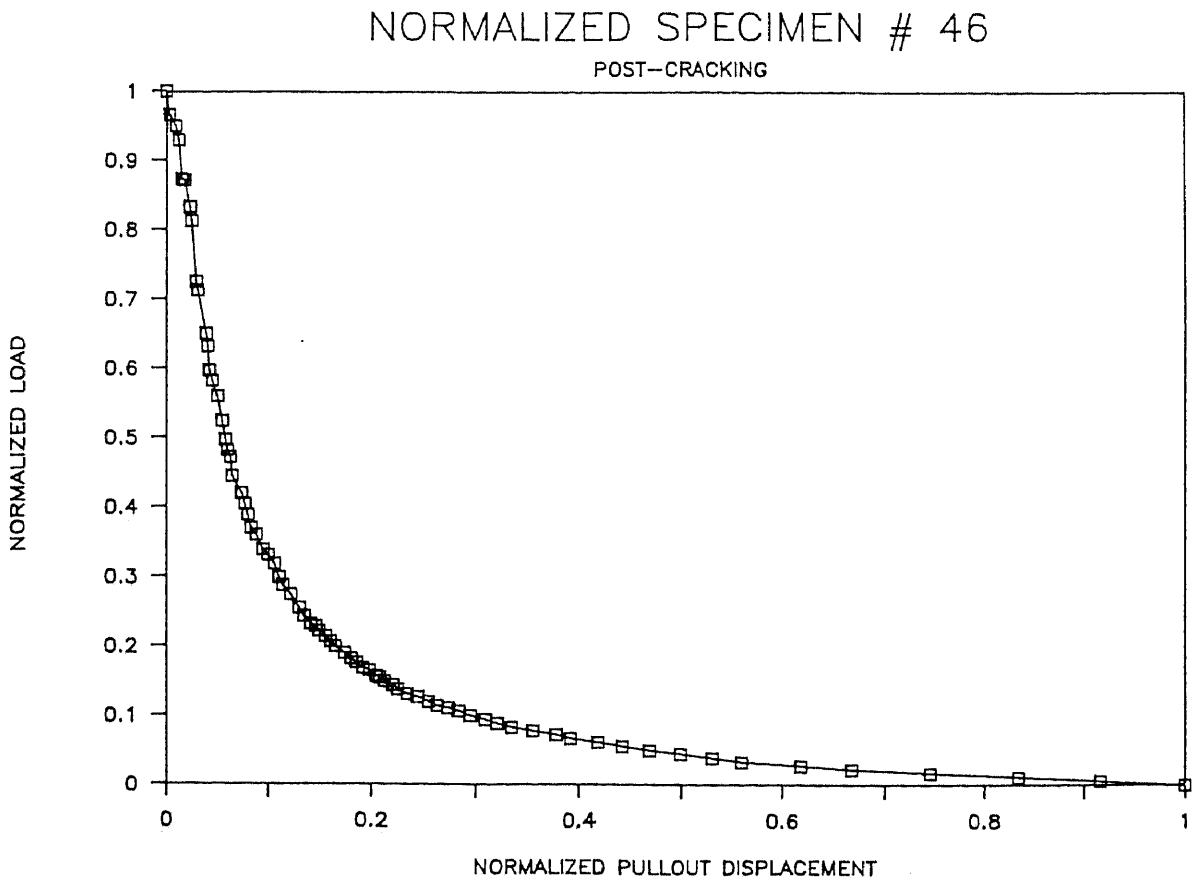
NORMALIZED SPECIMEN # 46
POST-CRACKING
NORMALIZED LOAD
NORMALIZED PULLOUT DISPLACEMENT
0
0.1
0.2
0.3
0.4
0.5
0.6
0.7
0.8
0.9
1
0
0.2
0.4
0.6
0.8
1

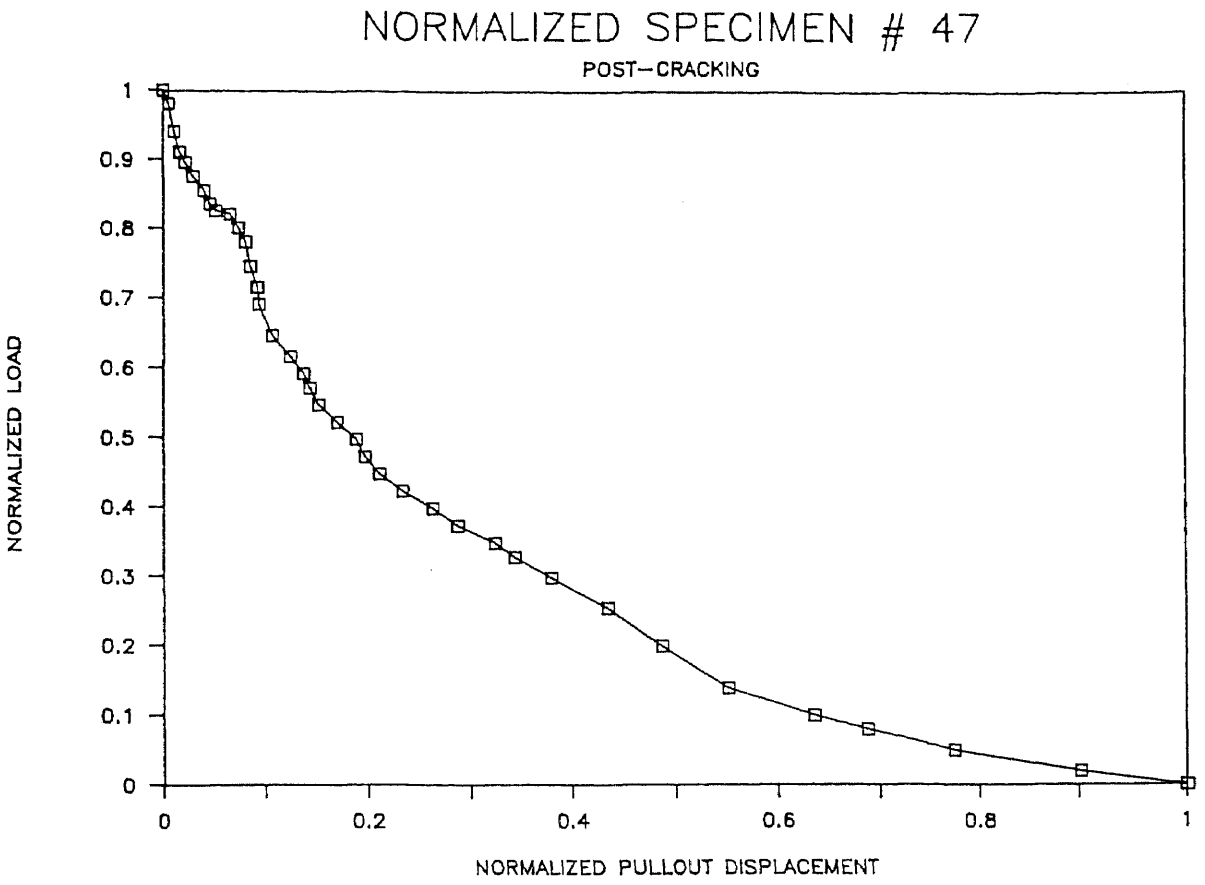
NORMALIZED SPECIMEN # 47
POST-CRACKING
NORMALIZED LOAD
NORMALIZED PULLOUT DISPLACEMENT
0
0.1
0.2
0.3
0.4
0.5
0.6
0.7
0.8
0.9
1
0
0.2
0.4
0.6
0.8
1

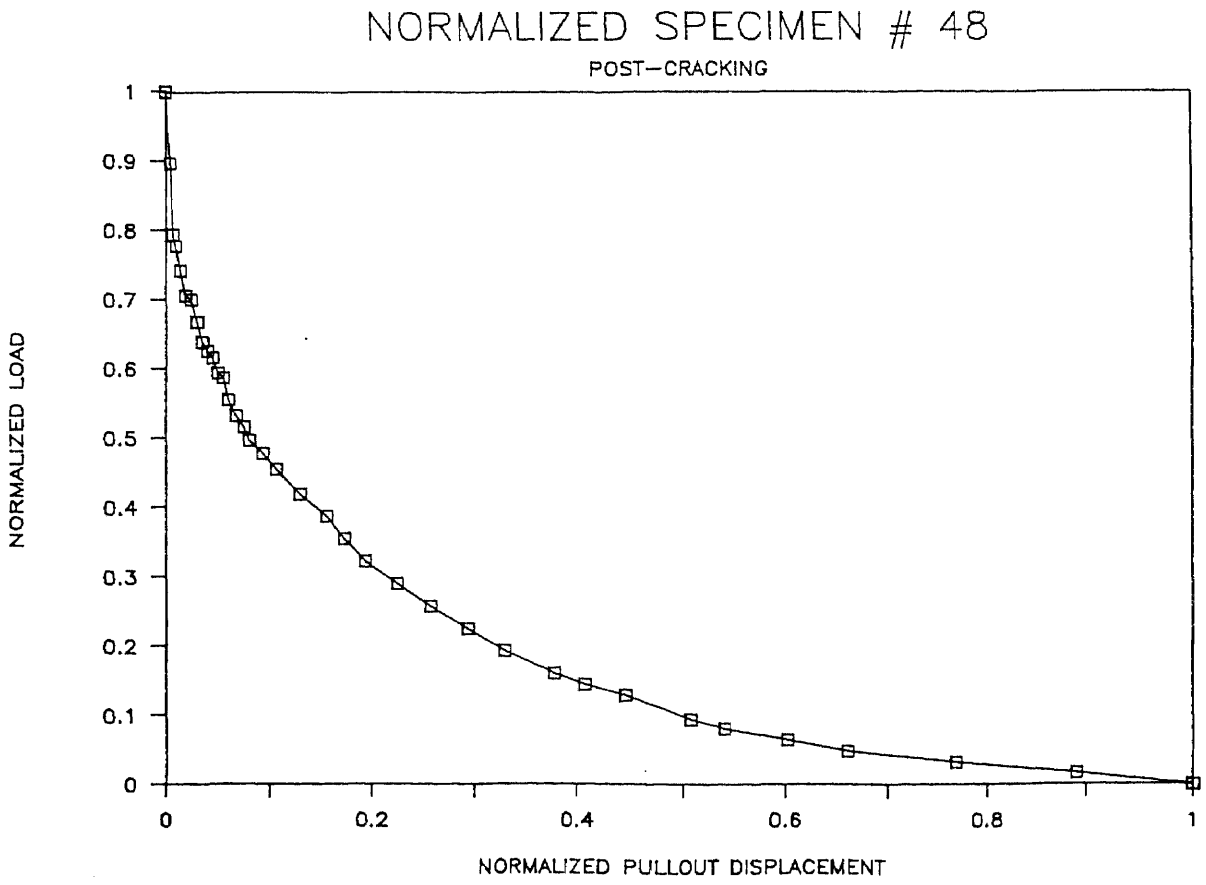
NORMALIZED SPECIMEN # 48
POST-CRACKING
NORMALIZED LOAD
NORMALIZED PULLOUT DISPLACEMENT
0
0.1
0.2
0.3
0.4
0.5
0.6
0.7
0.8
0.9
1
0
0.2
0.4
0.6
0.8
1

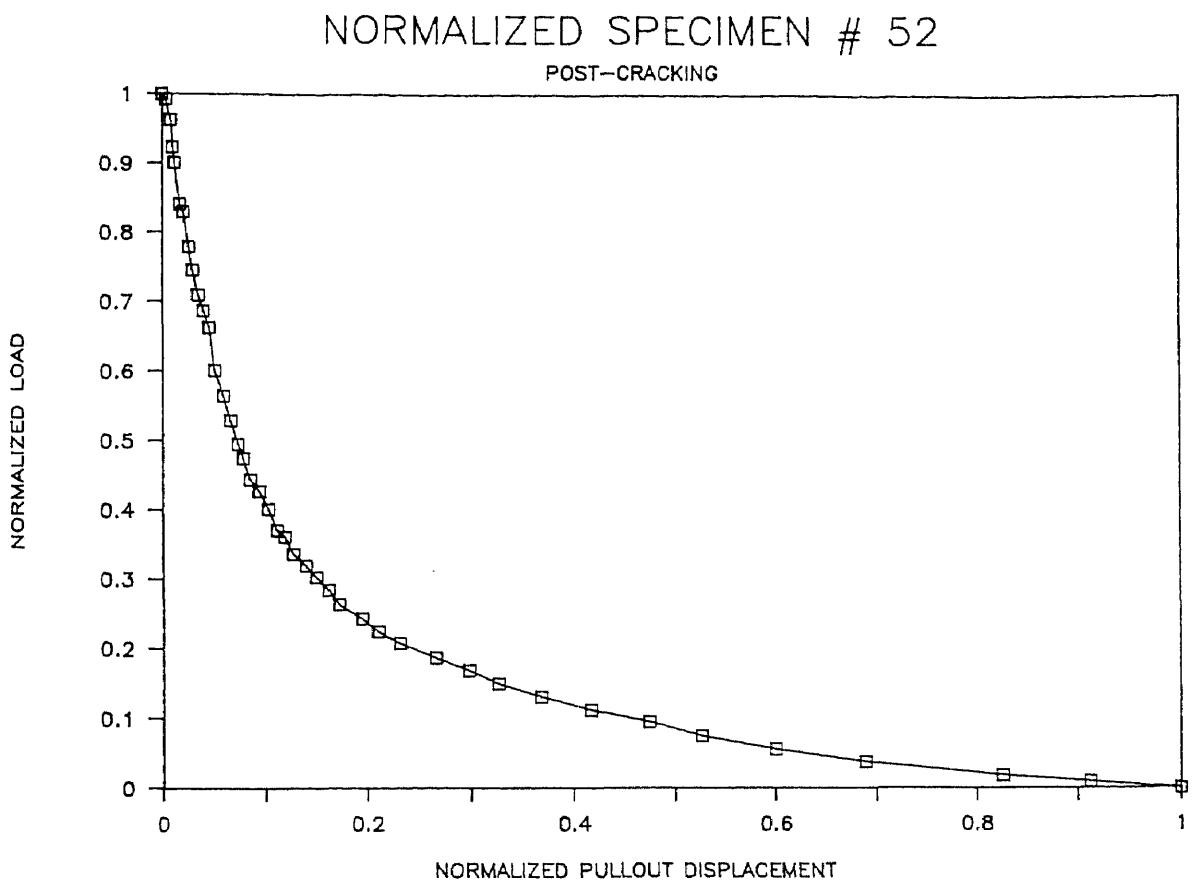
NORMALIZED SPECIMEN # 52
POST-CRACKING
NORMALIZED LOAD
1
0.9
0.8
0.7
0.6
0.5
0.4
0.3
0.2
0.1
0
0
0.2
0.4
0.6
0.8
1
NORMALIZED PULLOUT DISPLACEMENT

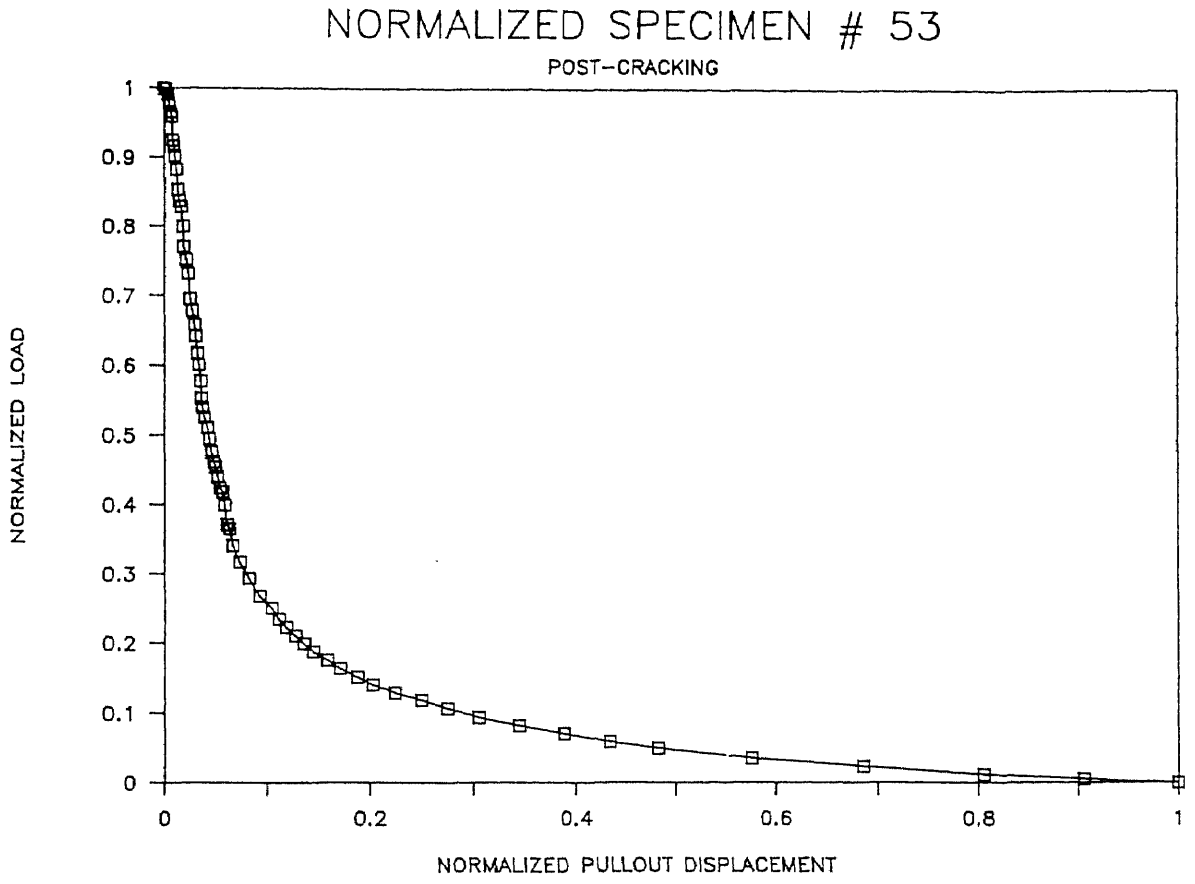
NORMALIZED SPECIMEN # 53
POST-CRACKING
NORMALIZED LOAD
NORMALIZED PULLOUT DISPLACEMENT
0
0.1
0.2
0.3
0.4
0.5
0.6
0.7
0.8
0.9
1
0.2
0.4
0.6
0.8

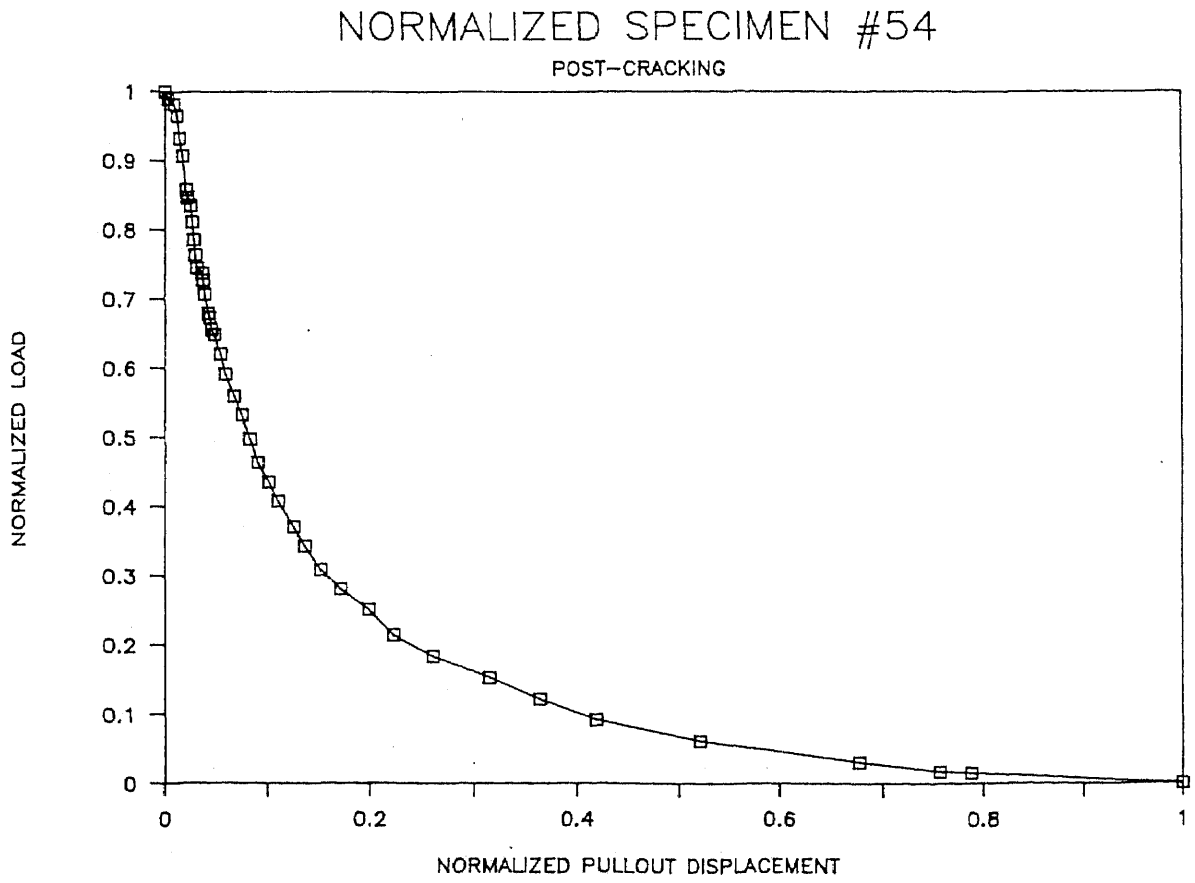
NORMALIZED SPECIMEN #54
POST-CRACKING
NORMALIZED LOAD
NORMALIZED PULLOUT DISPLACEMENT
0
0.1
0.2
0.3
0.4
0.5
0.6
0.7
0.8
0.9
1
0.2
0.4
0.6
0.8

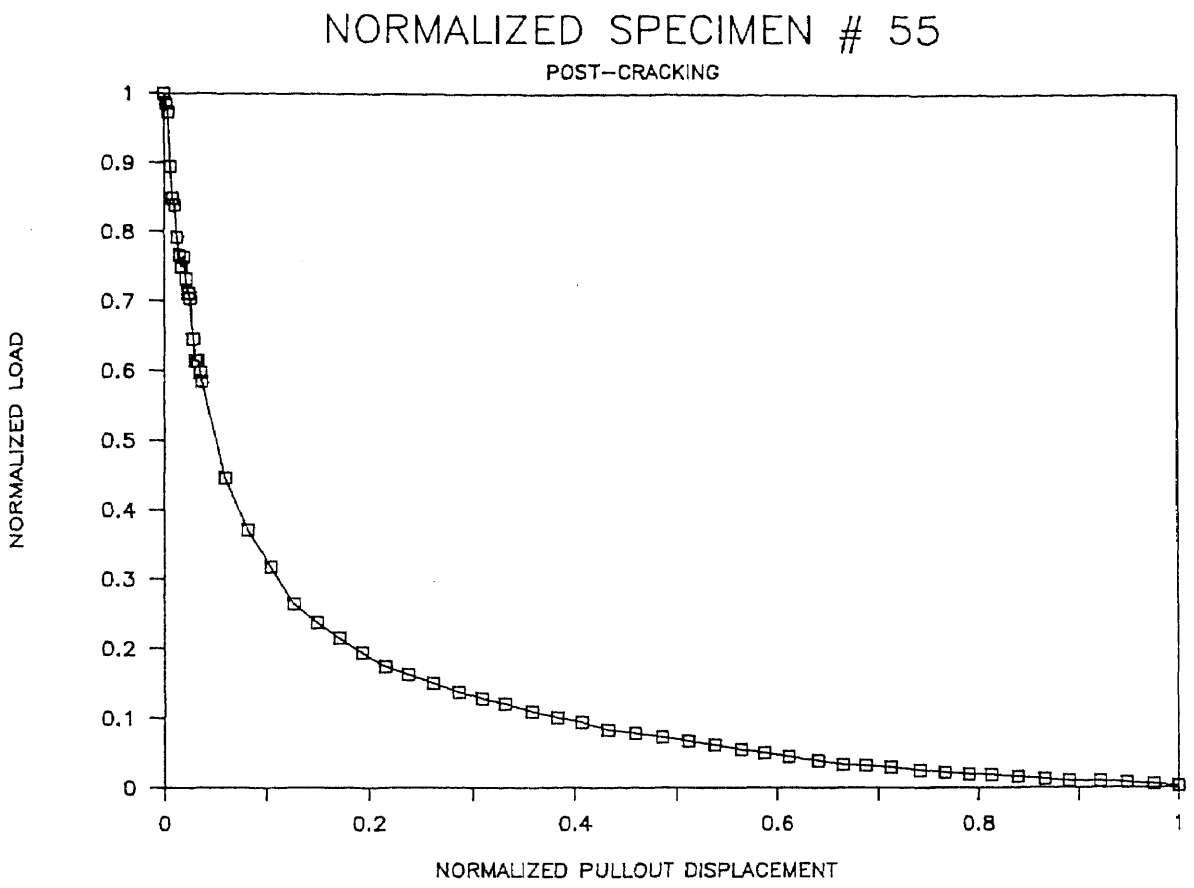
NORMALIZED SPECIMEN # 55
POST-CRACKING
NORMALIZED LOAD
0
0.1
0.2
0.3
0.4
0.5
0.6
0.7
0.8
0.9
1
0
0.2
0.4
0.6
0.8
1
NORMALIZED PULLOUT DISPLACEMENT

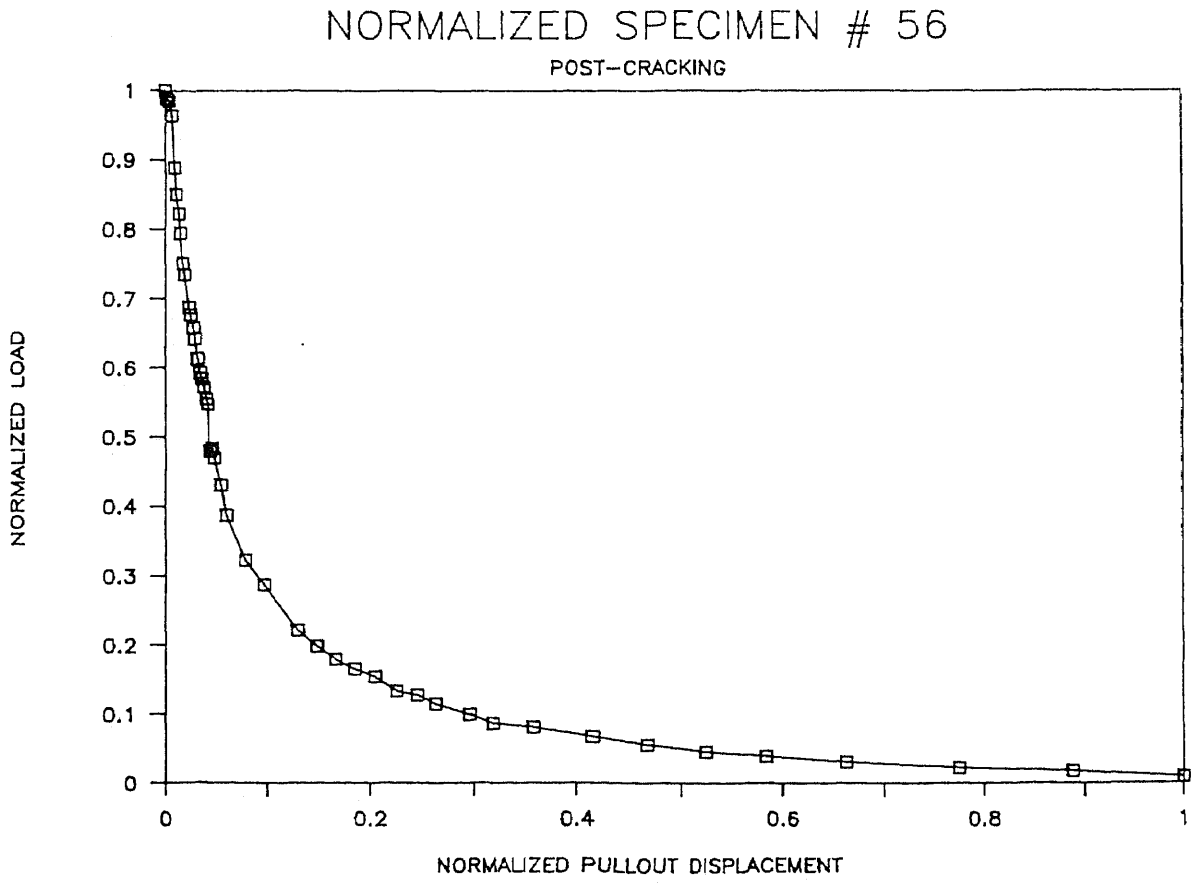
NORMALIZED SPECIMEN # 56
POST-CRACKING
NORMALIZED LOAD
0
0.1
0.2
0.3
0.4
0.5
0.6
0.7
0.8
0.9
1
0
0.2
0.4
0.6
0.8
1
NORMALIZED PULLOUT DISPLACEMENT

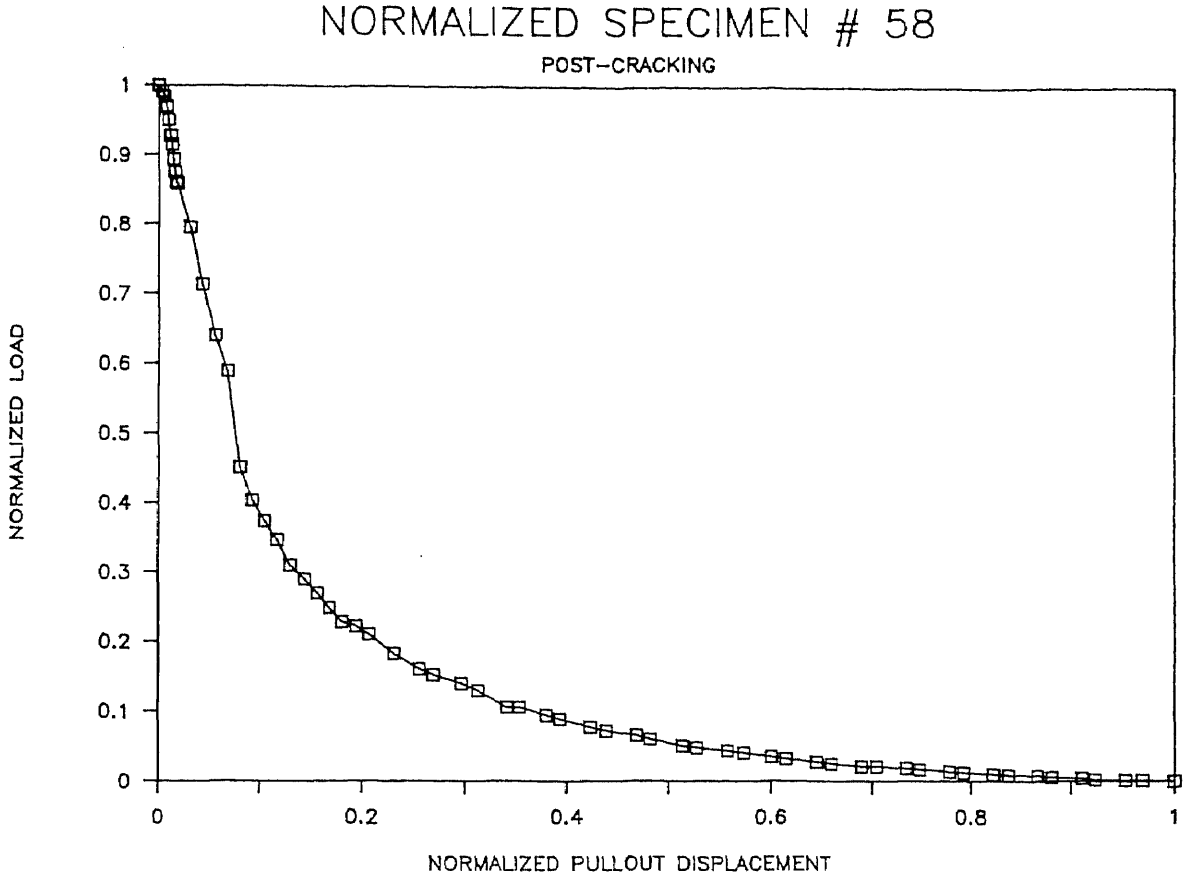
NORMALIZED SPECIMEN # 58
POST-CRACKING
NORMALIZED LOAD
NORMALIZED PULLOUT DISPLACEMENT
0
0.1
0.2
0.3
0.4
0.5
0.6
0.7
0.8
0.9
1
0
0.2
0.4
0.6
0.8
1

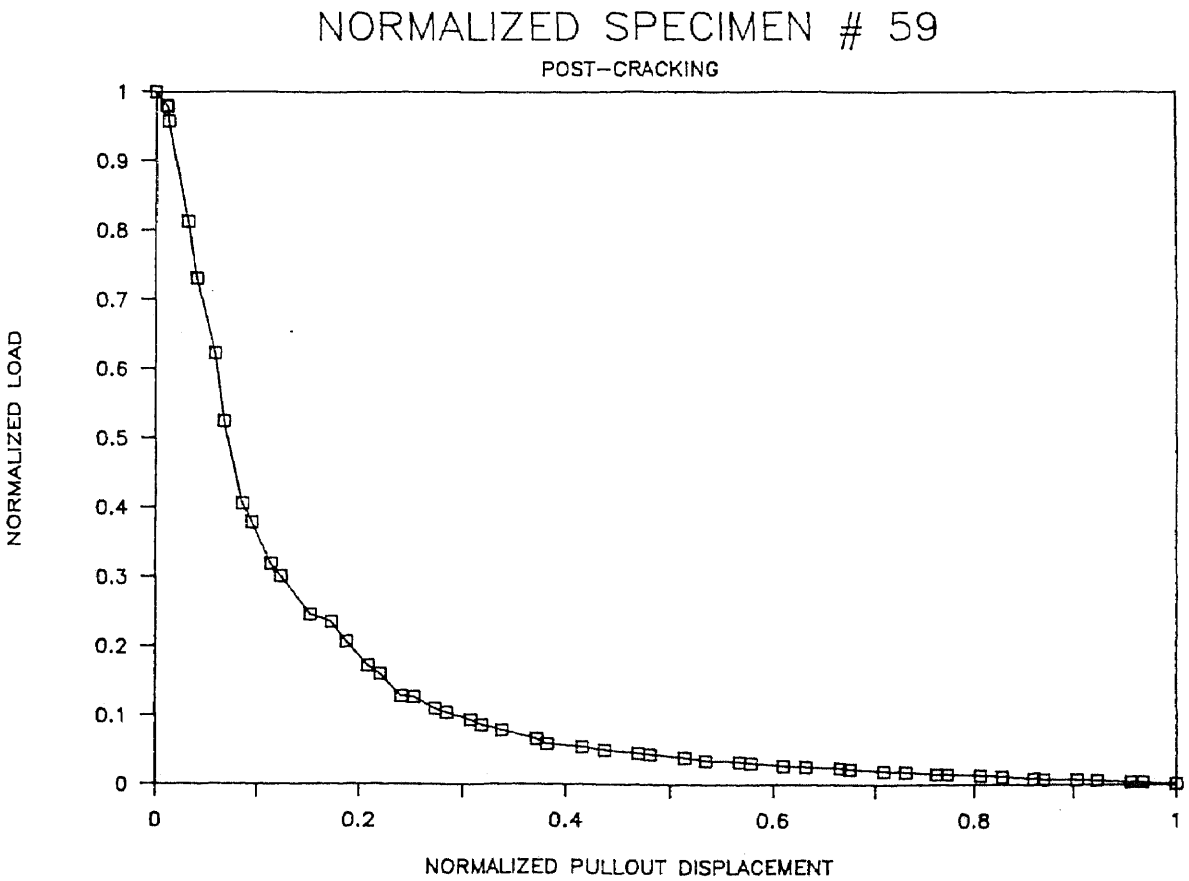
NORMALIZED SPECIMEN # 59
POST-CRACKING
NORMALIZED LOAD
NORMALIZED PULLOUT DISPLACEMENT
0
0.1
0.2
0.3
0.4
0.5
0.6
0.7
0.8
0.9
1
0
0.2
0.4
0.6
0.8
1

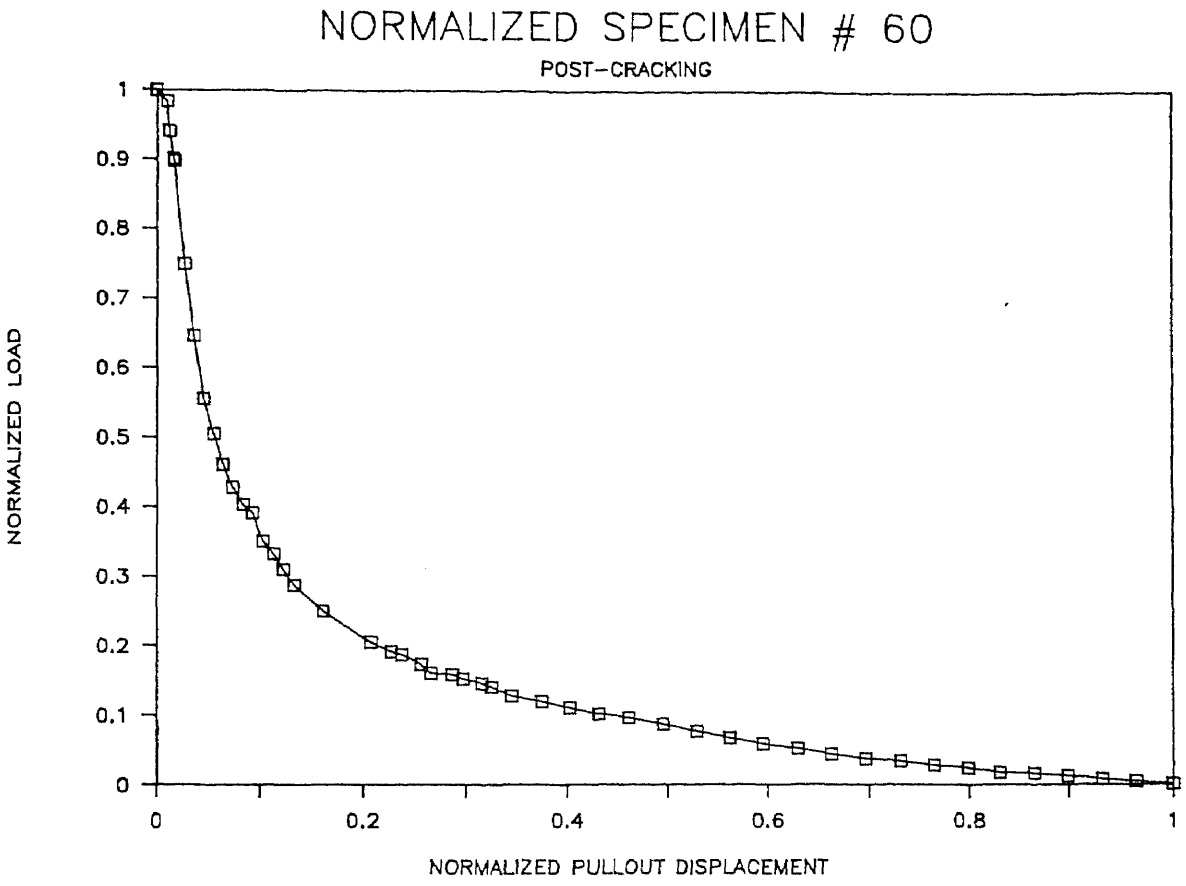
NORMALIZED SPECIMEN # 60
POST-CRACKING
NORMALIZED LOAD
NORMALIZED PULLOUT DISPLACEMENT
0
0.1
0.2
0.3
0.4
0.5
0.6
0.7
0.8
0.9
1
0
0.2
0.4
0.6
0.8
1

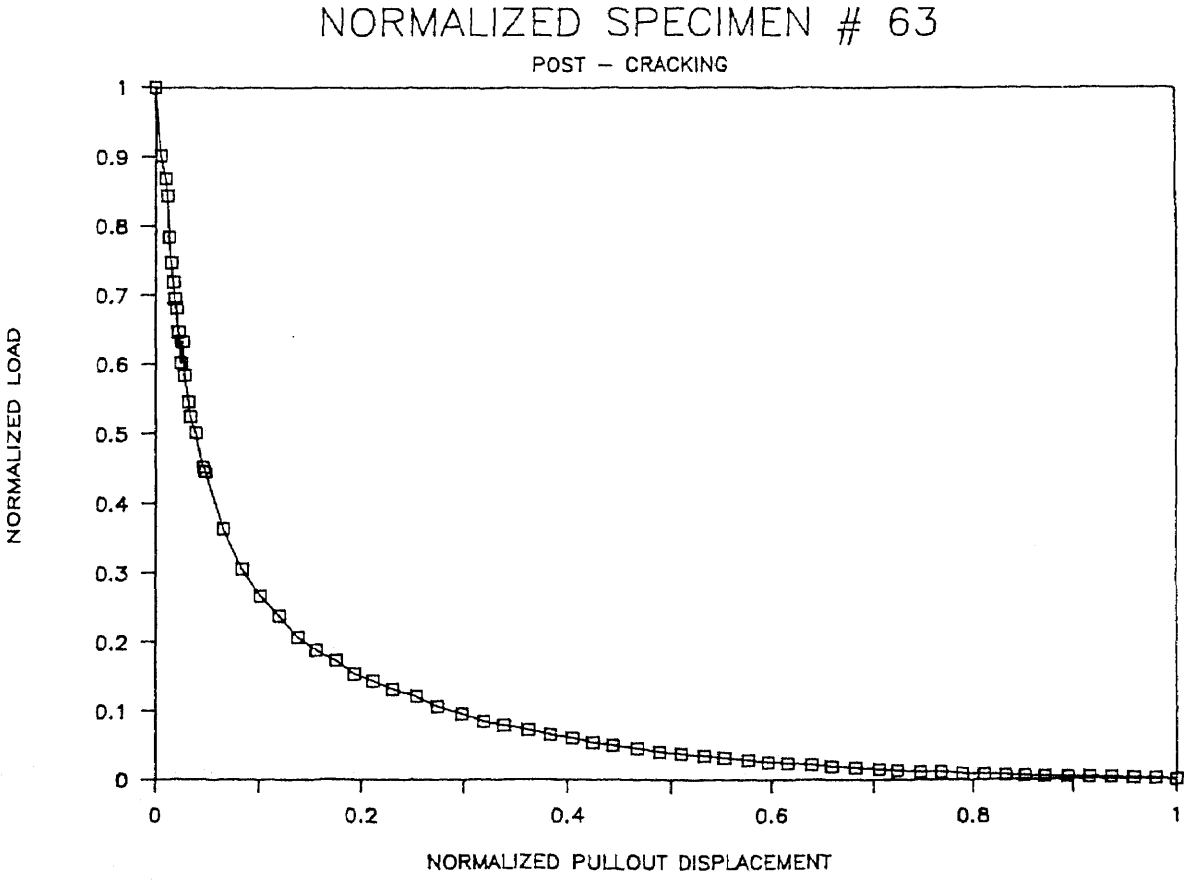
NORMALIZED SPECIMEN # 63
POST - CRACKING
NORMALIZED LOAD
NORMALIZED PULLOUT DISPLACEMENT
0
0.1
0.2
0.3
0.4
0.5
0.6
0.7
0.8
0.9
1
0
0.2
0.4
0.6
0.8
1

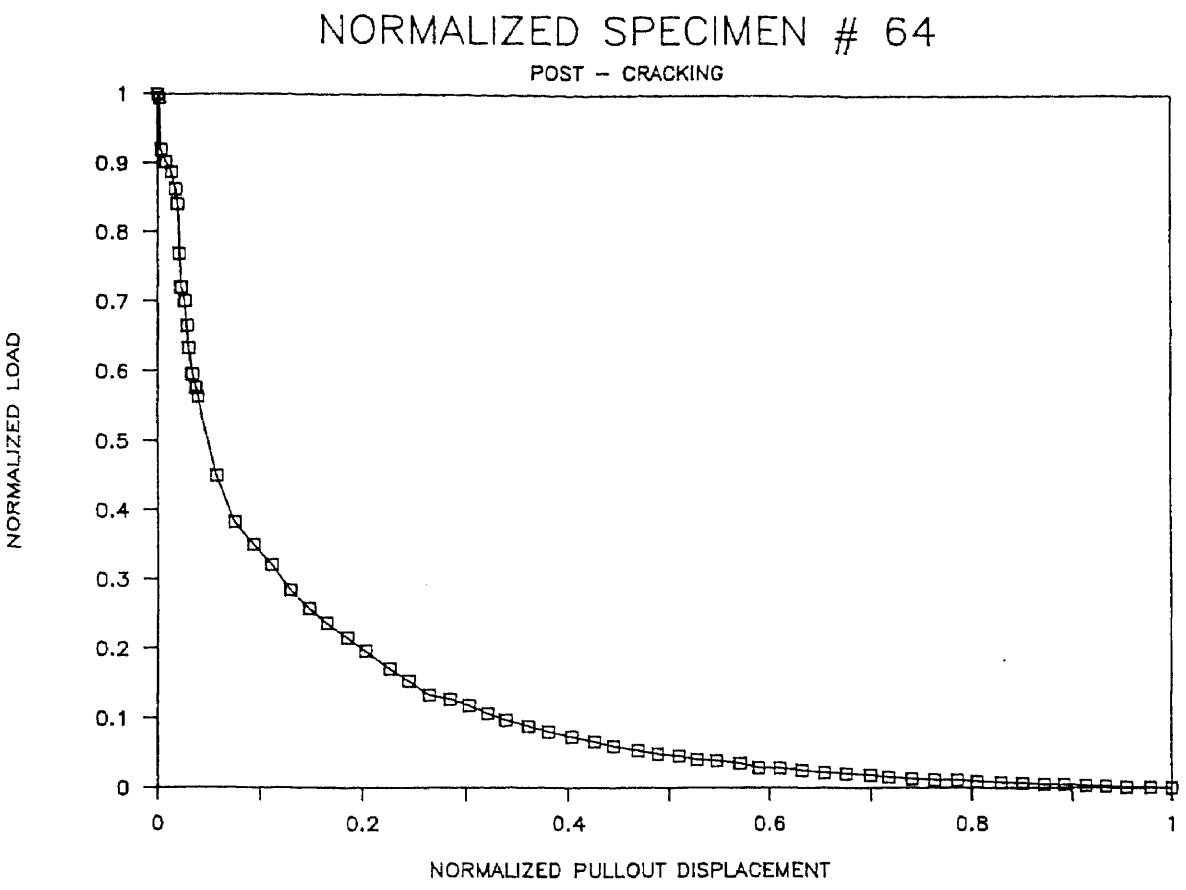
NORMALIZED SPECIMEN # 64
POST – CRACKING
NORMALIZED LOAD
NORMALIZED PULLOUT DISPLACEMENT
0
0.1
0.2
0.3
0.4
0.5
0.6
0.7
0.8
0.9
1
0
0.2
0.4
0.6
0.8
1

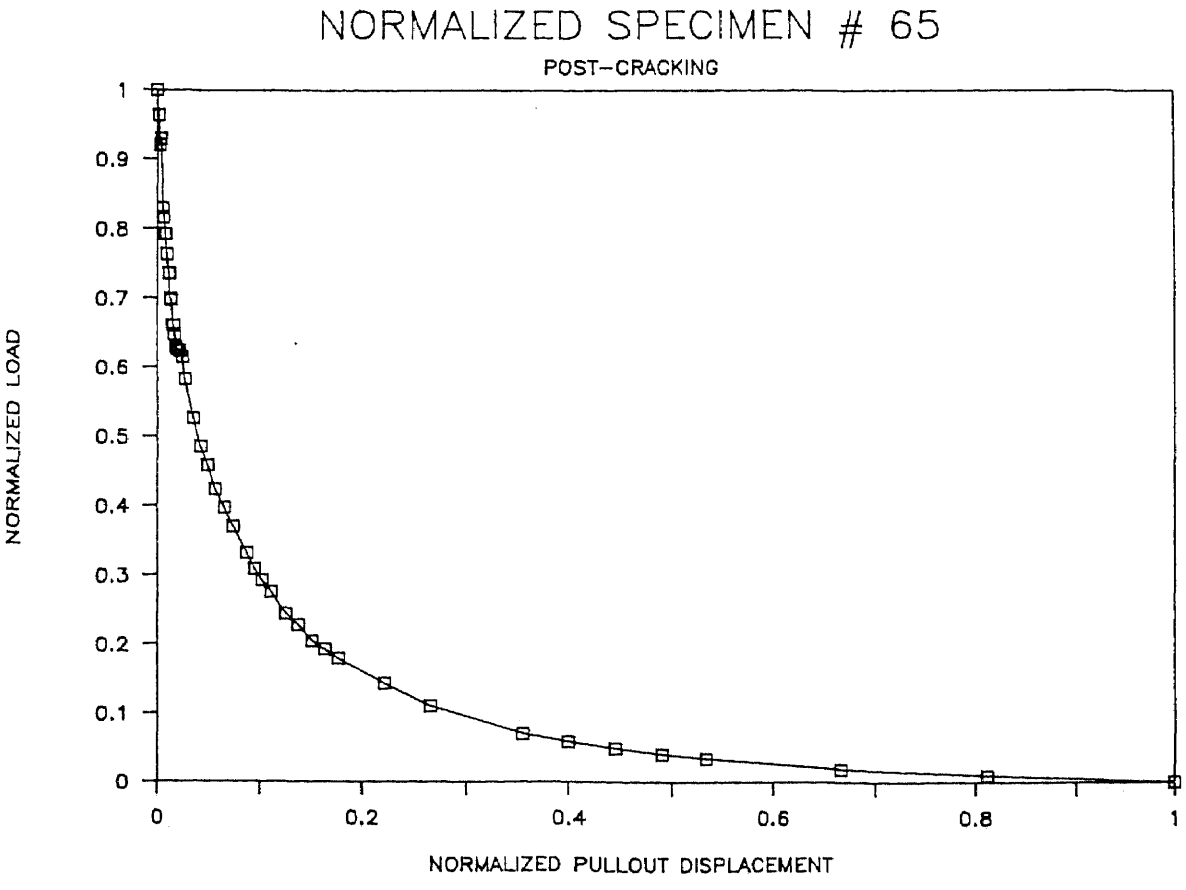
NORMALIZED SPECIMEN # 65
POST–CRACKING
NORMALIZED LOAD
NORMALIZED PULLOUT DISPLACEMENT
0
0.1
0.2
0.3
0.4
0.5
0.6
0.7
0.8
0.9
1
0
0.2
0.4
0.6
0.8
1

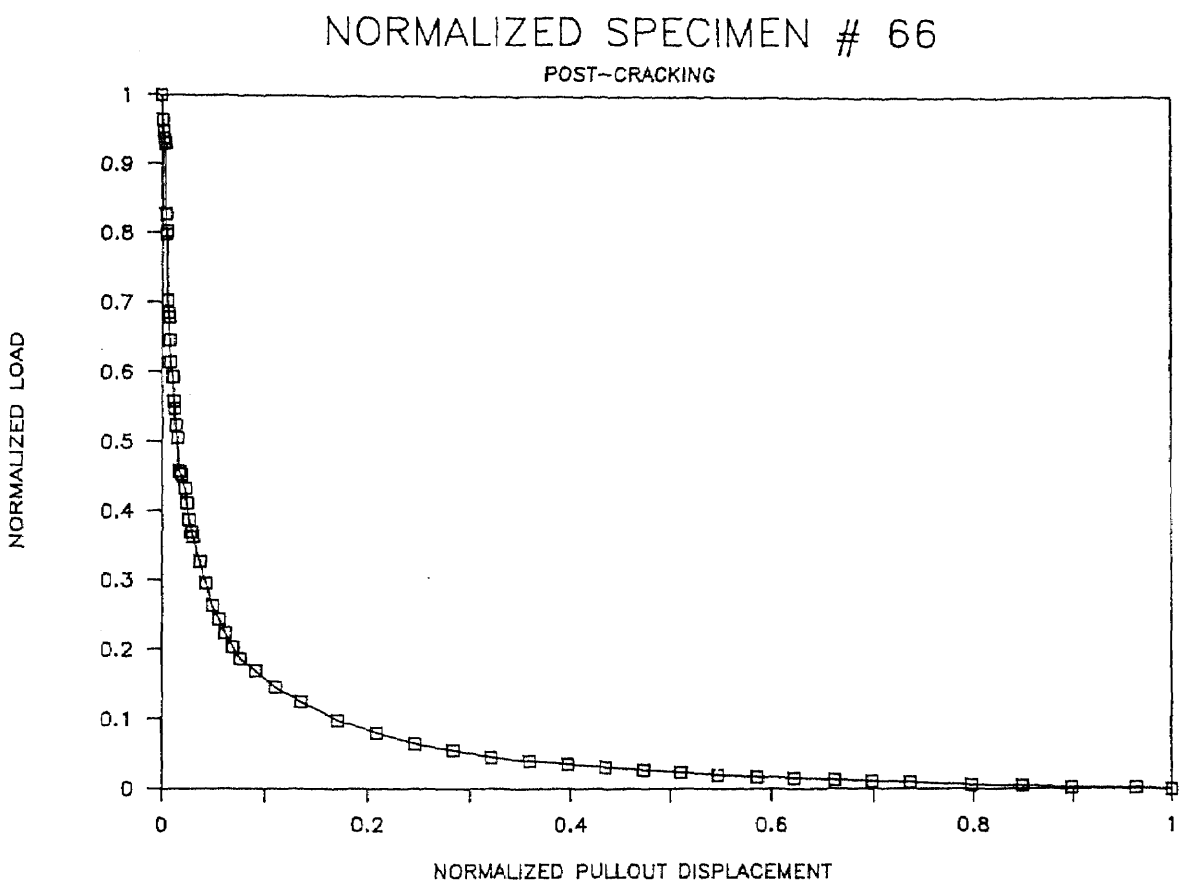
NORMALIZED SPECIMEN # 66
POST-CRACKING
NORMALIZED LOAD
NORMALIZED PULLOUT DISPLACEMENT
0
0.1
0.2
0.3
0.4
0.5
0.6
0.7
0.8
0.9
1
0
0.2
0.4
0.6
0.8
1

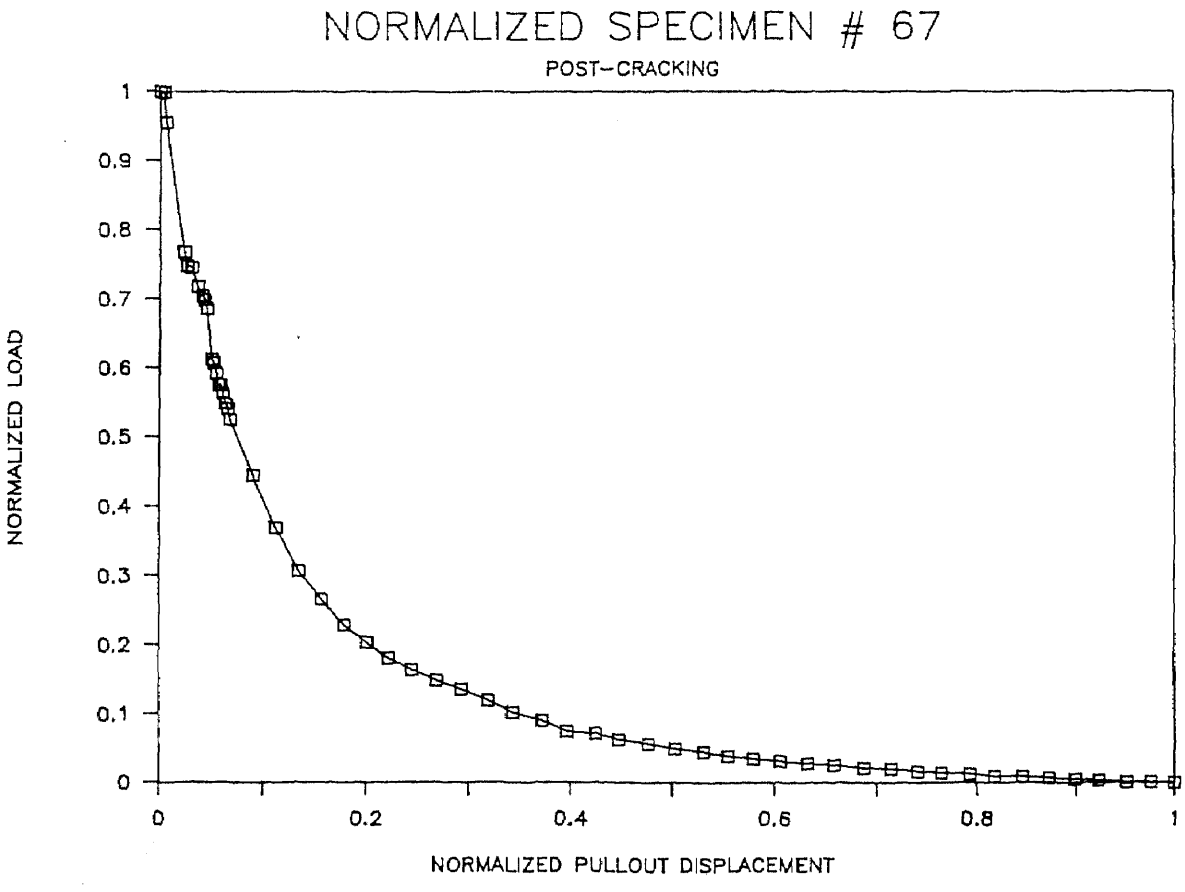
NORMALIZED SPECIMEN # 67
POST-CRACKING
NORMALIZED LOAD
NORMALIZED PULLOUT DISPLACEMENT
0
0.1
0.2
0.3
0.4
0.5
0.6
0.7
0.8
0.9
1
0
0.2
0.4
0.6
0.8
1

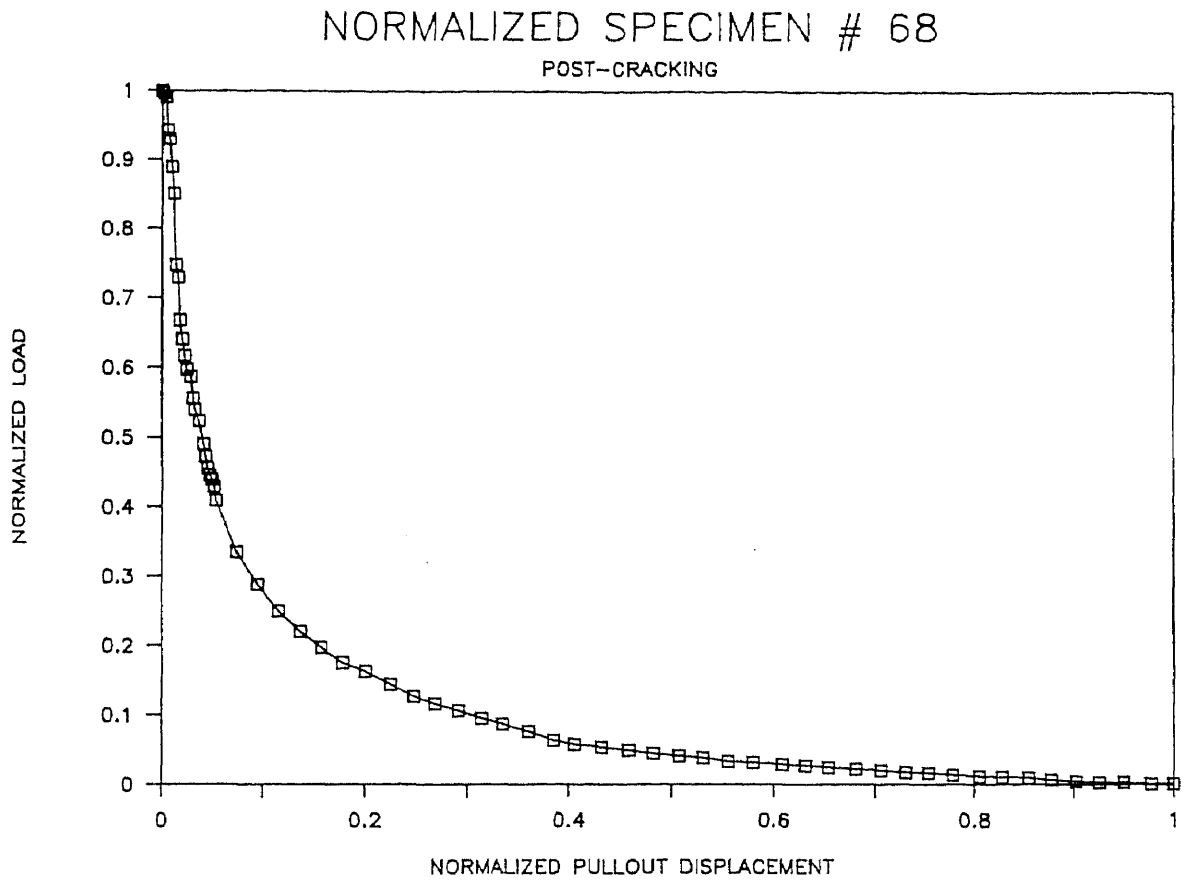
NORMALIZED SPECIMEN # 68
POST-CRACKING
NORMALIZED LOAD
NORMALIZED PULLOUT DISPLACEMENT
0
0.1
0.2
0.3
0.4
0.5
0.6
0.7
0.8
0.9
1
0
0.2
0.4
0.6
0.8
1

APPENDIX C

1	2	3	4	5	6	7	8	9	10	11
SPEC #	DATE CASTED	DATE TESTED	MIX PROPORTION C:S:G:W	GRAIN SIZE SIEVE NO	MAX LOAD lbs.	STRAIN AT MAX LOAD	MAX STRAIN E-4	COMPR. STRENGTH psi.	TENSILE STRENGTH psi.	G_f lb./in.
1	5/26/85	6/2/85	1:2:2:0.55	UNSIEVED	499	0.0004	194.0	N/A	178.21	0.34386
3	6/20/85	6/27/85	1:2:2:0.55	UNSIEVED	718	0.0003	168.0	5206	255.29	0.635217
4	6/24/85	7/1/85	1:2:2:0.55	UNSIEVED	441	0.0003	194.0	3750	441.00	0.328530
5	6/25/85	7/2/85	1:2:2:0.55	UNSIEVED	499	0.0004	194.0	N/A	183.46	0.50318
6	7/1/85	7/10/85	1:2:2:0.50	UNSIEVED	671	0.00034	INCONCL	4533	203.33	0.32853
7	7/1/85	7/11/85	1:2:2:0.50	UNSIEVED	547	0.00026	192.0	4533	223.33	0.71009
8	7/1/85	7/12/85	1:4:0.50	UNSIEVED	298	0.00033	193.4	N/A	132.33	0.48322
9	7/3/85	7/15/85	1:2:0.50	UNSIEVED	732	0.0005	193.3	4618	275.33	0.65545
20	7/10/85	8/7/85	1:2:2:0.45	UNSIEVED	682	0.00045	193.8	6686	207.93	0.80838
21	7/15/85	8/13/85	1:2:2:0.50	UNSIEVED	617	0.00045	316.6	5156	263.68	0.92208
22	7/15/85	8/14/85	1:2:2:0.50	UNSIEVED	554	0.00041	300.0	5156	236.75	1.00191
25	7/8/85	8/20/85	1:2:2:0.45	UNSIEVED	891	0.00037	336.7	7894	259.01	0.60832
26	7/8/85	8/21/85	1:2:2:0.45	UNSIEVED	785	0.00038	122.0	7894	288.60	0.49598
27	7/9/85	8/22/85	1:2:2:0.45	UNSIEVED	609	0.00042	237.1	6451	288.63	1.39580
28	7/9/85	8/26/85	1:2:2:0.45	UNSIEVED	751	0.00042	156.5	6451	261.67	0.51645
29	7/9/85	8/29/85	1:2:2:0.45	UNSIEVED	654	0.00026	306.5	6451	299.67	0.98822
32	7/12/85	9/10/85	1:2:2:0.45	10-40	760	0.00025	193.0	6960	249.59	0.51774
33	8/8/85	10/4/85	1:4:0.50	<70	255	0.00042	59.8	N/A	124.27	0.15492

1	2	3	4	5	6	7	8	9	10	11
SPEC #	DATE CASTED	DATE TESTED	MIX PROPORTION C:S:G:W	GRAIN SIZE SIEVE NO	MAX LOAD lbs.	STRAIN AT MAX LOAD	MAX STRAIN E-4	COMPR. STRENGTH psi.	TENSILE STRENGTH psi.	G_f lb./in.
34	8/12/85	10/11/85	1:2:0.50	40~70	502	0.00042	64.8	6663	246.08	0.22852
35	8/13/85	10/23/85	1:2:0.50	10~40	487	0.00042	120.3	7654	221.36	0.30020
36	8/13/85	10/24/85	1:2:0.50	10~40	579	0.00047	79.9	7654	261.99	0.29345
37	8/14/85	11/14/85	1:2:0.45	40~70	520	0.00033	56.2	9082	240.74	0.20951
38	8/19/85	1/6/86	1:2:0.40	10~40	506	0.00027	80.7	10356	220.00	0.27705
39	8/14/85	1/7/86	1:2:0.45	10~40	717	0.00036	77.8	8616	275.77	0.27228
40	12/23/85	2/26/86	1:2:0.50	10~40	518	0.00022	56.1	7068	261.30	0.27045
41	12/23/85	2/28/86	1:2:0.50	10~40	631	0.00030	106.8	7068	230.76	0.35930
42	1/8/86	3/9/86	1:2:0.45	40~70	776	0.00026	51.0	7378	391.44	0.29406
43	1/9/86	3/20/86	1:2:0.55	10~40	797	0.00036	82.8	7076	402.04	0.53062
44	1/13/86	3/21/86	1:2:0.55	40~70	859	0.00032	41.0	7233	391.99	0.32162
45	3/18/86	3/26/86	1:2:0.55	10~40	693	0.00023	75.9	6874	311.52	0.31892
46	3/18/86	4/2/86	1:2:0.55	10~40	899	0.00020	65.1	6874	375.74	0.32766
47	6/3/86	6/13/86	1:2:0.50	10~40	201	0.00040	39.0	6801	115.31	0.16947
48	6/3/86	8/6/86	1:2:0.50	10~40	310	0.00058	45.0	6801	176.36	0.18029
51	8/18/86	9/25/86	1:2:0.50	40~50	588	0.00036	FAILED	5080	268.32	********
52	8/15/86	9/26/86	1:2:0.50	40~50	533	0.00013	58.6	6021	226.55	0.21985
53	8/15/86	10/1/86	1:2:0.50	40~50	851	0.00033	104.3	6021	350.81	0.44754

1	2	3	4	5	6	7	8	9	10	11
SPEC #	DATE CASTED	DATE TESTED	MIX PROPORTION C:S:G:W	GRAIN SIZE SIEVE NO	MAX LOAD lbs.	STRAIN AT MAX LOAD	MAX STRAIN E-4	COMPR. STRENGTH psi.	TENSILE STRENGTH psi.	G_f lb./in.
54	8/18/86	10/10/86	1:2:0.50	40~50	649	0.00021	68.1	6783	271.48	0.31561
55	8/19/86	7/30/87	1:2:0.45	40~50	711	0.00033	48.2	7076	337.06	0.26759
56	8/19/86	7/31/87	1:2:0.45	40~50	676	0.0003	54.1	7076	400.59	0.28363
57	2/18/87	8/4/87	HIGH-STR	********	1022	0.00031	FAILED	********	454.22	********
58	8/20/86	8/5/87	1:2:0.45	40~50	711	0.00024	83.3	6450	297.42	0.38658
59	8/20/86	8/6/87	1:2:0.45	40~50	668	0.00035	113.0	6450	296.89	0.48645
60	8/21/86	8/10/87	1:2:0.45	30~40	614	0.00031	109.9	8140	207.92	0.36762
61	2/18/87	8/12/87	HIGH-STR	********	1205	0.00028	FAILED	********	476.04	********
62	8/21/86	8/18/87	1:2:0.45	30~40	1102	0.00026	FAILED	8140	489.78	********
63	8/27/86	9/1/87	1:2:0.40	10~30	1038	0.00023	58.2	9125	461.33	0.33020
64	8/22/86	9/1/87	1:2:0.40	30~40	1019	0.00028	58.3	9655	482.64	0.40879
65	8/26/86	9/3/87	1:2:0.40	10~30	878	0.00024	69.4	9106	390.22	0.33406
66	8/27/86	9/15/87	1:2:0.40	10~30	1148	0.00022	145.7	9125	408.18	0.42226
67	8/22/86	9/16/87	1:2:0.40	30~40	1026	0.00019	47.3	9655	456.00	0.33383
68	8/26/86	9/16/87	1:2:0.40	10~30	930	0.00024	50.7	9106	440.88	0.28998